Applied molecular bioprocess control using RNA thermometers

Exploiting temperature responsive elements
for rhamnolipid production

Dissertation to obtain the doctoral degree of
Natural Sciences (Dr. rer. nat.)

Faculty of Natural Sciences
University of Hohenheim

Institute of Food Science and Biotechnology

submitted by

Philipp Daniel Noll

from Ludwigshafen am Rhein
2022

Dean:	Prof. Dr. Uwe Beifuss

1^{rst} referee / examiner:	Prof. Dr. Rudolf Hausmann
2nd referee / examiner:	Prof. Dr. Christoph Syldatk
3rd examiner:	Prof. Dr. Ralf Kölling-Paternoga

Submitted:	March 23rd, 2022
Oral exam:	July 6th, 2022

This work was accepted on June 14th, 2022 by the Faculty of Natural Sciences of the University of Hohenheim as "Dissertation to obtain the doctoral degree of Natural Sciences".

The real problem in speech is not *precise* language.

The problem is *clear* language.

Richard Phillips Feynman

Acknowledgements

I would like to express my sincerest gratitude to...

Prof. Dr.-Ing. Rudolf Hausmann for the opportunity to complete my doctoral thesis in his department, for his guidance and helpful scientific discussions.

Prof. Dr. rer. nat. Christoph Syldatk the second reviewer of my thesis for the inspiring ideas and discussions.

Dr.-Ing. Marius Henkel for his supervision, interesting discussions and incredible patience. Thank you for providing the freedom to follow the topics I was interested in.

Dr. rer. nat. Lars Lilge for your friendly support and helpful input during meetings and seminars.

All members of the department of bioprocess engineering who created such a pleasant working environment. Especially my dear fellow doctoral students Mareen Hoffmann, Chantal Treinen, Peter Klausmann, Till Hennecke, Manuel Merkel, Malihe Vahidinasab and Dirk Kiefer.

My students who contributed to the development of this work in the form of a bachelor and master thesis or project works. Thank you for your valuable contribution to the collection of the enormous amount of data and for the opportunity to teach in a university format. Thank you: Sven Müller, Olivia Magosch, Isaac Thevathasan, Maximilian Möbus, Matheus Kolodziej, Jasmine Seidel, Vanessa Wienecke, Aline Zepezauer, Sina Maschek and Franziska Beck.

Prof. Dr. rer. nat. Thomas Rausch and the BBW-Forwerts program for providing the "bigger picture" of my research. Thank you for the valuable insights and the opportunity to make a contribution to the development of a sustainable bioeconomy.

Prof. Carlos Ariel Cardona Alzate, PhD for the opportunity to gain insights on industrial, economic and environmental assessment of biotechnological processes during my research stay at the Universidad Nacional de Colombia.

The Landesgraduiertenförderung of the University of Heidelberg for providing my individual doctoral fellowship.

My family and my girlfriend **Nariê Rinke** who supported me throughout my academic career.

Publications related to this work

Original research paper (peer-reviewed)

Philipp Noll, Chantal Treinen, Sven Müller, Lars Lilge, Rudolf Hausmann, and Marius Henkel (2021). "Exploiting RNA thermometer-driven molecular bioprocess control as a concept for heterologous rhamnolipid production".

In: *Scientific Reports* 11, pp. 1-12.
DOI: 10.1038/s41598-021-94400-4

Philipp Noll, Chantal Treinen, Sven Müller, Sabine Senkalla, Lars Lilge, Rudolf Hausmann, and Marius Henkel (2019). "Evaluating temperature-induced regulation of a ROSE-like RNA-thermometer for heterologous rhamnolipid production in *Pseudomonas putida* KT2440".

In: *AMB Express* 9.1, pp. 1–10.
DOI: 10.1186/s13568-019-0883-5.12

Horlamus, Felix, Andreas Wittgens, **Philipp Noll**, Jan Michler, Inga Müller, Fabiola Weggenmann, Claudia Oellig, Frank Rosenau, Marius Henkel, and Rudolf Hausmann (2019). "One-step bio-conversion of hemicellulose polymers to rhamnolipids with *Cellvibrio japonicus*: A proof-of-concept for a potential host strain in future bioeconomy".

In: *GCB Bioenergy* 11.1, pp. 260–268.
DOI: 10.1111/gcbb.12542

Review articles (peer-reviewed)

Ann-Kathrin Briem, Lars Bippus, Amira Oraby, **Philipp Noll**, Susanne Zibek, Stefan Albrecht (2022). "Environmental Impacts of Biosurfactants from a Life Cycle Perspective: A Systematic Literature Review".

In: *Advances in Biochemical Engineering/Biotechnology* book series, pp. 1-35.
DOI: 10.1007/10_2021_194.

Philipp Noll and Marius Henkel (2020). "History and evolution of modeling in biotechnology: modeling & simulation, application and hardware performance".

In: *Computational and Structural Biotechnology Journal* 18, pp. 3309–3323.
DOI: 10.1016/j.csbj.2020.10.018.

Philipp Noll, Lars Lilge, Rudolf Hausmann, and Marius Henkel (2020). "Modeling and exploiting microbial temperature response".

In: *Processes* 8.1, p. 121.
DOI: 10.3390/pr8010121.

Author contribution statement

Parts of this cumulative doctoral thesis are based on peer-reviewed research- and review articles. These articles are based on work accompanying this dissertation between March 2018 and July 2021. A list of published papers related to this work with the respective authors contribution, is provided below. Parts of this work have been previously published with the knowledge and approval of the supervisor Prof. Dr.-Ing. Rudolf Hausmann. Parts of the scientific work shown in this thesis were carried out in cooperation with co-authors from the University of Hohenheim.

Exploiting RNA thermometer-driven molecular bioprocess control as a concept for heterologous rhamnolipid production

Philipp Noll, Chantal Treinen, Sven Müller, Lars Lilge, Rudolf Hausmann, and Marius Henkel

Scientific Reports (2021) 11, pp. 1–12. DOI: 10.1038/s41598-021-94400-4

P.N. planned and executed the experiments, collected data, created the graphs and drafed the manuscript. C.T. and S.M. performed part of the experiments and cloning, collected and evaluated corresponding data. L.L. and R.H. contributed to evaluation of the data, design of the experiments and scientifc discussion. M.H. substantially contributed to conception, and design of the conducted experiments, interpretation and evaluation of the results and drafing of the manuscript. All authors read and approved the final version of the manuscript.

Evaluating temperature-induced regulation of a ROSE-like RNA-thermometer for heterologous rhamnolipid production in *Pseudomonas putida* KT2440

Philipp Noll, Chantal Treinen, Sven Müller, Sabine Senkalla, Lars Lilge, Rudolf Hausmann, and Marius Henkel

AMB Express (2019) 9.1, pp. 1–10. DOI: 10.1186/s13568-019-0883-5.12

P.N. planned and executed the experiments, collected data, created the graphs and drafted the manuscript. C.T., S.M. and S.S. performed part of the experiments and collected and evaluated corresponding data. L.L. and R.H. contributed to evaluation of the data, design of the experiments and scientifc discussion. M.H. substantially contributed to conception and design of the conducted experiments, interpretation of the results and drafting of the manuscript. All authors read and approved the final manuscript.

History and evolution of modeling in biotechnology: modeling & simulation, application and hardware performance

Philipp Noll and Marius Henkel

Comput. Struct. Biotechnol. J. (2020) 18, pp. 3309–3323. DOI: 10.1016/j.csbj.2020.10.018

P.N.: Conceptualization, Methodology, Formal analysis, Investigation, Writing - original draft, Writing - review & editing, Visualization. M.H.: Conceptualization, Methodology, Formal analysis, Investigation, Writing - original draft, Writing - review & editing, Visualization, Supervision, Project administration.

Modeling and exploiting microbial temperature response

Philipp Noll, Lars Lilge, Rudolf Hausmann, and Marius Henkel

Processes (2020) 8.1, p. 121. DOI: 10.3390/pr8010121

Conceptualization, **P.N.** and M.H.; Formal Analysis, **P.N.**, L.L., R.H. and M.H.; Investigation **P.N.**, L.L., R.H. and M.H.; Writing-Original Draft Preparation, **P.N.**; Writing-Review & Editing, **P.N.**, L.L., R.H. and M.H.; Supervision, M.H. All authors have read and agreed to the published version of the manuscript.

Abstract

"There is only one planet Earth, yet by 2050, the world will be consuming as if there were three" - The European Commission, 2020. Humanity will face several challenges in the twenty-first century, including a rapidly growing global population, limited fossil oil resources, climate change, and related issues such as increased demand for food, fuel, fiber, and feed. The initially quoted statement made by the European Commission backed by the Sustainable Development Goals (SDGs) of the United Nations indicates the urgency of a transition from a linear- to a circular economy. A part of the SDGs of the UN is the use of renewable resources for industrial products. This thesis represents a mosaic stone for the latter goal. A bioprocess with novel process design for the production of a microbial biosurfactant (in the following referred to as biosurfactant) from renewable resources is presented. The worldwide surfactant market was valued with 43.6 $ billion in 2017 and is expected to increase to 66.4 $ billion by 2025, corresponding to a compound annual growth rate of 5.4% (2018 – 2025). A large share of commercially available surfactants are derived from petrochemical or oleo-chemical sources. Some raw materials (e.g. 4-Nonylphenol) used for the chemical synthesis of surfactants display human- and environmental toxicity as well as low biodegradability respectively have an opposing social- and environmental impact (e.g. palm oil). In nowadays, consumer awareness and environmental legislation drive a transition towards sustainable and eco-friendly processes. Therefore, the production of biosurfactants on the basis of renewable substrates is becoming increasingly attractive for the industry. On the one hand, biosurfactants display beneficial properties like low toxicity, biodegradability, stability at extreme ambient conditions (pH, temperature, salinity) and high surfactant efficiencies. On the other hand, an economically feasible production of biosurfactants is challenging due to comparably low yields & titers, and comparably high downstream processing- as well as raw material costs. These hurdles are also present in production processes for rhamnolipids (RLs) which are among the best studied biosurfactants and natively produced in *Pseudomonas aeruginosa*. The pathogenicity and a complex quorum sensing mechanism regulating RL synthesis, make production in the native host undesirable. The close relative *Pseudomonas putida* KT2440 as a non-pathogenic host produces all precursors necessary for RL synthesis. With the transfer of the *rhlAB* genes encoded on the pSynpro8oT vector and constitutive expression of the rhamnosyltransferase 1 the metabolic gap for mono-RL synthesis was bridged. The highest titer reported for heterologous RL production is 14.9 g/L. However, biomass generation, as a large carbon sink, was a significant drawback in this

process with roughly 50% more biomass than product produced. This problem is addressed in this thesis leveraging temperature as control variable and a molecular temperature sensor, an RNA thermometer (RNAT). RNAT generally refers to secondary loop structures, typically present in the 5' untranslated region of the mRNA, that form at certain temperatures and therefore regulate translation in dependence of temperature. Usually RNATs mask the Shine-Dalgarno sequence or ribosome binding site and thus influence translation. When thermal energy is introduced into the system, the hydrogen bonds between the base pairs in the loop structure are destabilized, the secondary structure regresses, ribosomes can attach, and translation can take place. The ROSE (repression of heat shock gene expression) RNAT evaluated in the first original research article in the heterologous system *P. putida* KT2440 pSynpro8oT_*rhlAB* originates from *P. aeruginosa*. The ROSE element regulates, in dependence of ambient temperature, the translation of rhlA and via a polar effect also the translation of rhlB therefore indirectly RL synthesis. It was found that in the ROSE RNAT-controlled system, the RL production rate was 60% higher at cultivations of 37°C than at 30°C. However, besides the regulatory effect of the RNAT, as revealed by control experiments, multiple unspecific metabolic effects may be equally responsible for the increase in production rate. This first article marked an important step for the utilization of molecular temperature responsive elements as control units for temperature-based process design and control. After screening for even more efficient regulatory structures, a fourU RNAT was identified. Natively, this fourU RNAT regulates the expression of the small heat shock gene *agsA* of *Salmonella enterica* and its regulatory capability can easily be modified by site-directed mutagenesis. The experimental data collected in the second original research article confirms the functionality of the fourU RNAT in the heterologous RL production system. The data suggested improved regulatory capabilities of the fourU RNAT compared to the ROSE element and a major effect of temperature on RL production rates and yields. The average RL production rate increased by a factor of 11 between 25°C and 38°C. Control experiments confirmed that a major part of this increase originates from the regulatory effect of the fourU RNAT rather than from an unspecific metabolic effect. With this system $Y_{P/X}$ values well above 1 (about 1.4 g_{RL}/g_{BM}) could be achieved mitigating the problem of high biomass formation compared to product synthesis. Also $Y_{P/S}$ values of about 0.2 g_{RL}/g_{Glc} at elevated temperatures of 37-38°C were reached in shake flasks. The system was subsequently tested in a proof-of-concept bioreactor process involving a temperature switch. With this simple batch experiment and a temperature switch from 25°C to 38°C not only a partial decoupling of biomass formation from product synthesis was achieved but also an around 25% higher average specific rhamnolipid production rate reached compared to the so far best performing heterologous RL production process reported in literature (average specific production rate: 24 mg/(g h) vs. 32 mg/(g h)). This supports the potential to leverage temperature as control variable in combination with a functional RNAT e.g., to substitute (often expensive) chemical inducers. However, to achieve higher titers while reducing side product formation a suitable feeding strategy and more complex temperature profiles may be required. Temperature variations in turn cause several metabolic changes, many of which are complex and interdependent. Models that

describe biological processes as a function of temperature are thus essential for improved process understanding. The goal of the peer reviewed review article "Modeling and Exploiting Microbial Temperature Response", shown in this thesis, was to present an overview of various temperature models, aid comprehension of model intent and to facilitate selection and application. Since not all metabolic interdependencies and mechanisms during temperature variation are known for the reasonable connection of input-output relationships, a suitable modeling approach seemed to be neural networks. Neural networks as black box models do not require mechanistic *a priori* knowledge but representative historic datasets. The training of such a neural network was initiated during this thesis. In order to collect training data, different temperature profiles or constant temperatures for a bioreactor process with *P. putida* KT2440 pSynpro8oT_*rhlAB* were applied and concentration curves for biomass, glucose and RL recorded. Subsequently, the data was fed into the neural network to compute RL titer as output. An exponential temperature profile yielded at the highest RL value of approx. 9 g (around 13 g/L) less biomass (around 12 g/L) than product. These values were reached after only 30 h consuming just 45 g of glucose. Hence, at this timepoint 36 weight-% of the consumed glucose could be assigned to mono-RL ($Y_{P/S}$ = 0.19 g_{RL}/g_{Glc}) and biomass ($Y_{X/S}$ = 0.17 g_{BM}/g_{Glc}). The literature value for the theoretically possible maximum yield (Y_{max}) for mono-RL (Rha-C_{10}-C_{10}) from glucose (catabolism via Entner-Doudoroff-pathway) based on ATP-energy balancing is approximately 0.48 g_{RL}/g_{Glc} however i.a. absence of cell growth and no by-product formation was assumed. Hence 40% of Y_{max} was achieved in the mentioned process, using an exponential temperature profile. The so far best performing heterologous RL production process, yielded 23.2 g (14.9 g/L) mono-RL from >250 g of consumed glucose ($\sim$ $Y_{P/S}$ = 0.10 g_{RL}/g_{Glc} $\approx$ 21% of Y_{max}) in >70 h using the same strain and medium but a constant temperature of 30°C. This again supports the potential of exploiting temperature as a control variable by actively incorporating smart temperature variations in the process thereby increasing yields and time efficiency. Only a few (industrial) processes use temperature in process control or -optimization and none exploit RNATs in combination with temperature shifts for industrially relevant products like RLs as reported in this thesis.

In conclusion, an RNAT-controlled and temperature-dependent product formation was established using the example of RL synthesis in *P. putida* KT2440 pSynpro8oT_*rhlAB*. It was found that the type of RNAT used, and the host system are crucial for achieving an optimal separation of growth (30–32°C, *P. putida* KT2440) and product formation (37–38°C, RL). With a bioreactor process, partial decoupling of biomass growth and product formation was achieved. The potential for a more efficient process design was demonstrated, with increased yields and increased product formation rates. Data collection and training of an artificial neural network, to be used as an optional tool for future process optimization, was initiated. RNATs are functionally interchangeable between species and can be used with simple standard bioreactor peripherals. No additional probes or pumps are required, simply a temperature probe and suitable temperature control. These characteristics predestine the use of RNATs as molecular control switches in a bioprocess.

Zusammenfassung

"Es gibt nur einen Planeten Erde, aber bis 2050 wird die Welt so viel verbrauchen, als gäbe es drei" - Die Europäische Kommission, 2020. Im 21. Jahrhundert steht die Menschheit vor einer Reihe von Herausforderungen, darunter eine schnell wachsende Weltbevölkerung, begrenzte fossile Erdölressourcen, der Klimawandel und damit zusammenhängende Probleme wie die steigende Nachfrage nach Nahrungsmitteln, Brennstoffen, Textilien und Futtermitteln. Die eingangs zitierte Erklärung der Europäischen Kommission, die von den Zielen für nachhaltige Entwicklung (SDGs) der Vereinten Nationen unterstützt wird, weist auf die Dringlichkeit eines Übergangs von einer linearen Wirtschaftsform zu einer Kreislaufwirtschaft hin. Das Wirtschaftswachstum muss von der Umweltbelastung entkoppelt werden, wodurch die Ressourceneffizienz verbessert und die Menschen zu einem nachhaltigeren Leben ermutigt werden sollen. Ein Bestandteil der SDGs der UN ist die Nutzung erneuerbarer Ressourcen für nachhaltige Industrieprodukte. Die vorliegende Arbeit stellt einen Mosaikstein für das letztgenannte Ziel dar. Es wird ein Bioprozess mit neuartigem Prozessdesign für die nachhaltige Produktion von Biotensiden auf Basis nachwachsender Rohstoffe vorgestellt. Im Jahr 2017 wurde der weltweite Tensidmarkt mit 43,6 $ Milliarden bewertet und wird bis 2025 voraussichtlich auf 66,4 $ Milliarden expandieren, was einer durchschnittlichen jährlichen Wachstumsrate von 5,4% (2018 - 2025) entspricht. Ein großer Anteil der, im Handel erhältlichen, Tenside werden aus petrochemischen oder oleochemischen Quellen gewonnen. Rohstoffe (z. B. 4-Nonylphenol), die für die chemische Synthese dieser Tenside verwendet werden, weisen eine hohe Toxizität für Mensch und Umwelt sowie eine geringe biologische Abbaubarkeit auf bzw. haben ungünstige soziale und ökologische Folgewirkungen, wie im Falle von Palmöl. Heutzutage treiben das Verbraucherbewusstsein und die Umweltgesetzgebung den Übergang zu nachhaltigen und umweltfreundlichen Verfahren voran. Daher wird die Produktion von mikrobiellen Biotensiden (im Folgenden Biotenside genannt) auf der Basis erneuerbarer Substrate für die Industrie immer attraktiver. Einerseits weisen Biotenside vorteilhafte Eigenschaften wie geringe Toxizität, biologische Abbaubarkeit, Stabilität bei extremen Umgebungsbedingungen (pH-Wert, Temperatur, Salzgehalt) und hohe Tensidwirkung auf. Andererseits ist die wirtschaftliche Herstellung von Biotensiden eine Herausforderung, da die Ausbeuten vergleichsweise gering, und die Aufbereitungs- sowie die Rohstoffkosten vergleichsweise hoch sind. Diese Hürden bestehen auch bei den Produktionsverfahren für Rhamnolipide (RL), die zu den am besten untersuchten Biotensiden gehören und ursprünglich in *Pseudomonas aeruginosa* produziert wurden. Die Pathogenität und ein kom-

plexer Quorum-Sensing-Mechanismus, der die RL-Synthese reguliert, machen die Produktion im nativen Wirt unattraktiv. Der nahe Verwandte *Pseudomonas putida* KT2440 als nicht-pathogener Wirt produziert bereits alle für die RL-Synthese notwendigen Ausgangsstoffe. Mit dem Transfer der *rhlAB*-Gene in den pSynpro8oT-Vektor und der konstitutiven Expression der Rhamnosyltransferase 1 wurde die metabolische Lücke für die Mono-RL-Synthese überbrückt. Der höchste bisher berichtete Titer für die heterologe RL-Produktion liegt bei 14,9 g/L. Die Bildung von Biomasse als erhebliche Kohlenstoffsenke war jedoch ein wesentlicher Nachteil dieses Prozesses, da etwa 50% mehr Biomasse als Produkt gebildet wurde. Dieses Problem wird in dieser Arbeit durch den Einsatz der Temperatur als Kontrollgröße und eines molekularen Temperatursensors, eines RNA Thermometers (RNAT), adressiert. RNAT bezieht sich im Allgemeinen auf sekundäre Schleifen Strukturen, die sich typischerweise in der 5'-untranslatierten Region der mRNA befinden, sich bei bestimmten Temperaturen ausbilden und die Translation in Abhängigkeit dieser regulieren können. Normalerweise maskieren RNAT in ihrer Funktion als regulatorisches Element die Shine-Dalgarno-Sequenz oder die Ribosomen-Bindungsstelle und beeinflussen so die Translation. Wird thermische Energie in das System eingebracht, werden die Wasserstoffbrücken zwischen den Basenpaaren in der Schleifenstruktur destabilisiert, die Sekundärstruktur bildet sich zurück, Ribosomen können binden und die Translation beginnt. Das im ersten Forschungsartikel dieser kumulativen Arbeit untersuchten ROSE (repression of heat shock gene expression) RNAT im heterologen System *Pseudomonas putida* KT2440 pSynpro8oT_*rhlAB* stammt aus *P. aeruginosa*. Das ROSE-Element reguliert in Abhängigkeit von der Umgebungstemperatur die Translation von rhlA, über einen polaren Effekt auch die Translation von rhlB und damit indirekt die RL-Synthese. Es wurde festgestellt, dass im ROSE-RNAT gesteuerten System eine um 60% erhöhte RL-Produktionsrate bei einer Kultivierungstemperatur von 37°C im Vergleich zu 30°C vorlag. Neben der regulatorischen Wirkung des RNATs, die sich in den Kontrollexperimenten zeigte, könnten jedoch auch mehrere unspezifische Stoffwechseleffekte für die Erhöhung der Produktionsrate verantwortlich sein. Dieser erste Artikel markierte einen wichtigen Schritt für die Nutzung von molekularen temperaturabhängigen Elementen als Steuereinheiten für die temperaturbasierte Prozesskontrolle. Nach einem Screening für noch effizientere regulatorische Strukturen wurde ein fourU-RNAT identifiziert. Dieses fourU-RNAT reguliert nativ die Expression des kleinen Hitzeschockgens *agsA* von *Salmonella enterica* und seine Regulationsfähigkeit kann leicht durch gezielte Substitution einzelner Nukleotide verändert werden. Die experimentellen Daten, die im zweiten Forschungsartikel gesammelt wurden, bestätigen die Funktionalität des fourU-RNATs im heterologen RL-Produktionssystem. Die Daten deuten darauf hin, dass die Temperatur einen wesentlichen Einfluss auf die RL-Produktionsraten sowie Ausbeuten hat und dass das fourU-RNAT im Vergleich zum ROSE-Element verbesserte regulatorische Eigenschaften aufweist. Die durchschnittliche RL-Produktionsrate stieg zwischen 25°C und 38°C um das 11-fache. Kontrollexperimente bestätigten, dass ein Großteil dieses Anstiegs auf die regulatorische Wirkung des fourU-RNATs und nicht auf einen unspezifischen metabolischen Effekt zurückzuführen ist. Mit diesem System konnten $Y_{P/X}$-Werte deutlich über 1 (etwa 1,4 g_{RL}/g_{BM}) erreicht werden, wodurch das Problem der hohen Biomassebildung im Vergleich zur Produktsyn-

these gelöst wurde. Auch $Y_{P/S}$-Werte von etwa 0,2 g_{RL}/g_{Glc} bei erhöhten Temperaturen von 37-38°C wurden in Schüttelkolben erreicht. Das System wurde ferner in einem Proof-of-Concept-Bioreaktorprozess mit einem Temperaturswitch getestet. Bei diesem einfachen Batch-Experiment und einer Temperaturänderung von 25°C auf 38°C wurde nicht nur eine Trennung der Biomassebildung von der Produktsynthese erreicht, sondern auch eine um etwa 25% höhere durchschnittliche spezifische RL-Produktionsrate im Vergleich zu dem bisher besten in der Literatur beschriebenen heterologen RL-Produktionsprozess (mittlere spezifische Produktbildungsrate: 24 mg/(g h) vs. 32 mg/(g h)). Dies spricht für das Potenzial, die Temperatur als Stellgröße in Kombination mit einem funktionellen RNAT zu nutzen, um z. B. den Einsatz (oftmals teurer) chemischer Induktoren zu vermeiden. Um jedoch höhere Titer zu erreichen und gleichzeitig die Bildung von Nebenprodukten zu verringern, sind möglicherweise eine geeignete Fed-Batch-Strategie und komplexere Temperaturprofile erforderlich. Temperaturänderungen bewirken wiederum verschiedene metabolische Veränderungen, von denen viele komplex und voneinander abhängig sind. Modelle, die biologische Prozesse in Abhängigkeit von der Temperatur beschreiben, sind daher für ein besseres Prozessverständnis unerlässlich. Ziel des in dieser Arbeit gezeigten Review-Artikels "Modeling and Exploiting Microbial Temperature Response" war es, einen Überblick über verschiedene Temperaturmodelle zu geben, das Verständnis für die Intention der Modelle zu erleichtern und so die Auswahl und Anwendung zu vereinfachen. Da nicht alle metabolischen Abhängigkeiten und Mechanismen bei Temperaturvariationen für eine sinnvolle Verknüpfung von Input-Output-Beziehungen bekannt sind, schien ein geeigneter Modellierungsansatz die Verwendung neuronaler Netze zu sein. Neuronale Netze als Black-Box-Modelle benötigen kein mechanistisches *a priori* Wissen, sondern repräsentative historische Datensätze. Das Training eines solchen neuronalen Netzes wurde im Rahmen dieser Arbeit begonnen. Um Trainingsdaten zu sammeln, wurden verschiedene Temperaturprofile oder konstante Temperaturen für einen Bioreaktorprozess mit *P. putida* KT2440 pSynpro8oT_*rhlAB* getestet und Konzentrationskurven für Biomasse, Glukose und RL aufgenommen. Anschließend wurden die Daten in das neuronale Netz eingespeist, um den RL-Titer als Ausgabe zu berechnen. Ein exponentielles Temperaturprofil ergab beim höchsten RL-Wert von ca. 9 g (ca. 13 g/L) weniger Biomasse (ca. 12 g/L) als Produkt. Diese Werte wurden nach nur 30 Stunden erreicht, in denen lediglich 45 g Glukose verbraucht wurden. Somit konnten zu diesem Zeitpunkt 36 Gewichts-% der verbrauchten Glukose dem Mono-RL ($Y_{P/S}$ = 0,19 g_{RL}/g_{Glc}) und der Biomasse ($Y_{X/S}$ = 0,17 g_{BM}/g_{Glc}) zugeordnet werden. Der Literaturwert für die theoretisch mögliche Maximalausbeute (Y_{max}) für Mono-RL (Rha-C_{10}-C_{10}) aus Glukose (Katabolismus über den Entner-Doudoroff-Weg), welcher auf ATP-Energie-Bilanzierung basiert, liegt annäherungsweise bei 0,48 g_{RL}/g_{Glc}. Dabei wurde allerdings u. a. weder Zellwachstum noch Nebenproduktbildung berücksichtigt. Somit wurden 40% von Y_{max} in dem oben aufgeführten Prozess mit exponentiellem Temperaturprofil erreicht. Der bisher beste heterologe RL-Produktionsprozess lieferte 23,2 g (14,9 g/L) Mono-RL aus >250 g verbrauchter Glukose ($\sim Y_{P/S}$ = 0,10 $g_{RL}/g_{Glc} \approx$ 21% von Y_{max}) in >70 h wobei der gleiche Stamm und das gleiche Medium, aber eine konstante Temperatur von 30°C verwendet wurden. Dies unterstreicht erneut das Potenzial der Nutzung der Temperatur als Stellgröße durch

die aktive Einbeziehung intelligenter Temperaturänderungen in den Prozess, wodurch Ausbeute und Zeiteffizienz gesteigert werden. Nur wenige (industrielle) Prozesse Temperatur zur Prozesssteuerung oder -optimierung und kein bekannter Prozess verwendet RNAT in Kombination mit Temperaturänderungen für industriell relevante Produkte wie RL, wie in dieser Arbeit beschrieben.

Zusammenfassend wurde eine RNAT-gesteuerte und temperaturabhängige Produktbildung am Beispiel der RL-Synthese in *Pseudomonas putida* KT2440 pSynpro8oT_*rhlAB* in dieser Arbeit etabliert. Es wurde festgestellt, dass die Art des verwendeten RNATs und des Hostsystems entscheidend sind für eine optimal Trennung von Wachstum (30-32°C, *P. putida* KT2440) und Produktbildung (37-38°C, RL). Mit einem Bioreaktorprozess konnte eine teilweise Entkopplung von Biomassewachstum und Produktbildung erreicht werden. Das Potenzial für ein effizienteres Prozessdesign wurde aufgezeigt, wobei erhöhte Ausbeuten und Produktbildungsraten möglich sind. Es wurde mit der Trainingsdaten-Sammlung und dem Training eines künstlichen neuronalen Netzes begonnen, das als optionales Werkzeug für die künftige Prozessoptimierung verwendet werden kann. Die RNAT sind funktionell zwischen verschiedenen Spezies austauschbar und können mit einfacher Standard-Bioreaktorperipherie verwendet werden. Es sind keine zusätzlichen Sonden oder Pumpen erforderlich, sondern lediglich eine Temperatursonde und eine geeignete Temperaturregelung. Diese Eigenschaften prädestinieren RNAT für den Einsatz als molekulare Schalter in Bioprozessen.

Contents

Part I

General Introduction

1. Circular economy & biosurfactants

1.1 Circular economy

"There is only one planet Earth, yet by 2050, the world will be consuming as if there were three" [European Commission 2020]. Humanity will face a number of challenges in the twenty-first century, including a growing global population, limited fossil oil resources, climate change, and related issues such as increased demand for food, fuel, fiber, and feed [United Nations 2017]. In the next forty years, global consumption of commodities such as biomass, minerals & metals and fossil fuels is projected to double, while 3.40 billion tons of waste are generated annually by 2050 compared to 2.01 billion tons today [OECD 2019; Kaza *et al.* 2018; European Commission 2020]. According to the most recent estimates, the global population will reach 8.5 billion in 2030 and 9.7 billion in 2050 [United Nations 2019]. The presented challenges of the twenty-first century can be addressed by changing from the conventional linear economy to an alternative economic system – the circular economy. This alternativ form of economy is defined by the European parliament as follows:

"The circular economy is a model of production and consumption, which involves sharing, leasing, reusing, repairing, refurbishing and recycling existing materials and products as long as possible. In this way, the life cycle of products is extended."

- The European Parliament 2015

When it comes to sustainable consumption and production, the circular economy is about doing more with less. It is about separating economic growth from environmental damage, optimizing resource efficiency and encouraging people to live more sustainably [United Nations 2015a]. To tackle the current challenges, 17 critical main Sustainable Development Goals (SDGs) are defined by the United Nations including subgoals like worldwide food safety, sustainable farming methods, clean energy, reduction of greenhouse gas emissions and use of renewable resources for sustainable industrial products [United Nations 2015b]. This thesis represents a mosaic stone for the latter goal. The fundamental feasibility of a novel approach is presented for the production of a biosurfactant based on renewable resources.

1.2 Biosurfactants

Biosurfactants (BS) are surface-active, amphipathic molecules due to their composition of ≥1 hydrophilic and ≥1 hydrophobic moiety. The hydrophobic part usually consists of (hydroxy-) fatty acids with a chain length between 8 to 18 carbon atoms. The hydrophilic counterpart may exhibit carboxylate or phosphate groups, mono-, oligo- or polysaccharides, amino acids or peptides [Lang *et al.* 1999]. Most commercially available surfactants are derived from petrochemical or oleo-chemical sources. Some raw materials (e.g. the alkylphenol, 4-Nonylphenol) used for the chemical synthesis of these surfactants display human- and environmental toxicity as well as low biodegradability [Li *et al.* 2013; Van Bogaert *et al.* 2007] respectively have an opposing social- and environmental impact as in the case of palm oil [Meijaard *et al.* 2020]. Hence a growing number of successful applications either by replacing conventional surfactants or by opening new industrial areas due to specific BS activity have recently been reported and summarized [Banat *et al.* 2020]. In nowadays, consumer awareness and environmental legislation drive a transition towards sustainable and eco-friendly processes. Hence the production of BS based on renewable substrates in a sustainable way intensifies BS' attractivity for industry. In 2017, the worldwide surfactant market was valued with 43.6 $ billion and is expected to increase to 66.4 $ billion by 2025, corresponding to a compound annual growth rate of 5.4% (2018 – 2025) [Banat *et al.* 2020]. The exact value of the small share of BSs on the global surfactants market, on the other hand, remains unknown. This is due to incorrect and indiscriminate use of the term "biosurfactant" in market research reports [Banat *et al.* 2020]. The potential applications of BS are manifold. They may be used in the pharmaceutical sector (bactericides, fungicides, virucides) [Gaur *et al.* 2020; L. Jin *et al.* 2021; Crouzet *et al.* 2020], the cosmetic sector (personal care products) [Vecino *et al.* 2017], the food sector (emulsifiers or stabilizers) [Nitschke *et al.* 2007], bioremediation [Sáenz-Marta *et al.* 2015], microbial enhanced oil recovery [Banat 1995] and in household detergent formulations [El-Khordagui *et al.* 2021]. The beneficial properties of BS compared with their petrochemical competitors range from lower toxicity, higher biodegradability, stability at extreme ambient conditions (pH, temperature, salinity) to high surfactant efficiencies [Desai *et al.* 1997]. Unlike BS, chemically synthesized surfactants are produced at relatively low costs and are available in large quantities [Helmy *et al.* 2011]. It was recently suggested that using solid state fermentation can mitigate some of the challenges present in conventional submerged production of BS like foaming, contamination or in some cases lower titers and yields [El-Housseiny *et al.* 2019; Nene *et al.* 2020; Krieger *et al.* 2010]. To make BS more compatible and attractive for industrial exploitation, titers must be increased, overall production costs must be low, and technical limitations of downstream processing overcome [Banat *et al.* 2020; Helmy *et al.* 2011]. Partly responsible for these obstacles is the still relatively high production of biomass (roughly 50% more biomass than product), as a large carbon sink in the heterologous RL production process [Beuker *et al.* 2016a]. In this thesis an RNA thermometer and elevated temperatures (∼37-38°C) are used to effectively channel substrate carbon into the product, while keeping biomass concentration low, allowing $Y_{P/X}$ values well above 1 (about 1.4 g_{RL}/g_{BM}).

1.3 Rhamnolipids

1.3.1 Discovery & economics

Rhamnolipids (RLs) are biosurfactants and were first discussed in 1946 [Bergström *et al.* 1946]. Mono- respectively Di-RLs are glycolipids composed of 1 or 2 α-L-rhamnose and 1–3 hydroxy alkanoic acid chains (8–16 carbons) with around 60 known congeners or homologues reported [Lang *et al.* 1999; Abdel-Mawgoud *et al.* 2010]. Their structure was originally discovered in 1949 and examined in a *Pseudomonas aeruginosa* sample [Jarvis *et al.* 1949]. The figure below shows the timeline of RLs in research from discovery to the recent commercialization and planned industrial scale manufacturing by Evonik Industries (Essen, Germany) [Evonik Industries AG 2016; Evonik Industries AG 2022].

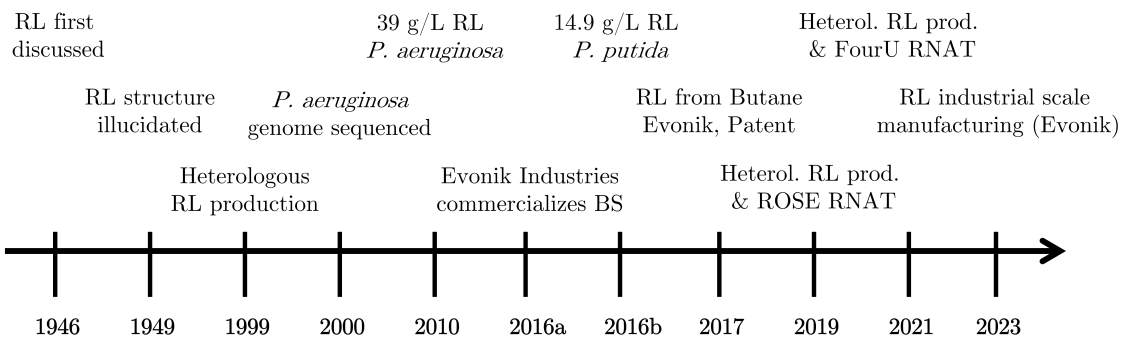

Figure 1.1: Timeline of important events for rhamnolipid (RL) biosurfactant (BS) in research from discovery to the recent commercialization by Evonik Industries [Bergström *et al.* 1946; Jarvis *et al.* 1949; Ochsner *et al.* 1995; Stover *et al.* 2000; Müller *et al.* 2010; Evonik Industries AG 2016; Beuker *et al.* 2016a; Thum *et al.* 2017; Noll *et al.* 2019; Noll *et al.* 2021; Evonik Industries AG 2022].

Recently the challenges of a RL production have been summarized [Chong *et al.* 2017]. Synthetic surfactants cost 1—3 $/kg, whereas rhamnolipids cost 20—25 $/kg, depending on the production scale [Lang *et al.* 1999]. So far, only using rhamnolipids in the preparation of high-priced goods such as cosmetics and pharmaceuticals in low volumes justifies the costs of a microbial fermentation [Makkar *et al.* 2002]. The three main factors that lead to the increased cost of BS production are (i) raw material costs, (ii) low BS yield by microorganisms, and (iii) downstream processing costs. Initial raw material costs are anticipated to account for about 10–30% overall cost of BS production. To overcome this obstacle several attempts have been made to produce BSs on low-cost substrates as summarized and analyzed before. The hypothetically cheapest substrate per kg Di-RL produced was reported to be stearic acid with 80–100 € per ton substrate hypothetically yielding 0.06–0.08 € substrate costs per kg Di-RL [Henkel *et al.* 2012].

1.3.2 Production hosts & commercialization

The native production organism *P. aeruginosa* has two drawbacks that make it undesirable for (commercial) RL synthesis. First, *P. aeruginosa* is an opportunistic human pathogen causing lung diseases [Williams *et al.* 2010]. Second, a regulation mechanism for RL production, quorum sensing complicates production and bioprocess design. Quorum sensing is a cell density-based control mechanism which aggravates efficient process design [Beuker *et al.* 2016b]. In 2009 orthologs of *rhlA*, *rhlB* and *rhlC* were reported in *Burkholderia thailandensis* a non-pathogenic organism able to produce RLs [Dubeau *et al.* 2009]. Also heterologous RL production systems were tested to resolve the drawbacks found in *P. aeruginosa* [Ochsner *et al.* 1995]. The close relative *Pseudomonas putida* as a heterologous host produced already both precursors dTDP-L-rhamnose and HAA (3-hydroxyalkanylalkanoate) needed for RL synthesis and comparably high RL titers after introduction of the missing genes. In 2016, the pBBR1MCS-3-based plasmid pSynpro8oT was used to transfer the *rhlAB* genes from *P. aeruginosa* into the nonpathogenic host *P. putida* KT2440. With the resulting constitutive expression of the rhamnosyl transferase genes (*rhlAB*) the metabolic gap for heterologous mono-RL production in *P. putida* KT2440 was bridged. In the same year a maximum of 14.9 g/L RL were produced in a fed batch process with model-based two-phase glucose feeding profile [Beuker *et al.* 2016a]. This titer for heterologous RL production has so far not been exceeded. However, heterologous RL production can still not compete with the titer (around 40 g/L) achieved by conventional production strains such as *P. aeruginosa* PAO1 [Müller *et al.* 2010]. A patent filed in 1997 claimed titers between 70-120 g/L RL produced by *P. aeruginosa*. This patent expired fee related in 2013 and the claimed titers could not be reached nor were reported elsewhere in literature. Furthermore, critical details like the applied quantification method are missing [Giani *et al.* 1997]. Yet, patents from recent years and the recent commercialization by Evonik Industries are indicative for the significance of rhamnolipids as industrial biotechnology products [Schafer *et al.* 2011; Schilling *et al.* 2013; Evonik Industries AG 2016].

1.3.3 Downstream processing & substrates

The downstream processing expenses typically account for 50–80% of the total production costs [Mnif *et al.* 2016; Thavasi *et al.* 2018]. The used purification methods for rhamnolipids have been summarized before [Heyd *et al.* 2008; Eslami *et al.* 2020]. For pure RL crystals the solvent extraction may be followed by (re)crystallization respectively chromatographic purification [Pajarron *et al.* 1993]. Ultrafiltration is yet another option to retain RL micelles when a membrane cutoff of 10 kDa is used [Mulligan *et al.* 1990]. Other methods include combinations of ammonium sulfate or acid precipitation and centrifugation and/or solvent extraction [Heyd *et al.* 2008; Schenk *et al.* 1995]. Furthermore, an integrated foam fractionation was proposed to be used during the fermentation process to separate rhamnolipids [Beuker *et al.* 2016b]. The production of RLs on different substrates was summarzied and compared to theoretically calculated maximum yields [Henkel *et al.* 2012]. The authors found experimentally achieved yields ranging from 0.058 (olive oil mill effluent)

over 0.06–0.11 (Glucose) to 0.62 (Soybean oil) $g_{RL}/g_{Substrate}$. This contrasts with the theoretically estimated maximum RL yields. The theoretical yields were calculated "assuming energy-limitation, no by-products, no cell-growth and the absence of other limiting factors (oxygen/carbon limitation, carbon limitation, redox-equivalents) and disregarding maintenance metabolism". Estimated yields ranged from 0.51 (Hemicellulose (Arabinose, Xylose)) over 0.52 (Glucose from vegetable starch) to 1.26 (stearic acid) $g_{RL}/g_{Substrate}$ [Henkel *et al.* 2012]. As indicated by these assumptions, there are some carbon sinks which claim substrate carbon, thus reducing product yields and at the same time potentially raising the costs to produce RLs. The so far best performing heterologous RL production process with a two-phase glucose feeding profile achieved a maximum concentration of 14.9 g/L RL. However, biomass generation, as a large carbon sink, was a significant drawback in this process with roughly 50% more biomass than product produced [Beuker *et al.* 2016a]. In this thesis it was shown that the ratio of product to biomass can be shifted in favor of the product by using an RNA thermometer and elevated temperatures (∼37–38°C). Thereby $Y_{P/X}$ values well above 1 (about 1.4 g_{RL}/g_{BM}) could be achieved.

2. Temperature sensing & response

2.1 Introduction

Bioprocesses are generally quite sensitive to most changes in the environment. Therefore temperature, pO_2, and pH, for example, are typically controlled at a narrow optimum. Deviations from the optimum values can result in a significant drop in total bioprocess productivity and influence repeatability [Hausmann *et al.* 2017]. Microorganisms in their natural habitat are usually exposed to a dynamic environment. This includes variations in pH, nutrient availability, and heightened or decreased temperature, among other factors. Especially temperature is a sensitive parameter for the survival of microorganisms as it affects the functionality of biomolecules like enzymes and, connected to that, metabolic reaction rate. The evolutionary development of temperature sensors for the detection of- and mechanisms for adaptation to temperature fluctuations was therefore crucial for the permanence of life forms. Since structure, stability and functionality of most biomolecules can be influenced by temperature, DNA, RNA, proteins, and lipids can be potential molecular thermosensors. An extensive review on microbial thermosensing was provided [Klinkert *et al.* 2009]. This chapter provides an overview of the effects of temperature on microbial metabolism and evolved coping mechanisms for non-physiological temperatures and outlines different ways on how temperature can be sensed. Furthermore, the potential of temperature as a control variable for industrial bioprocesses is highlighted.

2.2 Temperature changes and coping mechanisms

Prokaryotic life has been reported over a range of 127°C (-5°C – +122°C). This covers psychrophiles, mesophiles, thermophiles, and hyperthermophiles proliferating at temperatures ranging from -5°C (at high salinity, ∼24%, *Marinobacter* / *Halomonas*) to +122°C (at high pressure, 20 MPa, *Methanopyrus kandleri* strain 116) [Niederberger *et al.* 2010; Takai *et al.* 2008; Corkrey *et al.* 2014]. Temperature in those habitats is not always constant and can fluctuate. To deal with these fluctuations and survive potentially harmful environmental temperatures, microorganisms have developed a range of protective coping mechanisms. To deal with rapid drops or increases in ambient temperature, cold or heat-shock proteins can be expressed for example. A constant exposure (around 2000 generations) to suboptimal temperature in turn can lead to a more complex

adaptation and to a change in the overall performance optimum as reported for *E. coli* [Bennett *et al.* 1993]. However, the thermal niche breadth (see figure below) remained unchanged. This translates into a reshaped thermal growth curve in this example, with the same upper- and lower bounds but different thermal optima (greatest mean fitness relativ to ancestors) [Bennett *et al.* 1993].

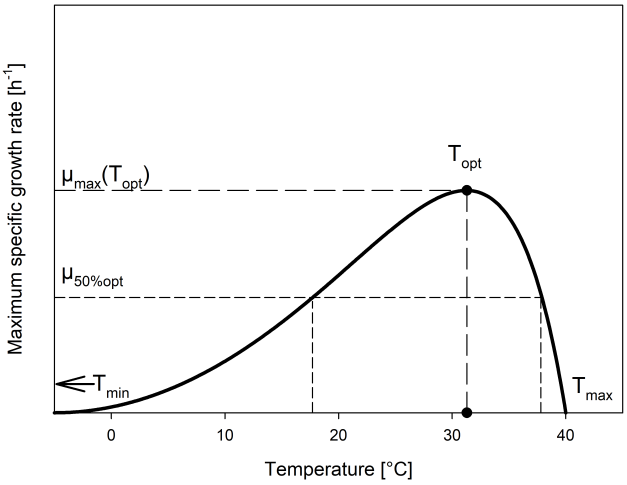

Figure 2.1: The temperature (°C) is plotted against the growth rate (h^{-1}) in this diagram of the thermal growth curve. Cardinal temperatures marking the lower and upper boundaries as well as the performance optimum of the thermal niche (T_{min}, T_{opt}, and T_{max}) are shown [adapted from Noll *et al.* 2020b]

.

2.3 Cold shock response

A cold shock occurs when the ambient temperature drops sharply (e.g., 37°C to 15°C). It was hypothesized that the cold shock response takes place in 3 stages, (i) acclimatization phase, (ii) recovery phase and (iii) stationary phase [M. H. Weber *et al.* 2003]. Structural changes of biomolecules occur during cold shock, which a bacterial cell must counteract with an adequate response. These structural changes and its consequences may include the reduction of membrane fluidity, hinderance of translation by rigid RNA structures and affect molecular dynamics as dictated by the law of Arrhenius [Arrhenius 1889] where the velocity of (enzyme-catalyzed) biochemical reactions is exponentially decreased [M. H. Weber *et al.* 2003; Arrhenius 1889]. After a cold shock, the synthesis of a series of proteins is induced to reduce potential damage and maintain an active metabolism. The produced cold shock proteins can interact directly or indirectly with nucleic acids. They primarily include nucleases, helicases and ribosome-associated components. Whereas, no alternative sigma factor is known which controls the cold shock response as in the case of the alternative sigma factor 32 (σ^{32}) during heat shock [M. H. Weber *et al.* 2003]. Other cold shock related reactions involve adaptation of the cellular membrane by so called homeoviscous adaption. The membrane is involved in energy generation, transport and cell division. During adaptation, short fatty acids with low melting points are embedded in the membrane to maintain membrane integrity and function

[Sinensky 1974]. During cold shock, the translational machinery of a cell may be modified. This can for example happen in form of interference of elongation by inter-ribosomal secondary mRNA structures [M. H. Weber *et al.* 2003]. Temperature reduction was also reported to be a decisive signal for plant pathogens like *Pseudomonas* or *Erwinia*. These organisms were found to cause the "cold weather" disease as a result of host invasion with subsequent activation of virulence gene expression upon cold shock. The synthesis of the virulence factor INA by *P. syringae* during cold shock promotes ice-crystal formation at plant leaves. The ice crystals in turn contribute to the breach of the membrane envelope of the plant cells and cause the release of nutrients which the bacterium needs for its growth [Smirnova *et al.* 2001; Lanham *et al.* 1991; Cochet *et al.* 2000].

2.4 Heat shock & high temperature response

The heat shock response of *E. coli* is a widely studied example of metabolic adaptation to external heat stress. During heat shock (30 to 42°C), genome-wide analyses revealed that almost 130 genes are up-regulated and initially up to 20 different heat shock proteins (HSPs) are overproduced up to 15-fold. The global regulator and alternative sigma factor σ^{32} guides the RNA polymerase to heat shock promotors resulting in elevated heat shock gene expression. Other HSPs are involved in protein degradation and repair (proteases e.g. ClpB and chaperones e.g. HtpG), energy and intermediary metabolism (e.g. GapA), DNA-replication, repair and modification (e.g. Mfd and TopA) as well as other heat shock related but non-classified proteins [Arsène *et al.* 2000; Zhao *et al.* 2005]. A change in ambient temperature can also mean the successful invasion of a host. In contrast to the non-physiological heat shock temperature and its response, ambient temperature after host invasion is in the physiological range for mesophilic bacterial growth. The response of this moderate temperature change needs to be distinguished from heat shock conditions. It may therefore be referred to as "high temperature response". Human pathogens, for example change their metabolism due to the usually moderately increased temperature of the host (37°C) compared to ambient temperature resulting in the induction of virulence genes. *Pseudomonas aeruginosa* as an example for an opportunistic human pathogen, produces the virulence factor rhamnolipid (RL). RLs are described to permeabilize respiratory epithelial cells by altering tight junctions which facilitates the invasion of host cells [Grosso-Becerra *et al.* 2014; Zulianello *et al.* 2006]. As shown by the aforementioned necessary responsive actions to cold shock, heat shock or host invasion, cellular survival depends on the capability of a timely detection of incoming temperature stimuli to induce the appropriate metabolic response. Now the key question arises:

- How is temperature sensed by microorganisms? –

2.5 Molecular thermosensors

The figure below shows selected examples of different mechanisms of molecular temperature sensing discussed in this section. These examples include DNA (2.5.1), Protein (2.5.2), Membrane (2.5.3) and RNA sensors (2.5.4).

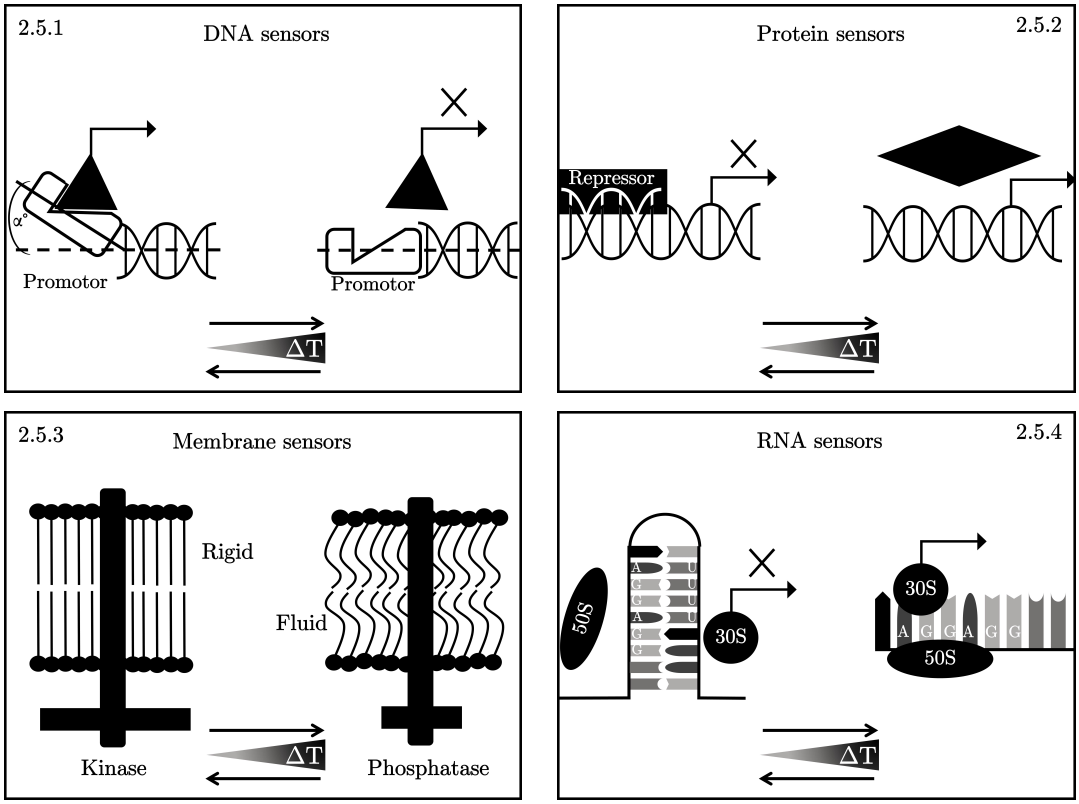

Figure 2.2: Selected examples for different mechanisms of molecular temperature sensing in a prokaryotic cell including DNA (2.5.1), protein (2.5.2), membrane (2.5.3) and RNA sensors (2.5.4). From L–R: Bended DNA at low temperatures improving affinity for RNA polymerase in *Clostridium perfringens*; conformational change upon temperature increase of specific repressor RheA for the *hsp18* gene of *Streptomyces albus*; temperature and membrane fluidity dependent change of DesK Kinase/Phosphatase activity of *Bacillus subtilis* involved in modulation of response regulator DesR; temperature dependent conformational change of a fourU RNA thermometer controlling small heat shock gene *agsA* expression in *Salmonella enterica* [Katayama *et al.* 1999; Servant *et al.* 2000; Abriata *et al.* 2017; Waldminghaus *et al.* 2007b; Uniprot Databse – P0A6Y8 2007; Uniprot Database – O34757 1998].

2.5.1 DNA sensors

The transcriptional machinerys' access to DNA is critical for transferring genetic information from RNA to a protein, and it is temperature sensitive [Klinkert *et al.* 2009]. Temperature changes are mostly reported to alter DNA accessibility in two ways. First, global (supercoiling) respectively local (DNA curvature) DNA topology can be affected. Second, temperature changes trigger the

development and the binding of transcription repressing histone-like nucleoid structuring protein. These actions ultimately effect gene expression and attribute temperature-sensing properties to the DNA itself [Shapiro *et al.* 2012].

DNA supercoiling

In its right-handed relaxed B form one helical turn of the DNA duplex contains 10.5 base pairs. Positive supercoiling occurs when the number of turns is increased whereby the axis of the helix winds around itself to maintain a minimal energy conformation. The opposite effect, negative supercoiling occurs when turns are removed [Sinden 1994; Dorman 2019]. Isolated plasmid DNA is commonly used by most studies as a reference for determining global DNA topology. But since DNA-binding proteins limit DNA supercoiling, plasmid topology can only be utilized as a rough estimate for global chromosomal supercoiling respectively local DNA structures [López-García *et al.* 2000]. The plasmid DNA of mesophilic bacteria usually reported to be negatively supercoiled [Wang 1987] whereas relaxed or positively supercoiled plasmid DNA is commonly found in hyperthermophilic archaea with a growth optimum around 80°C [Forterre *et al.* 1996]. The degree of supercoiling differs and is mainly depending on the organism, chromosomal localization, growth stage, nutrients available and environmental factors such as temperature [Lal *et al.* 2016; Klinkert *et al.* 2009]. For mesophiles (e.g. in *E. coli*) [López-García *et al.* 2000; Mizushima *et al.* 1997] and hyperthermophiles (*Sulfolobales* & *Thermococcales*) [López-García *et al.* 1997; López-García *et al.* 2000], a temporary increase in positive supercoiling is reported following a heat shock and a temporary increase in negative supercoiling following a cold shock. For returning DNA topography to its initial state after exposure to non-physiological temperatures, positive supercoils can be removed by DNA gyrase, while negative supercoils may be relaxed by DNA topoisomerases I and/or IV. The activity of these enzymes in turn is also temperature dependent [Dorman 2019]. Furthermore, the proteins HU (small DNA binding protein) and DnaK (heat shock protein) have been identified to regulate topological changes in DNA in response to temperature [Ogata *et al.* 1996; Ogata *et al.* 1997].

DNA curvature & Histone-like nucleoid structuring proteins

In 2010 it was reported *in vitro* that temperature affects promotor activity and gene expression of a reporter gene solely via DNA curvature alterations [Prosseda *et al.* 2010]. By changing the temperature and a resulting change in DNA curvature transcriptional activity could be increased by a factor of 2.5 relative to unbent DNA [Prosseda *et al.* 2010]. It was also reported that transcriptional activity increases without the participation of trans-acting regulators only by primitive DNA bending at low temperatures e.g. for the α-toxin (phospholipase C gene) of *Clostridium perfrigens* [Katayama *et al.* 1999]. Another element, the histone-like nucleoid structuring protein is reported to repress transcription in a temperature dependent manner. These proteins cause DNA looping and trap the RNA polymerase which hinders its progression and consequently inhibits gene expression as has been reported by multiple studies [Schröder *et al.* 2000; Shin *et al.* 2005;

Lim *et al.* 2012; Kotlajich *et al.* 2015]. Over two thirds of the temperature regulated genes in *E. coli* K-12 and more than 200 of temperature regulated genes in *Salmonella* sp. are reported to be controlled via temperature dependent regulators such as the histone-like nucleoid structuring proteins [Ono *et al.* 2005; White-Ziegler *et al.* 2009].

2.5.2 Protein sensors

Protein (mis)folding and alteration in protein function is a common phenomenon when ambient temperature exceeds the optimal working temperature of a protein. Hence, proteins are well suited for sensing temperature changes because their tertiary respectively quaternary structure is susceptible to temperature changes. Several protein structures have been identified that allow temperature-dependent regulation of various processes. These processes include, protein stability or degradation, transcription, motility, host invasion and signal transduction. Protein structures that play a role in these processes are manifold. They include for example chaperones respectively proteases, global regulators, methyl-accepting chemotaxis proteins (MCPs), and sensor kinases as has been summarized previously [Klinkert *et al.* 2009].

Protein quality control

An interesting example for temperature dependent protein quality control is the protease DegP (HtrA). This hexameric chaperone / (serine) protease is located in the periplasmic space of *E. coli* and *Thermotoga maritima*. Its functional status can be switched between chaperone- (≤ 28°C) and protease activity (≥ 28°C). The protease domain of DegP is inactive in the chaperone conformation resulting in switched off substrate binding and catalysis and vice versa [Rai *et al.* 2015; Krojer *et al.* 2008].

Global regulator

CtsR is a master regulator that inhibits DNA transcription at non permissive temperatures. It was reported to be involved in the regulation of "protein quality control" during heat stress in gram positive bacteria. This is possible due to intrinsic heat sensing capabilities via a glycine rich loop in the global repressor. When temperature is raised to a threshold CtsR dissociates from the DNA and permitts transcription [Elsholz *et al.* 2010].

Methyl-accepting chemotaxis proteins

Methyl-accepting chemotaxis proteins (MCPs) represent a large share of chemoreceptors in bacteria [Zhulin 2001]. They are transmembrane receptors that have a periplasmic ligand-binding domain and a cytosolic signaling domain [Krell *et al.* 2010]. In *E.coli*, the MCPs Trg, Tsr, Tar and Tap sense chemical and temperature gradients. The bacterium can then navigate for example spatial thermal gradients by adjusting flagella motility to either tumble or smooth swimming when heading towards an un-/favorable direction [Sengupta *et al.* 2013]. Amongst the best understood

MCP mechanisms is the Tar transmembrane protein. Depending on whether aspartate is present or absent, Tar acts as a heat or cold sensor. The presence of aspartate and subsequent methylation on, at least one till up to four sites, favors the conversion of Tar from a heat to a cold sensor. This results in an adaptation of the MCP and decreases signaling of CheA (histidine kinase) and CheY (response regulator). The latter two proteins ultimately influence flagellar motor function respectively motility [Sengupta *et al.* 2013; Nishiyama *et al.* 1999; Ottemann *et al.* 1999].

Virulence

In 2011, it was reported that a protein thermometer is involved in motility-dependent host infection by *Listeria monocytogenes*. The foodborn pathogen forms flagella for locomotion outside a host. The flagella also play a role during host invasion, but their formation is repressed at the hosts temperature of 37°C following a successful invasion. The molecular mechanism behind these actions is a temperature-dependent conformational change of the protein thermosensor GamR. Subsequently, this leads to a dissociation of MogR. MogR, dissociated from GamR, represses all flagellar motility genes, as well as the transcription of *gmaR*. The downregulation of flagella motility is in turn necessary for the virulence of *L. monocytogenes* [Kamp *et al.* 2011]. Temperature sensitive usually membrane-associated (histidine) kinases in combination with a cytoplasmic response regulator are involved in temperature response of *Agrobacterium tumefaciens'* virulence. VirA is a temperature sensitive kinase and VirG the respective regulatory element that controls virulence. At temperatures below 32°C, *A. tumefaciens* is reported to be able to induce tumors in plants as a result of active, phosphorylated VirA and VirG. Thereby autophosphorylation of VirA, consecutive transfer of phosphor to VirG and the expression of *vir* gene occur in this two component system [S. Jin *et al.* 1993].

Protein-lipid interaction

The DesK kinase/phosphatase of *Bacillus subtilis* is involved in maintaining an appropriate membrane fluidity at low temperatures by modulating the response regulator DesR. The regulator controls the expression of the *des* gene coding for a Δ5-acyl lipid desaturase which can restore membrane fluidity by introducing *cis* double bonds into acyl chains at the phospholipid membrane. A report from 2017 showed that temperature sensing of DesK most likely depends on the reversible two-helix coiled coil formation of the fifth transmembrane segment and temperature-dependent membrane properties namely thickness, fluidity, and water permeability. At high temperatures and a fluid membrane, the coiled coil is compact and phosphatase activity of DesK is favored. Whereas at low temperatures and thicker rigid membrane, the coiled coil is destabilized, phosphatase activity abolished, and kinase activity switched on [Abriata *et al.* 2017]. This membrane bound sensor which mechanism of action is connected to temperature dependent membrane properties leads to the next subsection “Membrane fluidity”.

2.5.3 Membrane sensors

The cellular membrane protects the intracellular components and is also susceptible to changing ambient temperature. Sudden temperature shifts can cause alterations in membrane fluidity and -function. The changes in membrane fluidity must be adapted rapidly in order to prevent constant cell damage [Vigh *et al.* 1998]. The fatty acid composition and saturation state of membrane lipids were reported to change with temperature in different microorganism families [Mykytczuk *et al.* 2010; Matsuno *et al.* 2009; Paulucci *et al.* 2011]. Low temperatures alter DNA topology patterns that govern the temperature-dependent expression levels of various desaturases especially the gene *desB* coding for ω-3 desaturase in cyanobacterium *Syncheosystis*. The desaturase can alter membrane fluidity to maintain membrane homeostasis at low temperatures, via the increase of *cis*-unsaturation of pre-existing fatty acid side chains in the membrane [Los 2004]. Evidence has been presented that heat shock genes, like the *hsp17*, are strongly influenced by the physical order but not degree of saturation of the lipid membrane. It was reported that signal transduction of heat stress involved the membrane of *Syncheosystis* in the function of a cellular thermometer and the Hsp17. Heat shock proteins support maintaining membrane function by adhering to the membrane. Hsp17 has thereby a particular tendency to interact with non-bilayer phase forming lipids, which accumulate during heat shock in the membrane [Horváth *et al.* 2008]. Carratu et al. suggested that the ratio of saturated to unsaturated fatty acids and lipid membrane perturbation participate in temperature sensing and induction of heat shock gene expression. After introducing a mutation into the *ole1* gene (Δ9-desaturase) of *Saccharomyces cerevisiae*, the yeast was not able to produce unsaturated fatty acids. In consequence the composition of the cell membrane changed. The altered ratio of saturated to unsaturated fatty acids in turn had a significant influence on *hsp70* and *hsp82* transcription [Carratù *et al.* 1996].

2.5.4 RNA sensors

The mRNA formed during transcription is crucial for subsequent translation. At this level of gene expression, so-called RNA thermometers (RNAT) have proven to be particularly important for the microbial temperature response. RNAT generally refer to secondary structures, typically present in the 5' untranslated region (5'UTR) of the mRNA, that form at certain temperatures. They can regulate translation in a temperature dependent manner due to their 3D structure. The formed mRNA double strands are called hairpin or loop structures. They usually mask the Shine-Dalgarno sequence (SD) or ribosome binding site (RBS) in their function as a regulatory element and thus influence translation initiation. When thermal energy is introduced into the system, the hydrogen bridges between the base pairs in the loop structure melt, the secondary structure regresses, ribosomes can attach, and translation can take place [Wei *et al.* 2016; Chowdhury *et al.* 2006; Klinkert *et al.* 2009]. One of the earliest reported *cis* encoded RNA temperature responsive elements was found to regulate the *cIII* gene of bacteriophage α [Altuvia *et al.* 1989]. In 1999 the term "RNA thermometer" was coined by the work of G. Storz on the heat shock sigma factor

32 (RpoH) of *E. coli* [Storz 1999]. The characterization of an RNAT is usually based on its melting temperature or structural integrity and stability and the associated number of inhibitory loops. The stability of the loop structures in turn depends on non-/canonical base pairings and mismatches within the regulatory structure [Wei *et al.* 2016; Klinkert *et al.* 2009]. Nowadays, essentially two families and two regulatory roles of RNATs are distinguished. The first family includes the so-called ROSE elements (Repression Of heat Shock gene Expression) and the second family the fourU RNATs. The latter are so called because they contain four consecutive uracil bases in their regulatory loop. Typically, fourU RNATs are composed of 1–5 loop structures, 40–$>$ 270 nucleotides (*htrA, E. coli – shuA, S. dysenteriae*) in length and located in the 5'UTR of a gene [Kouse *et al.* 2021; G. G. Weber *et al.* 2014; Klinkert *et al.* 2012]. The ROSE RNAT is usually formed of 2–4 stem loops (60–100 nucleotides). The conserved nucleotide sequence UXGCU (X is a pyrimidine) pair with the SD sequence and is unique for the ROSE RNAT. In the final hairpin of the ROSE RNAT, the SD sequence and sometimes the AUG start codon are masked [Waldminghaus *et al.* 2005; Narberhaus *et al.* 2006]. Other types of RNAT that could not be clearly assigned to one of the main families, have been identified in the past and novel RNA regulatory elements are still reported until today [Wei *et al.* 2016; Nocker *et al.* 2001a; Johansson *et al.* 2002; Waldminghaus *et al.* 2007a; Kortmann *et al.* 2012; Eichner *et al.* 2021; Quinn *et al.* 2019; Catalan-Moreno *et al.* 2021, table below]. The functions of RNATs in general are largely concerned with the regulation of the heat shock response and the regulation of virulence of a pathogen upon host invasion. The key bacterial processes under the control of RNATs have been extensively reviewed by Wei [Wei *et al.* 2016] and a short overview with (recent) reports on RNA elements and their regulatory role is presented in the table below.

Table 2.1: RNA elements and their regulatory role in prokaryotes (N/A* = not available)

Gene (RNAT)	**Function**	**Organism**	**Reference**
		Temperature shock response	
"sHsps" (ROSE)		*Bradyrhizobium japonicum*	[Nocker *et al.* 2001b]
hspX, hspY (N/A*)	Small heat shock proteins & chaperones	*Pseudomonas putida*	[Krajewski *et al.* 2014]
agsA (fourU)		*Salmonella enterica*	[Waldminghaus *et al.* 2007b]
cspB, cspC (N/A*)	Cold shock proteins	*Staphylococcus aureus*	[Catalan-Moreno *et al.* 2021]
rpoH (N/A*)	Alternative sigma factors (σ^{32})	*Escherichia coli*	[Storz 1999]
htrA (N/A*)	Proteases	*Escherichia coli* & *Salmonella*	[Klinkert *et al.* 2012]
		Virulence	
ligA, ligB (N/A*)	Adhesion (lipoproteins)	*Leptospira interrogans*	[Matsunaga *et al.* 2013]
shuA, chuA (fourU)	Nutrient acquisition	*Shigella dysenteriae* & *Escherichia coli*	[Kouse *et al.* 2021]
cpsA, bcs1 (N/A*)	Immune system evasion	*Streptococcus pneumoniae* & *Haemophilus influenzae*	[Eichner *et al.* 2021]
rhlAB (ROSE)	Host invasion	*Pseudomonas aeruginosa*	[Grosso-Becerra *et al.* 2014]
rhlR, lasI (ROSE)	Quorum sensing	*Pseudomonas aeruginosa*	[Grosso-Becerra *et al.* 2014]
cssA (N/A*)	Encapsulation	*Neisseria meningitidis*	[Karlsson *et al.* 2020]
cnfY (N/A*)	Toxin formation	*Yersinia pseudotuberculosis*	[Twittenhoff *et al.* 2020]
tviA (fourU)	Transcription regulation of virulence	*Salmonella enterica* serovar Typhi	[Twittenhoff *et al.* 2020]

De novo design of RNA sensors

RNATs are relatively simple structures. Furthermore, it is mostly understood what constitutes to the functionality of an RNAT and how this may be influenced [Rinnenthal *et al.* 2011, see above]. Therefore, it is not surprising that attempts have been made to create artificial "Designer RNAT" structures with tailored regulatory capabilities. In 2008, first attempts of a *de novo* design of RNA regulatory elements were made [Neupert *et al.* 2008]. This involved the design of 12 simple RNA sequences (13 when including the control sequence). These sequences were transformed via plasmid vectors into *E. coli*. Subsequently the expression of the GFP encoded on the plasmid and regulated by the respective RNAT sequence was measured after growth at 4 different temperatures (17–37°C). A year later, in 2009 a step-by-step protocol for the design and use of artificial RNA structures was released. The authors reported that an RNAT can be designed, produced, tested and optimized in just 2–3 weeks [Neupert *et al.* 2009]. In 2013 so called “thermozymes” have been designed. Thermozymes are a combination of a fourU RNAT from *Salmonella* and a hammerhead ribozyme that cleaves itself while liberating a ribosome binding site allowing downstream gene expression. The thermozyme exhibits the reversed effect upon temperature-controlled gene expression in comparison to the wildtype RNAT. Elevated temperatures melt the RNAT structure, which consequently impairs self-cleavage of the ribozyme as well as liberation of the ribosome-binding site and gene expression is therefore switched off at high temperatures [Saragliadis *et al.* 2013]. A toolset for designing RNAT with tailored temperature responses was reported in 2017. The RNAT toolbox was designed by using thermodynamic calculations such as minimum free energy structures or melting profiles, as well as *in vitro* activity benchmarking to yield RNATs with different sensitivity and threshold profiles. Thereby RNA sequences were identified with different temperature response profiles in the range of 29–37°C [Sen *et al.* 2017].

2.6 A ROSE fourU - The (hi)story & its relation to this thesis

The initial description of the ROSE RNA element was reported in 2001 for *Bradyrhizobium japonicum* as: “Expression of [...] small heat shock proteins (sHsps), is under the control of ROSE (repression of heat shock gene expression). This negatively *cis*-acting DNA element confers temperature control to a σ70-type promoter.” [Nocker *et al.* 2001b]. The authors noted that these regulatory elements “are functionally interchangeable between species” [Nocker *et al.* 2001b]. This statement becomes important for this thesis where two different RNATs are used as heterologous control element for rhamnolipid (RL) production by *Pseudomonas putida* KT2440 [Noll *et al.* 2019; Noll *et al.* 2021]. The ROSE element evaluated in the first mentioned article originates from the close relative *P. aeruginosa* where it regulates the expression of the *rhlAB* operon and indirectly the synthesis of the virulence factor RL. As the name ROSE (repression of heat shock gene expression) suggests, it normally occurs as a control element of heat shock genes. The virulence factor RL is the only known exception to this rule so far [Grosso-Becerra *et al.* 2014; Wei *et al.* 2016]. The ROSE element regulates, in dependence of ambient temperature, the translation of rhlA and via a

so-called polar effect also the translation of rhlB and as such indirectly RL production. The *rhlAB* genes code for the RhlA and RhlB proteins which form an acyltransferase [Deziel *et al.* 2003] and the rhamnosyltransferase 1 required for RL production; both in the native host *P. aeruginosa* and in the heterologous host *P. putida* KT2440 [Grosso-Becerra *et al.* 2014; Noll *et al.* 2019]. RNA elements are often responsible for temperature dependent control of virulence factor synthesis in pathogens like *P. aeruginosa*. As described above, the ROSE element represents an exception here regulating usually heat shock gene expression. In fact, the second RNAT family, the fourU RNATs, is responsible for most of the temperature dependent translational control of virulence genes. So far only two fourU RNATs are reported to be involved in the control of heat shock proteins [Wei *et al.* 2016, see table above]. Among the first reports of genes regulated by a fourU RNAT were the virulence genes of *Yersina pestis lcrF* (*virF*) and, the exception to the rule, the small heat shock gene *agsA* of *Salmonella enterica* [Hoe *et al.* 1993; Waldminghaus *et al.* 2007b]. The later fourU element is of particular interest for this thesis because it was identified to more efficiently regulate translation than the ROSE element [Noll *et al.* 2019; Noll *et al.* 2021]. Furthermore, its regulatory capability can easily be modified by a point mutation [Rinnenthal *et al.* 2011]. The following figure summarizes important historic developments of RNAT and RL research and assigns the original research of this thesis.

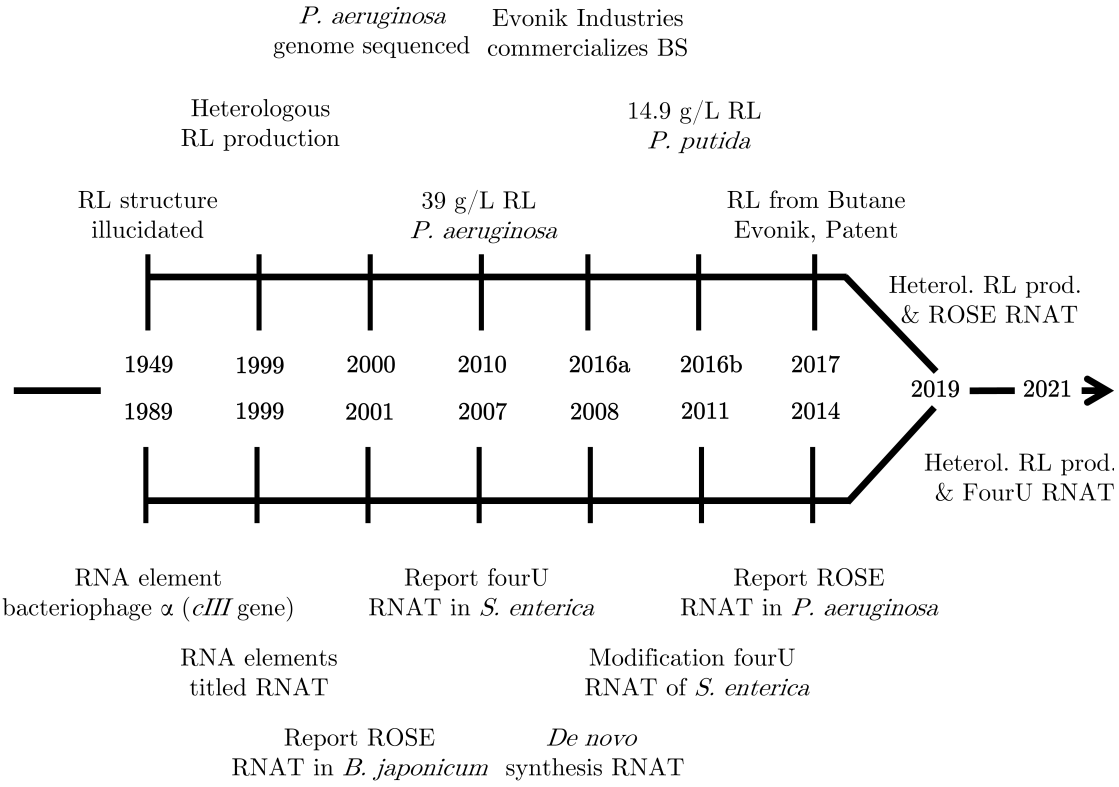

Figure 2.3: Timeline of important events for RNA thermometer (RNAT) & rhamnolipid (RL) biosurfactant (BS) research [Altuvia *et al.* 1989; Storz 1999; Nocker *et al.* 2001b; Waldminghaus *et al.* 2007b; Neupert *et al.* 2008; Rinnenthal *et al.* 2011; Grosso-Becerra *et al.* 2014; Noll *et al.* 2019; Noll *et al.* 2021].

The enhanced molecular control options of the described fourU element of *S. enterica* have so far not been exploited for industrial bioprocesses. As such this molecular thermo switch permits to leverage temperature as an additional control variable for a bioprocess. A detailed overview on advantages and disadvantageous of temperature as control variable and RNAT as molecular control elements is presented in the General Discussion below. Briefly, the use of temperature as a physical inducer for separation biomass growth from product formation phases has advantages over the current chemical inducers. Changing the temperature rather than using chemical inducers like IPTG is thought to be more cost effective. Also compared to the addition of a chemical inducer to a closed system, the possibility of contamination can be avoided merely by adjusting the temperature. This could be valuable for process validation in the pharmaceutical industry, for example. Furthermore, in large scale productions reactor systems must be cooled due to metabolic heat. Cultivations at higher temperatures would require less cooling effort or an autoinduction of a process may be possible when temperature increases over time of cultivation. Temperature variations in turn cause several metabolic changes, many of which are complex and interdependent as described in this chapter. Models that describe biological processes as a function of temperature are thus essential for decreasing complexity and better comprehending those relationships. The goal of the review article "Modeling and Exploiting Microbial Temperature Response", shown in the following chapter, was to present an overview of various temperature models in order to aid comprehension of model intent selection and application. Only a few (industrial) bioprocesses exploit temperature for process control, -monitoring or -optimization. None of them uses a molecular RNAT in combination with a temperature shift (see table 2 of review article). The combination of directed temperature control with temperature responsive RNA elements to conduct the course of a bioprocess (in our case heterologous rhamnolipid production) is presented in the original research articles in the following chapter.

Part II

Publications

The following article was published in 2019 in *AMB Express*, 9.1, 154 as

- Evaluating temperature-induced regulation of a ROSE-like RNA-thermometer for heterologous rhamnolipid production in *Pseudomonas putida* KT2440 -

Philipp Noll, Chantal Treinen, Sven Müller, Sabine Senkalla, Lars Lilge, Rudolf Hausmann and Marius Henkel

DOI: 10.1186/s13568-019-0883-5

Noll *et al. AMB Expr* (2019) 9:154
https://doi.org/10.1186/s13568-019-0883-5

AMB Express

ORIGINAL ARTICLE Open Access

Evaluating temperature-induced regulation of a ROSE-like RNA-thermometer for heterologous rhamnolipid production in *Pseudomonas putida* KT2440

Philipp Noll, Chantal Treinen, Sven Müller, Sabine Senkalla, Lars Lilge, Rudolf Hausmann and Marius Henkel*

Abstract

The microbial production of rhamnolipids has been in the focus of research for the last decades. Today, mainly heterologous production systems are targeted due to the advantage of non-pathogenic hosts as well as uncoupling from complex quorum sensing regulatory networks compared to their natural producer *Pseudomonas aeruginosa*. In the recent past, the presence and function of a ROSE-like RNA-thermometer located in the 5′UTR of the rhamnosyltransferase genes *rhlAB* has been reported in wild type *P. aeruginosa*. In this study, the temperature-induced regulation of this native RNA-thermometer for heterologous rhamnolipid production was evaluated and its potential application for process control is discussed. For this purpose, the non-pathogenic production host *P. putida* KT2440 containing the *rhlAB* genes with the native *P. aeruginosa* 5′-UTR region was used. The system was evaluated and characterized regarding the effect of temperature on growth and product formation, as represented by efficiency parameters and yields. Experimental data suggests a major effect of temperature on specific rhamnolipid production rates. With maximum values of 0.23 g/(g h) at 37 °C, this constitutes a more than 60% increase compared to the production rate of 0.14 g/(g h) at the growth optimum of 30 °C. Interestingly however, control experiments unveiled that besides the regulatory effect of the RNA-thermometer, multiple metabolic effects may contribute equally to the observed increase in production rate. As such, this work constitutes an important step towards the utilization of temperature-based process designs and enables the possibility for novel approaches for process control.

Keywords: Thermoregulation, RNA thermometer, Heterologous rhamnolipid biosynthesis, *Pseudomonas putida*, Biosurfactant

Introduction

Temperature has a direct effect on fundamental biological systems, including enzyme activity and correct folding of proteins. In nature, bacteria experience temperatures that are far from the optimum for growth, and more extreme temperatures can be detrimental for cells. While high temperatures account for denatured and misfolded proteins, low temperatures may cause damage to membranes. Consequently, bacteria have developed different systems to sense changes in environmental conditions such as temperature and induce an adaptation of metabolism and gene expression. Many different principles of thermoregulation have been identified in bacteria, which can be assigned to the class of protein-, DNA- or RNA-thermosensors. The principle of action behind these strategies is the conversion of temperature signals into either transcriptional or translational responses. The different principles have been extensively reviewed (Klinkert and Narberhaus 2009; Shapiro and Cowen 2012; Sengupta and Garrity 2013). Protein-based thermosensors are a very diverse group including transcriptional regulators, sensor kinases, chaperones or

*Correspondence: Marius.Henkel@uni-hohenheim.de
Institute of Food Science and Biotechnology, Department of Bioprocess Engineering (150 k), University of Hohenheim, Fruwirthstr. 12, 70599 Stuttgart, Germany

proteases (reviewed in Klinkert and Narberhaus 2009). Due to the inherent diversity in the underlying mechanisms, protein-based thermosensors affect different cellular processes such as transcription, translation, protein stability, signal transduction as well as proteolytic processes. Changes in temperature are typically sensed as a result of conformation changes of protein structure as well as misfolded proteins. These thermosensors are part of a regulatory network, such as the production of heat shock proteins mediated by sigma factor 32 (RpoH) in *Escherichia coli* or the transcriptional repressor of heat-shock genes HrcA in *Bacillus subtilis* (Hecker et al. 1996; Narberhaus 1999).

DNA thermosensors, also referred to as DNA thermometer, are AT-rich sequences that alter the structure and bending of DNA in response to temperature. DNA thermometer are known to be present in promoter region where they can affect binding and interaction with regulatory proteins such as transcription factors and RNA polymerase resulting in temperature-dependent transcription (Nickerson and Achberger 1995; Katayama et al. 1999).

The third class of thermosensing is based on the temperature-dependent conformation of specific RNA sequences, which are termed RNA-thermometer (RNAT). These sequences typically include the 5′-untranslated region in mRNA including the ribosome binding site (Shine-Dalgarno sequence) and in some cases the start codon (Klinkert and Narberhaus 2009). The temperature-dependent three-dimensional structure formed by the RNA occludes ribosome binding at low temperatures. At higher temperatures, the structure destabilizes and normal translation is facilitated (Chowdhury et al. 2006). The first cis-encoded temperature-sensitive RNA sequence which regulates translation was discovered in 1989 (Altuvia et al. 1989). Several examples for bacterial genes which are induced by a shift in temperature due to the presence of RNA-thermometer have been reported up to today, and many are linked to heat-shock and virulence associated genes (Nocker et al. 2001; Johansson et al. 2002; Waldminghaus et al. 2007; Kortmann and Narberhaus 2012). Even though most RNA-thermometers have been reported to be present in the 5′-UTR, exceptions like the *rpoH* RNA-thermometer have been reported to include significant parts of the coding region in the transcript. More than 200 nucleotides of the coding region of *rpoH*, divided into two segments, are involved in the temperature response of the transcript. Furthermore, the Shine-Dalgarno sequence in the *rpoH* mRNA is, unlike to the majority of described RNATs, not completely blocked (Morita et al. 1999). One of the most abundant sequences present in the 5′-UTR of many different bacteria controlling heat shock response is referred to as ROSE (repression of heat-shock gene expression) element (Nocker et al. 2001; Balsiger et al. 2004; Wei and Murphy 2016). Besides these simplest single-loop conformations, RNA-thermometers with up to five loops have been reported (Klinkert et al. 2012; Kouse et al. 2013). RNA-thermometer, unlike riboswitches, do not require a ligand to function properly, and the temperature-dependent regulatory function is mediated solely by the sequence of the RNA (Chowdhury et al. 2006; Serganov and Nudler 2013). For pathogenic bacteria, a change of environmental temperature is a key stimulus that may indicate infection of the host. To facilitate efficient growth under these conditions, and as defense against immune response of the host, the expression of virulence factors needs to be closely regulated. In many pathogenic bacteria, expression of virulence genes is induced at 37 °C, and the underlying mechanisms are often based on RNA-thermometers (Johansson et al. 2002; Böhme et al. 2012; Weber et al. 2014). *Pseudomonas aeruginosa* is an opportunistic human pathogen, which is known for infections of the respiratory tract, the eyes as well as the skin.

Pseudomonas aeruginosa furthermore is known for the production of rhamnolipid biosurfactants, which are glycolipids consisting of a (hydroxyalkanoyloxy)alkanoic acid (HAA) hydrophobic fatty acid tail and a hydrophilic head of one or two rhamnose molecules. While the expression of virulence associated genes as well as genes involved in rhamnolipid biosynthesis is under control of a complex quorum sensing dependent regulatory network, the effect of RNA-thermometers is not well-understood. The presence of an RNA-thermometer in the *rhlAB* operon coding for the rhamnosyltransferase complex required for rhamnolipid biosynthesis, was first predicted in silico in the past (Waldminghaus et al. 2007), and first experimental evidence of its function was recently provided by Grosso-Becerra et al. (2014). Expression of *rhlA* was shown to be increased at 37 °C, which is reported to be caused by a ROSE-like element in the 5′-UTR. At temperatures ≤ 30 °C, an inhibitory loop structure blocks *rhlA* translation, which subsequently results in a polar effect of *rhlB* transcription that is initiated at the *rhlA* promotor (Grosso-Becerra et al. 2014).

The microbial production of rhamnolipids has been in the focus of research for the last decades. As green alternatives to petrochemically derived surfactants, rhamnolipids have gained more and more attention over the last decades. The relevance of rhamnolipids as products of industrial biotechnology is furthermore emphasized by patents from the last years as well as the recent commercialization by Evonik Industries (Schaffer et al. 2011; Schilling et al. 2013; Evonik Industries 2016). In current research, heterologous production

systems are targeted due to the advantage of non-pathogenic hosts as well as uncoupling from complex quorum sensing regulatory networks compared to their natural producer *Pseudomonas aeruginosa*.

Even though the structure and function of the native RNA-thermometer from *P. aeruginosa* PAO1 has been reported in the past, its potential has not yet been evaluated for application in process development and heterologous production processes. Using temperature as a physical inductor poses advantages over chemical inducers used today. Changing temperature is regarded as more cost efficient as opposed to adding chemical inducers (e.g. IPTG). Furthermore, the risk of contamination can be avoided when simply changing the temperature compared to the addition of a chemical inducer to a closed system, which may be beneficial for process validation, such as in the pharmaceutical environment.

In this study, the temperature response and potential application for process control of this native RNA-thermometer for heterologous rhamnolipid production was evaluated. The plasmid-based system contained the *rhlAB* genes with the native *P. aeruginosa* 5′-UTR region and RNA-thermometer sequence under control of a synthetic promoter as described previously (Beuker et al. 2016b) (Fig. 1). The system was evaluated and characterized regarding the effect of temperature on growth and product formation, as represented by efficiency parameters and yields. As such, this work constitutes a fundamental step toward establishing temperature-based process design and control.

Materials and methods

Chemicals and reference substances

All chemicals used in the current study were purchased from Carl Roth GmbH (Karlsruhe, Germany) if not stated otherwise. All chemicals for analytic procedures were of analytical/MS grade. The di-rhamnolipid (Rha-Rha-C_{10}-C_{10}) standard for HPTLC analysis was a gift from former Hoechst AG (Frankfurt-Hoechst, Germany). The mono-rhamnolipid (Rha-C_{10}-C_{10}) standard was obtained from Sigma-Aldrich Laborchemikalien GmbH (Seelze, Germany). Rhamnolipid derivatization was performed as described by Schenk et al. (1995), and for this purpose, 4-bromophenacylbromide and triethylamine were obtained from Sigma-Aldrich Laborchemikalien GmbH (Seelze, Germany).

Microorganism and plasmids

Pseudomonas putida KT2440 with plasmid pSynPro8oT_*rhlAB* producing mono-rhamnolipids was used as described previously (Beuker et al. 2016b). As control with no RNA-thermometer effect, plasmid pSynPro8oT_*rhlAB-oT* which carries the RNA-thermometer sequence inactivated by randomization was constructed. The pBBR1MCS-3 based plasmid pSynPro8oT_*rhlAB* was extracted from *Pseudomonas putida* KT2440 pSynPro8oT_*rhlAB.* The template plasmid pSynPro8oT_*rhlAB* was modified in a polymerase chain reaction using a Q5 High-Fidelity Polymerase (NEB, Ipswitch, MA, USA), the forward primer 5′ TGA CTT CAA TTG TTC TGG TTA GTA ATG CTA TGA GTG AAC GGG GGC TGA AGT TGG GAG GTG TGA AAT GCG GC 3′ and the reverse primer

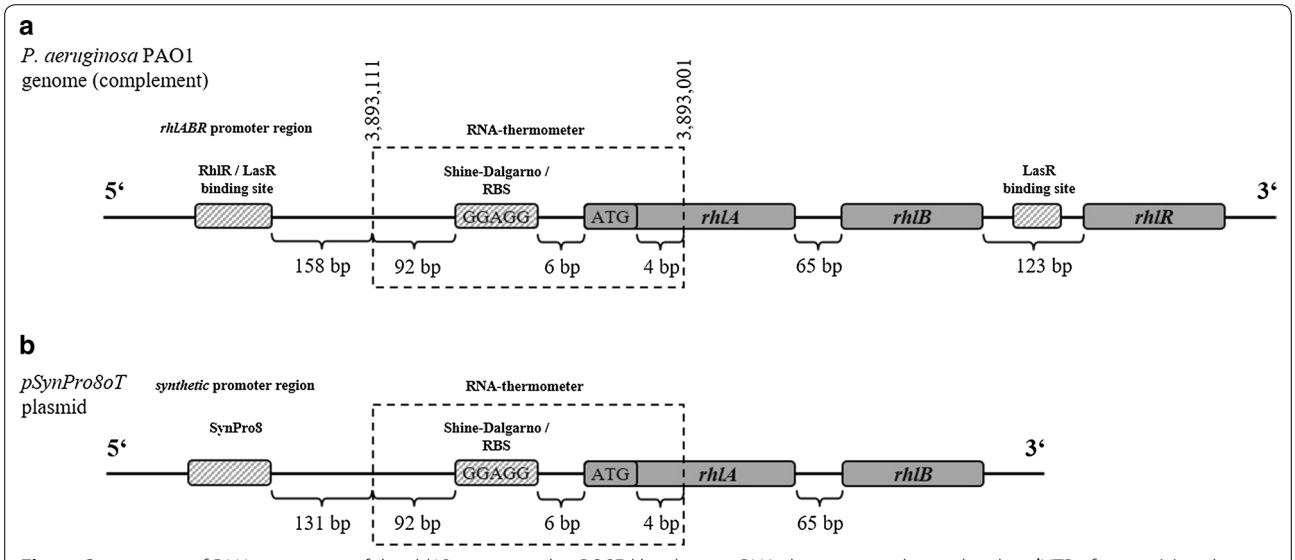

Fig. 1 Comparison of DNA sequences of the *rhlAB* operon with a ROSE-like element RNA-thermometer located in the 5′UTR of native (**a**) and heterologous (**b**) rhamnolipid production hosts *P. aeruginosa* PAO1 and *Pseudomonas putida* KT2440 pSynpro8oT_*rhlAB* (Beuker et al. 2016b)

5′ TGA TGT CAA TTG GTC CAT TTG GTT AAT TCA TGT ATG ATC GAG ATA GGC TGA TAA ACT CAG CGG CCA TCC GC 3′. The primers were designed to contain a 5′ overhang of 6 bp, a MfeI restriction site to produce sticky ends facilitating later religation with T4 DNA Ligase of the linearized vector containing the randomized sequence. The randomized sequence is of equal length like the to be exchanged RNAT. The plasmid containing the randomized sequence instead of the RNAT was transformed into electro competent *Pseudomonas putida* KT2440 wild type cells. Electro competent *Pseudomonas putida* KT2440 wt were prepared according to Choi et al. (2006). The solution containing the PCR product (NoRNAT) was desalted using a 0.025 µm nitrocellulose membrane. Electroporation of electro competent cells was performed using an electroporation device (Eporator, Eppendorf AG, Hamburg, Germany) with voltage set to 2.5 kV. After transformation cells were transferred to 1 mL LB-Medium and incubated for 3 h at 30 °C and 120 rpm. Consequently, cells were plated on LB-Agar containing 20 mg/L Tetracycline as selection marker and incubated overnight at 30 °C. After streaking on LB-Agar containing 20 mg/L Tetracycline an isolated single colony was selected for preparation of glycerol stocks, cultivation and sequence confirmation of *Pseudomonas putida* KT2440 pSynPro8oT_*rhlAB-oT*.

Media preparation

All growth media (LB, ModR, SupM) were prepared as described by Beuker et al. (2016a).

Cultivation conditions

All shake flasks were inoculated in a shake incubator (New Brunswick /Innova 44, chamber, Eppendorf AG, Hamburg, Germany) at 120 rpm and a temperature between 26 and 40 °C, as indicated for each individual experiment. First precultures were prepared by inoculating 25 mL LB medium in a 250 mL baffled shake flask with 50 µL from a glycerol stock solution of *P. putida* KT2440 pSynPro8oT_*rhlAB and* pSynPro8oT_*rhlAB-oT* and incubation at 30 °C for 24 h. From these first precultures, grown for 24 h, seed cultures were prepared for all preformed experiments in shake flasks as described by Beuker et al. (2016a). For each seed culture, grown for 15 h, 1 mL of the first preculture was used to inoculate 100 mL SupM medium in 1 L shake flasks. The main culture in ModR medium was inoculated with the second preculture to an OD_{600} of 0.3.

Sampling and sample processing

Sample processing was performed as described by Beuker et al. (2016a). For extraction of rhamnolipids, culture supernatant was acidified 1:100 (*v*/*v*) with phosphoric acid and extracted twice with 1.25:1 (*v*/*v*) ethyl acetate, pooled and evaporated in a vacuum centrifuge at 40 °C for 40 min and 10 mbar (RVC 2-25 Cdplus, Martin Christ Gefriertrocknungsanlagen GmbH, Osterode am Harz, Germany).

HPTLC for quantification of rhamnolipids

Rhamnolipid detection was performed as described by Schenk et al. (1995) with modifications for a protocol suitable for HPTLC (Horlamus et al. 2018). Evaporated rhamnolipid samples were dissolved in acetonitrile and derivatized for 90 min at 1400 rpm and 60 °C using a 1:1 mixture of 135 mM bromphenacylbromid and 67.5 mM tri-ethyl-ammonium/-amin as described by Cooper and Anders (1974). If Rhamnolipid concentrations above 2 g/L were to be expected samples were diluted prior to derivatization. Measurements of derivatized samples were performed on silica gel 60 HPTLC plates with fluorescence marker F^{254} (Merck, Darmstadt, Germany). A HPTLC system for quantitative analysis (CAMAG Chemie-Erzeugnisse & Adsorptionstechnik AG, Muttenz, Switzerland) was used. Samples were applied with the Automatic TLC Sampler 4 (ATS 4). Development of plates was performed with the automatic Developing Chamber 2 (ADC 2) equipped with a 20 cm × 10 cm twin-trough chamber. After development, plates were analyzed using the TLC Scanner 4. The HPTLC system is controlled via an HPTLC imaging and data analysis software (winCATS 1.4.7.2018 software, CAMAG, Muttenz, Switzerland). For sample application the filling speed of the syringe was adjusted to 15 µL/s and dosage speed to 150 nL/s. In between sample application the syringe was rinsed with methanol. Band width was adjusted to 6 mm and application start was at 15 mm from the left and 8 mm from the lower edge. Mobile phase for plate development was composed of 30:5:2.5:1 isopropyl acetate:ethanol:water:acetic acid. Tank saturation was adjusted to 5 min and drying with an air stream was carried out for 5 min afterwards. A deuterium (D2) lamp with slit dimensions of 3 mm × 0.3 mm was used for scanning. Scanning was performed at 263 nm at which wavelength bromphenacyl-derivatized rhamnolipid congeners absorb. Data resolution and scanning speed were set to 1 nm/step and 100 nm/s respectively.

Enzymatic assays

The concentration of glucose was detected from the culture supernatant of samples using glucose enzymatic assay kits (R-Biopharm AG, Darmstadt, Germany), according to the manufacturers' instructions.

Software for graphical analysis, regression and replicates

Regression analysis of measured data was performed using scientific graphing and data analysis software (SigmaPlot, Systat Software Inc., San Jose, CA). Specific rhamnolipid production rates and growth rates were calculated using a four-parameter logistic fit for biomass and rhamnolipid concentration (Henkel et al. 2014). All data was obtained as duplicates from at least two independent biological experiments, and measurement results are presented as mean ± standard deviation.

Software for parameter optimization, modeling and simulation

All parameter fitting and simulation for temperature-dependency models, as described in "Results" section, was performed in MATLAB (The MathWorks, Natick, MA, USA). For parameter optimization, the Nelder-Mead numerical algorithm implemented in the embedded functions "fmincon" and "fminsearch" by minimizing the error of simulation data and measured data according to a least-square error function was applied. To visualize and describe temperature dependency of rhamnolipid production rates, a modified Ratkowsky model according to Zwietering et al. (1991; Ratkowsky et al. 1983) was used to derive a fitting curve.

$$q_{RL}(T) = \frac{[b \cdot (T - T_{min})]^2 \cdot \left\{1 - e^{c \cdot (T - T_{max})}\right\}}{a} \quad (1)$$

For the maximum specific growth rate μ_{max}, a fitting curve was derived using a model proposed by Roels et al. (1983).

$$\mu_{max}(T) = \frac{A \cdot e^{\left(\frac{-E_G}{RT}\right)}}{1 + B \cdot e^{\left(\frac{-\Delta G_d}{RT}\right)}} \quad (2)$$

Results

To visualize the effect of temperature on rhamnolipid production and growth, a first experiment was performed comparing cultivations at 30 °C (growth optimum, Fig. 2a) and 37 °C (suggested induction, Fig. 2b). There was no apparent lag phase detected in either cultivation, but a significantly lower biomass concentration was achieved at 37 °C of 0.6 g/L, while 3 g/L were obtained at 30 °C. Even though significantly lower biomass concentrations (approx. 1/5th) were produced at 37 °C, the maximum rhamnolipid concentration was only slightly lower when comparing 30 °C (1.2 g/L) and 37 °C (0.9 g/L). Visualization of this effect is further supported by plotting of specific rhamnolipid production rates over the course of cultivation (Fig. 2c) for 30 °C and 37 °C, which reveals approx. 60% increased specific rhamnolipid productivity from 0.14 g/(g h) to 0.23 g/(g h).

This temperature-dependency of rhamnolipid production (Fig. 2) was further investigated at temperatures between 26 and 40 °C and is shown in Fig. 3. As a fitting curve for the maximum specific rhamnolipid production rate, a modified Ratkowsky model (Eq. 1) according to Zwietering et al. (1991) was used, as described in "Materials and methods". The productivity increased in a linear way until a maximum of 0.23 g/(g h) was reached, which, according to the model with parameter fitting performed for the obtained data, is slightly above 36 °C or, when comparing experimental data, 0.24 g/(g h) at 37 °C. At temperatures above 37 °C, rhamnolipid productivity decreased rapidly. When comparing the average sp. productivity to the maximum sp. productivity, the average productivity was unaffected and constant at a value of approximately 0.05 g/(g h) at temperatures between 26 °C and approximately 35 °C. At temperatures above 35 °C however, the average productivity increased nearly threefold to values of 0.14 g/(g h).

Rhamnolipid-per-glucose yields ($Y_{P|S}$) and total rhamnolipid-per-biomass yields ($Y_{P|X}$) are shown for different temperatures in Fig. 4a. There was no apparent correlation of rhamnolipid-per-glucose yield and temperature and $Y_{P|S}$ stayed almost constant at values of 0.06–0.08 g/g over the entire investigated temperature range. The total rhamnolipid-per-biomass yield was also almost unaffected by temperature between 26 °C and approximately 35 °C. At temperatures above 35 °C however, $Y_{P|X}$ reached values of up to 0.75 g/g at 38.5 °C, which were approximately 2.5-fold increased when comparing to $Y_{P|X}$ at lower temperatures. At 40 °C however, this highest value decreased significantly to approx. 0.4 g/g (Fig. 4a).

In addition to rhamnolipid production rates and yields, growth rates and substrate-to-biomass were furthermore investigated for all cultivations (Fig. 4b). Data reveals that the optimum temperature for growth was at approximately 30–32 °C. The maximum specific growth rate $\mu_{max} = 0.7–0.8$ 1/h was determined by a fitting curve of a temperature dependent equation (Eq. 2) according to Roels et al. (1983). While glucose-to-biomass yields ($Y_{X|S}$) were relatively constant at values of 0.35–0.40 g/g at the growth optimum and temperatures below, there was a decrease in yield at temperatures above 32 °C to below 0.2 g/g (Fig. 4b).

As a control, a plasmid with inactivated RNAT was used to determine the increase in specific rhamnolipid production rate by performing comparing cultivations with both constructs (Fig. 5). For *P. putida* KT2440 pSynpro80T_*rhlAB*, an average increase in specific

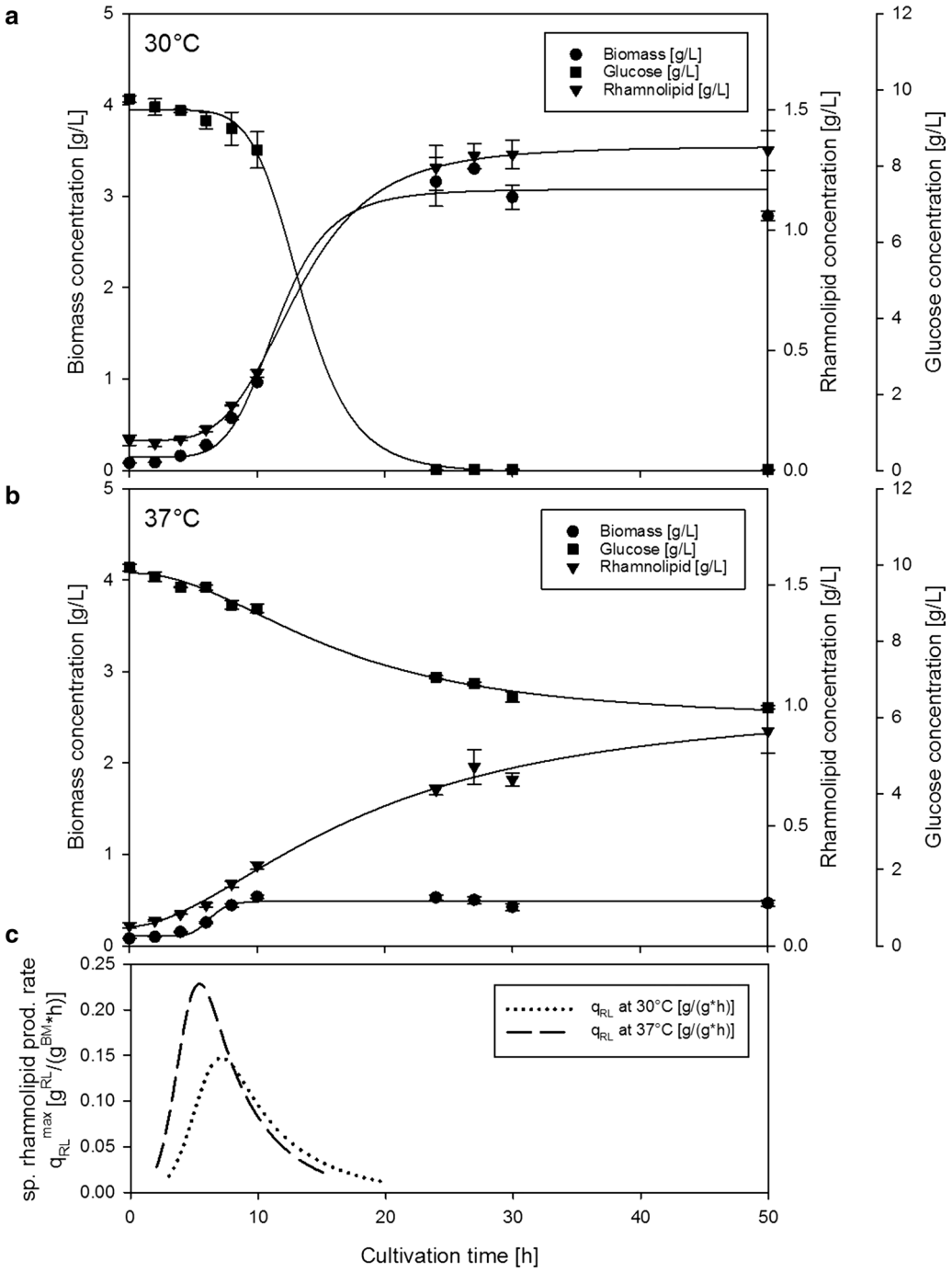

Fig. 2 Time course of biomass concentration (circles), rhamnolipid concentration (triangles) and glucose concentration (squares) during shaking flask cultivation of *Pseudomonas putida* KT2440 pSynpro8oT_*rhlAB* on ModR medium with 10 g/L glucose at 30 °C (**a**) and 37 °C (**b**), and corresponding course of specific rhamnolipid production rate (**c**)

productivity of approx. 36% was measured when comparing cultivations at 30 °C and 37 °C, respectively (see also Fig. 3). For cultivations of *P. putida* KT2440 including the plasmid with randomized and inactivated RNA-thermometer (open conformation) at 30 °C and 37 °C, an average increase in specific rhamnolipid production rate of approx. 23% was detected.

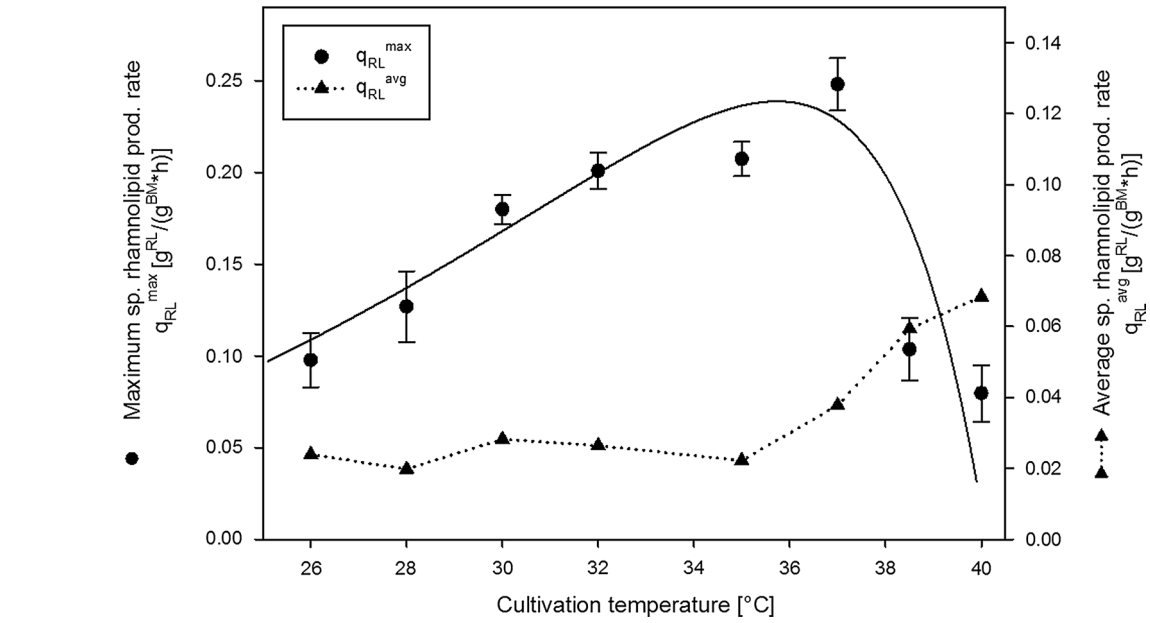

Fig. 3 Maximum (circles) and average (triangles) specific rhamnolipid production rates at different cultivation temperatures. Maximum specific rhamnolipid production rates as a function of temperature was described using the empirical modified Ratkowsky equation (Eq. 1) (Ratkowsky et al. 1983; Zwietering et al. 1991), with parameter fitting performed for the obtained data (black line)

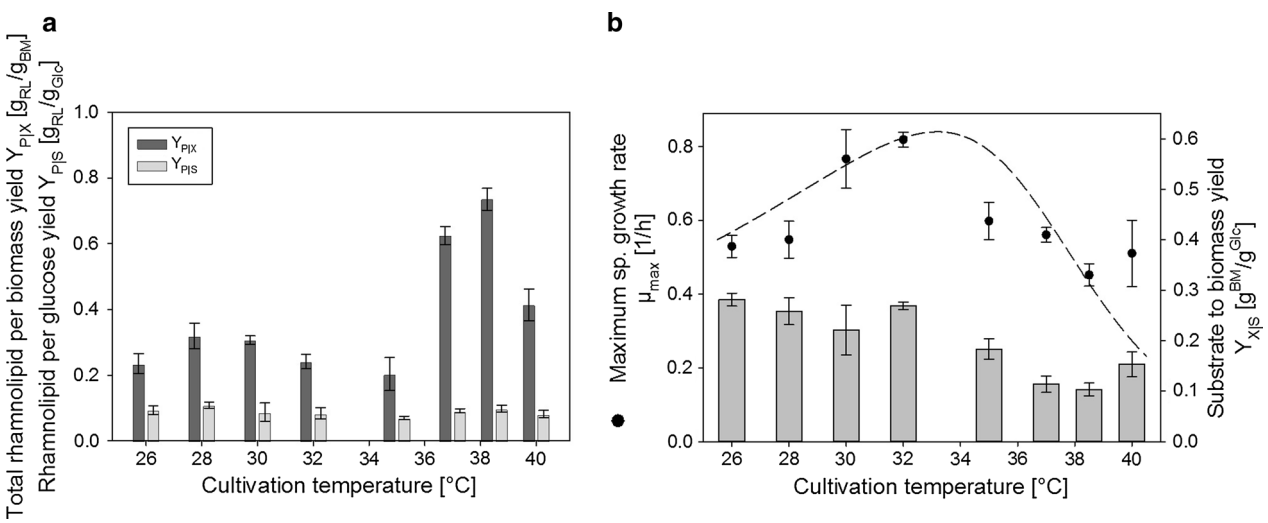

Fig. 4 Effect of temperature on rhamnolipid-per-glucose yields ($Y_{P|S}$) and rhamnolipid-per-biomass yields ($Y_{P|X}$) (**a**) as well as effect of temperature on maximum specific growth rate μ_{max} and substrate-to-biomass yields ($Y_{X|S}$) (**b**). Maximum specific growth rate as a function of temperature was described using an equation proposed by Roels et al. (1983) (Eq. 2) with parameter fitting performed for the obtained data (dashed line)

Discussion

When comparing the time courses of biomass concentration during cultivations at 30 °C to 37 °C, final biomass at 37 °C was significantly lower while the final rhamnolipid concentration remained nearly comparable to what was obtained at 30 °C (Fig. 2a, b). Therefore, it can be reasoned that a higher biomass specific productivity was reached at 37 °C. After calculating specific productivity over time using data from continuous curve fits (Fig. 2c), a similarly shaped time course of productivities

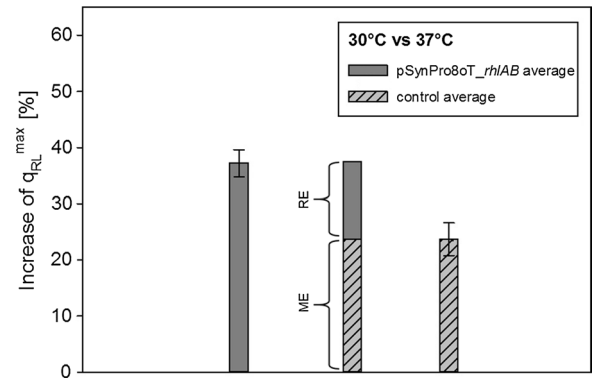

Fig. 5 Comparison of increase in specific rhamnolipid production rate of *Pseudomonas putida* KT2440 pSynpro8oT_*rhlAB* and control plasmid with inactivated RNA-thermometer at 30 °C and 37 °C respectively. Average differences in production rate calculated from individual biological data are shown with derived metabolic effect (ME) and regulatory (RE) effect

was observed, and the main difference between 30 °C and 37 °C was the overall extension and height (Fig. 2c). This suggests that indeed, specific production rates are higher at a cultivation temperature of 37 °C instead of being attributed to other phenomena such as increased duration of the productive phase.

As a next step, the temperature-dependency of rhamnolipid production was investigated in a range between 26 and 40 °C (Fig. 3). An almost linear increase of rhamnolipid productivity between 26 °C until the optimum at 37–38 °C could be observed in the recorded temperature range of 26–40 °C. Assuming rhamnosyltransferase concentration and rhamnolipid production rate to be proportional in the absence of limitations, this correlation mirrors what is known on RNA-thermometers regulation behavior. It is reported that the RNA loop typically never completely prevents translation but shows a gradually increasing temperature-response profile when thermal energy is introduced into the system because of the destabilizing effect of elevated temperatures on the inhibitory loop structure (Chowdhury et al. 2006; Rinnenthal et al. 2010). After reaching the optimal rhamnolipid production temperature, productivities rapidly decrease when temperatures are further increased. This may be due to different effects elevated temperatures can have on bacteria. Furthermore, possible indirect effects on rhamnolipid formation have to be considered, which are due to altered bacterial metabolism resulting in a decreased precursor concentration causing a bottleneck for rhamnolipid production. Rhamnolipid synthesis itself may be negatively affected by temperatures above the optimal production temperature by defective or altered function or substrate binding capacity of RhlA respectively RhlB towards the precursors HAA and dTDP-rhamnose.

When comparing how the average specific rhamnolipid production rate is effected by cultivation temperature (Fig. 3), interestingly, an increase is only detected once temperature of highest rhamnolipid production is surpassed. The average specific rhamnolipid production rate may represent an important target parameter for optimization for evaluation of the total productivity of the process. It is important to note, however, that the average specific rhamnolipid production rate is calculated from shake-flask with a defined and limited cultivation time. In contrast this may not be the case for optimized prolonged processes with a fed-batch design for instance. Total rhamnolipid yield per biomass or glucose moreover represent important target optimization parameters for bulk chemical production processes. In terms of development of an economical process, it should be noted that observed increase in rhamnolipid yield per biomass (Fig. 4a) correlates with the maximum specific production rate (Fig. 3). This would generally allow for a process design with both increased as well as more efficient rhamnolipid production.

To determine what proportion of the observed effect of increase in rhamnolipid production can be attributed to a regulatory effect, control experiments using a plasmid with randomized, inactive sequence of the RNA-thermometer (open conformation) were performed. The increase in specific rhamnolipid production rate comparing cultivations of 30 °C to 37 °C of *P. putida* KT2440 pSynpro8oT_*rhlAB* with functional RNAT was quantified to be approx. 36% (Fig. 5, see also Fig. 3). This increase may be assigned to two different (overlapping) effects. First a regulatory effect caused by the inhibitory structure of the RNAT and second by multiple (overlapping) metabolic effects. When assuming no regulatory effect by the RNA-thermometer, the increase for the control strain (with inactivated RNAT) would be expected to be approx. equal to the increase in specific rhamnolipid production rate of the strain with functional RNAT. Metabolic effects would then solely cause this increase. When assuming no overlapping metabolic effects, and increases in production rate were assumed to be fully attributed to the RNA-thermometer regulation, the increase in specific rhamnolipid production rate of the control strain should be close to 0% due to an inactivated RNAT.

Interestingly, control experiments unveiled that besides the regulatory effect ('RE', Fig. 5) of the RNA-thermometer, a major part of the increase in specific rhamnolipid production rate is not due to regulation of the RNA-thermometer. The average increase in specific production rate with the control plasmid of around 23% can be attributed to metabolic effects ('ME', Fig. 5). However, these results confirm the action of the employed ROSE-like temperature-sensitive regulatory element in

a heterologous host, as results obtained with the RNAT plasmid lead to a higher average increase of 36% (Fig. 5).

As temperature has a broad effect on bacterial metabolism and regulation, different hypothesis may provide an explanation for this observed behavior. Firstly, it should be mentioned that RNA-thermometers are generally reported to display a comparably high degree of "leakiness" and inefficiency when inhibiting translation (Chowdhury et al. 2003), which could result in a leveling out of differences in production rates. Furthermore, temperature has an effect on plasmid replication and copy numbers, and therefore also on the number of gene copies present per bacterial cell. Along with effects of increasing temperature on plasmid replication, there are furthermore physical effects that need to be considered, such as a shift in oxygen solubility and therefore availability comparing cultivation temperatures of 30 °C and 37 °C.

Altogether, in this study, the RNA-thermometer effect of a ROSE-like regulatory element could be confirmed in the heterologous host *P. putida* KT2440. Findings from this study along with quantitative data from comparison of efficiency parameters and yields provides a basis of how temperature effects rhamnolipid production and growth. A high potential for using temperature to design and control a process for rhamnolipid production is revealed by the observed strong increase in production rate of up to 60%. Interestingly however, regulation of translation due the RNA-thermometer does not seem to play the major part in the observed effect. As temperature effects a wide range of biological and physical properties, it is difficult to attribute to what extent each individual effect constitutes a part in this effect. Future work could include molecular data such as transcriptome and metabolome data, which would allow insight into bottlenecks, existing effects and limitations during protein biosynthesis. Furthermore, a variety of regulatory RNAT structures are available and may be exploited for process design and control in future studies. RNAT consist of a comparably straightforward structure and mechanism. Therefore, attempts have been made to provide guidelines for in silico design, experimental benchmarking and optimization of synthetic thermosensitive nucleic acids, a procedure that takes only 2–3 weeks claimed by Neupert et al. (2008). In 2017, a toolbox was presented to design RNA-thermometers that offer various temperature responses. The RNATs were designed by Sen et al. (2017) to differ in sensitivity and threshold. The design of the RNAT toolbox for various temperature responses was based on thermodynamic calculations like minimum free energy structures or melting profiles, as well as on experimental activity benchmarking in vitro. A wide range of structures has been found and evaluated to give a varying temperature response within a range between 29 and 37 °C. In the here presented study, even though individual effects are not yet clear, a proof-of-concept for a straightforward method to efficiently increase rhamnolipid production levels is presented. As such, this work constitutes an important step towards the utilization of temperature-based process designs and enables the possibility for novel approaches for process control.

Abbreviations

RNAT: RNA-thermometer; ROSE: repression of heat shock gene expression (element); RL: rhamnolipid; UTR: untranslated region; HPTLC: high-performance thin layer chromatography; HAA: (hydroxyalkanoyloxy)alkanoic acid.

Acknowledgements

The authors would like thank Dr. Frank Rosenau and Dr. Andreas Wittgens (Institute for Pharmaceutical Biotechnology, Ulm University, Germany) for constructive scientific discussion and for providing the initial plasmid pSynPro8.

Authors' contributions

PN planned and executed the experiments, collected data, created the graphs and drafted the manuscript. CT, SM and SS performed part of the experiments and collected and evaluated corresponding data. LL and RH contributed to evaluation of the data, design of the experiments and scientific discussion. MH substantially contributed to conception and design of the conducted experiments, interpretation of the results and drafting of the manuscript. All authors read and approved the final manuscript.

Funding

This work was partially funded by the Fachagentur Nachwachsende Rohstoffe e.V. (Funding Code 22004513). PN is a member of the "BBW ForWerts" graduate program and receives a scholarship within the frame of the Baden-Wuerttemberg Landesgraduiertenfoerderung (LGF) awarded by the Ministry of Science, Research and the Arts (MWK) of Baden-Württemberg, Germany.

Availability of data and materials

All discussed data have been included into the manuscript. Please turn to the corresponding author for all other requests.

Ethics approval and consent to participate

Not applicable.

Consent for publication

Not applicable.

Competing interests

The authors declare that they have no competing interests.

Received: 5 August 2019 Accepted: 17 September 2019
Published online: 25 September 2019

References

Altuvia S, Kornitzer D, Teff D, Oppenheim AB (1989) Alternative mRNA structures of the cIII gene of bacteriophage λ determine the rate of its translation initiation. J Mol Biol 210:265–280. https://doi.org/10.1016/0022-2836(89)90329-X

Balsiger S, Ragaz C, Baron C, Narberhaus F (2004) Replicon-specific regulation of small heat shock genes in *Agrobacterium tumefaciens*. J Bacteriol 186:6824–6829. https://doi.org/10.1128/JB.186.20.6824-6829.2004

Beuker J, Barth T, Steier A, Wittgens A, Rosenau F, Henkel M, Hausmann R (2016a) High titer heterologous rhamnolipid production. AMB Express 6:124. https://doi.org/10.1186/s13568-016-0298-5

Beuker J, Steier A, Wittgens A, Rosenau F, Henkel M, Hausmann R (2016b) Integrated foam fractionation for heterologous rhamnolipid production with

recombinant *Pseudomonas putida* in a bioreactor. AMB Express 6:1–10. https://doi.org/10.1186/s13568-016-0183-2
Böhme K, Steinmann R, Kortmann J, Seekircher S, Heroven AK, Berger E, Pisano F, Thiermann T, Wolf-Watz H, Narberhaus F, Dersch P (2012) Concerted actions of a thermo-labile regulator and a unique intergenic RNA thermosensor control *Yersinia* virulence. PLoS Pathog. https://doi.org/10.1371/journal.ppat.1002518
Choi KH, Kumar A, Schweizer HP (2006) A 10-min method for preparation of highly electrocompetent *Pseudomonas aeruginosa* cells: application for DNA fragment transfer between chromosomes and plasmid transformation. J Microbiol Methods 64:391–397. https://doi.org/10.1016/j.mimet.2005.06.001
Chowdhury S, Ragaz C, Kreuger E, Narberhaus F (2003) Temperature-controlled structural alterations of an RNA thermometer. J Biol Chem 278:47915–47921. https://doi.org/10.1074/jbc.M306874200
Chowdhury S, Maris C, Allain FHT, Narberhaus F (2006) Molecular basis for temperature sensing by an RNA thermometer. EMBO J 25:2487–2497. https://doi.org/10.1038/sj.emboj.7601128
Cooper MJ, Anders MW (1974) Determination of long chain fatty acids as 2-naphthacyl esters by high pressure liquid chromatography and mass spectrometry. Anal Chem 46:1849–1852. https://doi.org/10.1021/ac60348a035
Evonik Industries (2016) Evonik commercializes biosurfactants. Press release:https://corporate.evonik.com/media/pressattachments/c483/n60276/a28986.pdf. Accessed 21 Jun 2016
Grosso-Becerra MV, Croda-Garcia G, Merino E, Servin-Gonzalez L, Mojica-Espinosa R, Soberon-Chavez G (2014) Regulation of *Pseudomonas aeruginosa* virulence factors by two novel RNA thermometers. Proc Natl Acad Sci USA 111:15562–15567. https://doi.org/10.1073/pnas.1402536111
Hecker M, Schumann W, Volker U (1996) Heat-shock and general stress response in *Bacillus subtilis*.: DISCOVER: all subjects. Mol Microbiol 19:417–428
Henkel M, Schmidberger A, Vogelbacher M, Kühnert C, Beuker J, Bernard T, Schwartz T, Syldatk C, Hausmann R (2014) Kinetic modeling of rhamnolipid production by *Pseudomonas aeruginosa* PAO1 including cell density-dependent regulation. Appl Microbiol Biotechnol 98:7013–7025. https://doi.org/10.1007/s00253-014-5750-3
Horlamus F, Wittgens A, Noll P, Michler J, Müller I, Weggenmann F, Oellig C, Rosenau F, Henkel M, Hausmann R (2018) One-step bioconversion of hemicellulose polymers to rhamnolipids with *Cellvibrio japonicus*: a proof-of-concept for a potential host strain in future bioeconomy. GCB Bioenergy. https://doi.org/10.1111/gcbb.12542
Johansson J, Mandin P, Adriana R, Chiaruttini C, Springer M, Cossart P (2002) An RNA thermosensor controls expression of virulence genes in *Listeria monocytogenes*. Cell 110:551–561. https://doi.org/10.1016/S0092-8674(02)00905-4
Katayama S, Matsushita O, Jung CM, Minami J, Okabe A (1999) Promoter upstream bent DNA activates the transcription of the *Clostridium perfringens* phospholipase C gene in a low temperature-dependent manner. EMBO J 18:3442–3450. https://doi.org/10.1093/emboj/18.12.3442
Klinkert B, Narberhaus F (2009) Microbial thermosensors. Cell Mol Life Sci 66:2661–2676. https://doi.org/10.1007/s00018-009-0041-3
Klinkert B, Cimdins A, Gaubig LC, Roßmanith J, Aschke-Sonnenborn U, Narberhaus F (2012) Thermogenetic tools to monitor temperature-dependent gene expression in bacteria. J Biotechnol 160:55–63. https://doi.org/10.1016/j.jbiotec.2012.01.007
Kortmann J, Narberhaus F (2012) Bacterial RNA thermometers: molecular zippers and switches. Nat Rev Microbiol 10:255–265. https://doi.org/10.1038/nrmicro2730
Kouse AB, Righetti F, Kortmann J, Narberhaus F, Murphy ER (2013) RNA-mediated thermoregulation of iron-acquisition genes in *Shigella dysenteriae* and pathogenic *Escherichia coli*. PLoS ONE. https://doi.org/10.1371/journal.pone.0063781
Morita M, Kanemori M, Yanagi H, Yura T (1999) Heat-induced synthesis of σ 32 in *Escherichia coli*: structural and functional dissection of rpoH mRNA secondary structure. J Bacteriol 181:401–410
Narberhaus F (1999) Negative regulation of bacterial heat shock genes. Mol Microbiol 31:1–8. https://doi.org/10.1046/j.1365-2958.1999.01166.x
Neupert J, Karcher D, Bock R (2008) Design of simple synthetic RNA thermometers for temperature-controlled gene expression in *Escherichia coli*. Nucleic Acids Res 36:1–9. https://doi.org/10.1093/nar/gkn545
Nickerson C, Achberger E (1995) Role of curved DNA in binding of *Escherichia coli* RNA polymerase to promoters. J Bacteriol 177:5756–5761. https://doi.org/10.1128/jb.177.20.5756-5761.1995
Nocker A, Hausherr T, Balsiger S, Krstulovic NP, Hennecke H, Narberhaus F (2001) A mRNA-based thermosensor controls expression of rhizobial heat shock genes. Nucleic Acids Res 29:4800–4807. https://doi.org/10.1093/nar/29.23.4800
Roels J (1983) Energetics and kinetics in biotechnology. Elsevier Biomedical Press. ISBN 0444804420
Ratkowsky DA, Lowry RK, McMeekin TA, Stokes AN, Chandler RE (1983) Model for bacterial culture growth rate throughout the entire biokinetic temperature range. J Bacteriol 154:1222–1226
Rinnenthal J, Klinkert B, Narberhaus F, Schwalbe H (2010) Direct observation of the temperature-induced melting process of the *Salmonella* fourU RNA thermometer at base-pair resolution. Nucleic Acids Res 38:3834–3847. https://doi.org/10.1093/nar/gkq124
Schenk T, Schuphan I, Schmidt B (1995) High-performance liquid chromatographic determination of the rhamnolipids produced by *Pseudomonas aeruginosa*. J Chromatogr A 693:7–13. https://doi.org/10.1016/0021-9673(94)01127-Z
Schaffer S, Wessel M, Thiessenhusen A, Stein N (2011) Cells and method for producing rhamnolipids. EU patent EP2598646B1, 20 Jul 2011
Schilling M, Rueterming M, Dahl V, Cabirol F (2013) Process for the isolation of rhamnolipids. EU patent EP2735605B1, 29 Oct 2013
Sen S, Apurva D, Satija R, Siegal D, Murray RM (2017) Design of a toolbox of RNA thermometers. ACS Synth Biol 6:1461–1470. https://doi.org/10.1021/acssynbio.6b00301
Sengupta P, Garrity P (2013) Sensing temperature. Curr Biol 23:R304–R307. https://doi.org/10.1016/j.cub.2013.03.009
Serganov A, Nudler E (2013) A decade of riboswitches. Cell 152:17–24. https://doi.org/10.1016/j.cell.2012.12.024
Shapiro RS, Cowen LE (2012) Thermal control of microbial development and virulence: molecular mechanisms of microbial temperature sensing. MBio 3:1–6. https://doi.org/10.1128/mbio.00238-12
Waldminghaus T, Gaubig LC, Narberhaus F (2007) Genome-wide bioinformatic prediction and experimental evaluation of potential RNA thermometers. Mol Genet Genomics 278:555–564. https://doi.org/10.1007/s00438-007-0272-7
Weber GG, Kortmann J, Narberhaus F, Klose KE (2014) RNA thermometer controls temperature-dependent virulence factor expression in *Vibrio cholerae*. Proc Natl Acad Sci 111:14241–14246. https://doi.org/10.1073/pnas.1411570111
Wei Y, Murphy ER (2016) Temperature-dependent regulation of bacterial gene expression by RNA thermometers. Nucleic Acid. https://doi.org/10.5772/61968
Zwietering MH, de Koos JT, Hasenack BE, de Witt JC, van't Riet K (1991) Modeling of bacterial growth as a function of temperature. Appl Environ Microbiol 57:1094–1101

Publisher's Note

The following article was published in 2020 in *Processes*, 8.1, 121 as

- Modeling and Exploiting Microbial Temperature Response -

Philipp Noll, Lars Lilge, Rudolf Hausmann and Marius Henkel

DOI: 10.3390/pr8010121

processes

MDPI

Review

Modeling and Exploiting Microbial Temperature Response

Philipp Noll, Lars Lilge, Rudolf Hausmann and Marius Henkel *

Institute of Food Science and Biotechnology, Department of Bioprocess Engineering (150k), University of Hohenheim, Fruwirthstr. 12, 70599 Stuttgart, Germany; philipp.noll@uni-hohenheim.de (P.N.); lars.lilge@uni-hohenheim.de (L.L.); rudolf.hausmann@uni-hohenheim.de (R.H.)

* Correspondence: marius.henkel@uni-hohenheim.de

Received: 15 December 2019; Accepted: 14 January 2020; Published: 17 January 2020

Abstract: Temperature is an important parameter in bioprocesses, influencing the structure and functionality of almost every biomolecule, as well as affecting metabolic reaction rates. In industrial biotechnology, the temperature is usually tightly controlled at an optimum value. Smart variation of the temperature to optimize the performance of a bioprocess brings about multiple complex and interconnected metabolic changes and is so far only rarely applied. Mathematical descriptions and models facilitate a reduction in complexity, as well as an understanding, of these interconnections. Starting in the 19th century with the "primal" temperature model of Svante Arrhenius, a variety of models have evolved over time to describe growth and enzymatic reaction rates as functions of temperature. Data-driven empirical approaches, as well as complex mechanistic models based on thermodynamic knowledge of biomolecular behavior at different temperatures, have been developed. Even though underlying biological mechanisms and mathematical models have been well-described, temperature as a control variable is only scarcely applied in bioprocess engineering, and as a conclusion, an exploitation strategy merging both in context has not yet been established. In this review, the most important models for physiological, biochemical, and physical properties governed by temperature are presented and discussed, along with application perspectives. As such, this review provides a toolset for future exploitation perspectives of temperature in bioprocess engineering.

Keywords: thermal growth curve; temperature modeling; thermoregulation; monitoring and control; bioprocess engineering; calorimetry

1. Introduction

Predetermined by the applied system, bioprocesses are generally very sensitive to most changes in environmental conditions. It is for this reason that conditions such as temperature, pO_2, or pH are generally tightly controlled. In most cases, even small deviations from optimum values may lead to a significant reduction in the overall productivity and reproducibility of the process. Therefore, special consideration must be given to control tasks, which are typically defined by maintaining process variables within a narrow optimum [1]. In contrast to artificial laboratory conditions, microorganisms are usually exposed to a changing environment, with changes in pH, nutrient availability, competitors, and elevated or decreased temperature, etc. A crucial environmental factor for microorganisms is temperature. It affects the folding, structure, and stability of almost every biomolecule, as well as the metabolic reaction rate. Detection of temperature changes and subsequent adaptation of the metabolism are essential for microbial survival, such as by pathogens sensing intrusion into a host. Organisms can sense temperature shifts indirectly or by specialized sensing systems that evolved to detect changes in temperature in order to respond with adapted gene expression. This was extensively reviewed by Klinkert and Narberhaus [2]. Indirect temperature sensing is possible via the accumulation

of aggregated proteins after a heat shock and via stalled ribosomes after a cold shock. Molecular thermosensors may consist of DNA, RNA, proteins, or lipids. DNA topology changes, e.g., supercoiling caused by heat stress, stable RNA structures preventing translation at sub-optimal temperatures, temperature-responsive regulatory proteins, and alterations in lipid membrane stability with respective to fluidity are just a few examples for direct temperature sensing. Temperature plays an essential role and has a crucial effect on biological processes. Targeted temperature adjustments for triggering a desired response may also be exploited for biotechnological applications. Noll et al. published an example for a thermosensitive structure to direct the carbon flow of a substrate into a product rather than into biomass, by exploiting an RNA thermometer to optimize the heterologous production of rhamnolipid biosurfactants [3].

Alterations in temperature lead to multiple, often complex, interconnected metabolic changes. Models describing a biological process as a function of temperature are therefore indispensable to reducing complexity and facilitating understanding of those interconnections. Mathematical descriptions of how (bio-)chemical reactions respond to high or low temperatures emerged as early as in the 1900s with the "primal" temperature model of Arrhenius [4]. He investigated the reaction kinetics for sugar cane inversion by acids, depending on temperature. Popularized by Arrhenius, a variety of temperature models evolved over time, as shown in Figure 1. These models range from data-driven empirical approaches to complex mechanistic models that are based on thermodynamic knowledge of biomolecular behavior at different temperatures. Models are readily available to be used as a tool for process control and design. An overview of the current state of thermo-modeling is crucial to reasonably selecting a suitable model for the bioprocess to be monitored or optimized. The aim of this review is to provide an overview of available temperature models to facilitate understanding of model intention and reasonable selection for application. So far, only a few applications for temperature in (industrial) process design, monitoring, and control have been described. Applied model approaches are usually based on fuzzy logic or artificial neural networks and do not harvest the full potential of deterministic approaches. There are a few examples for applied model-assisted temperature control strategies in industrial biotechnology. These include heat balancing for an estimation of metabolic activity to improve batch-to-batch reproducibility by applying a process control module which uses the difference between the culture temperature and temperature of a coolant to predict oxygen mass transfer rates and k_La values [5–7]. Furthermore, deterministic process models can be used to describe a biological process as a function of a physical condition, like the temperature. They may be used in the food sector to estimate product shelf life, determining critical control points of a process, or to maximize productivities and ensure safe distribution chains [8]. These examples highlight a potential for temperature and deterministic models in process design. An approach for experimental design to optimize processes depending on multiple parameters is the Response Surface Method (RSM): "RSM is a collection of statistical techniques used for studying the relationships between measured responses and independent input variables" [9]. This method may be used for optimization purposes in experimental design in the shape of a metamodel. It connects the response of an objective function to input variables and determines its relations, for example, by the means of first- or second-order polynomial equations. The Matlab software package from The Mathworks, Inc. (Natick, MA, USA) [10] or the Minitab statistic software (GMSL s.r.l., UK) [11] may be used to conduct an RSM analysis. In bioprocesses, usually very few process variables are available online that continuously display a process course. Furthermore, arguably the only control variable to direct a bioprocess towards a desired outcome is, in most cases, the addition of fresh media. Other variables like pH, temperature, or pO_2 are typically controlled at a constant value. Therefore, investigating and exploiting novel potentially available monitoring and control variables like temperature is a reasonable strategy to extend existing toolsets of bioprocess monitoring and control. Even though several systems inducible by temperature have been discovered and made available to biotechnologists in the last decades, only a few have been exploited for practical purposes, such as for process design or optimization [12]. For monitoring and control purposes, calorimetric approaches have been presented [5,6,13,14]. For control purposes,

temperature may be used to directly address biological traits like RNA-thermometers to provoke a desired response, as previously evaluated [3]. Furthermore, indirect metabolic effects may be exploited, like elevated metabolic rates at high temperatures or the correct folding of proteins at low temperatures. Even though knowledge on microbial temperature responses and adaptation, along with descriptions developed by mathematical means, is available, its potential for applied industrial bioprocesses has not been sufficiently exploited. This review provides an overview on available thermo-models with the potential to develop model-assisted or model-derived process control strategies using temperature as a crucial parameter.

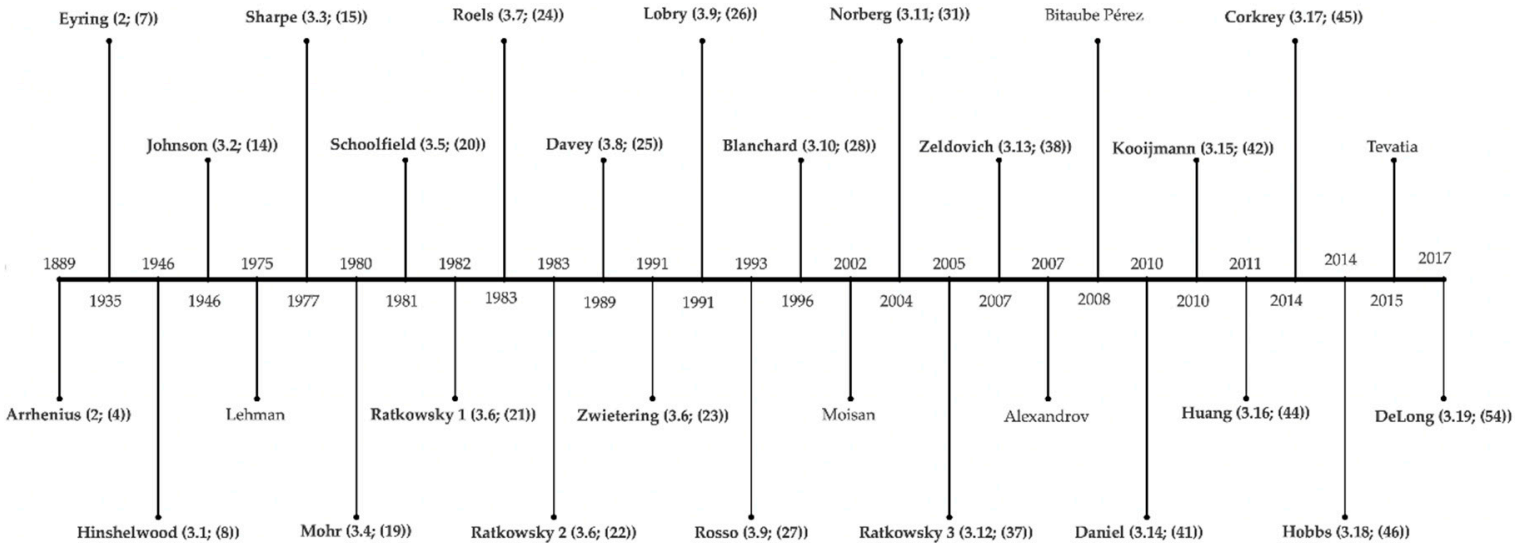

Figure 1. Timeline of temperature models described in paragraphs 2–3 starting in 1889 with the semi-empirical Arrhenius model. First author of the described model (paragraph number; equation number). Models marked with bold letters are described in detail and the remaining models in non-bold letters are summarized in Table 1.

2. History of Temperature Modeling—17th–20th Century

As early as the 17th century, there were theories on temperature being a form of particle movement. The kinetic theory of gases, with its origins in the 18th century, first specifically associated translational motions of molecules with heat and not with their vibrational or rotational motions [15]. Daniel Bernoulli was the pioneer of the kinetic theory of gases. He hypothesized that gases consist of a finite number of small spherical particles, which move through space along a straight line with high velocities. He assumed that heat increases the particle speed (v) and demonstrated that air pressure correlates with v^2. Air temperature can therefore be measured by this pressure at a constant density, making temperature proportional to v^2 [16,17]. The kinetic energies of the molecules are correlated with the ideal gas law of Equation (1), whose history began with the French engineer Émile Clapeyron in 1834 [18,19]. In the following, only SI units are used. Parameters with non-SI units, used by cited authors, were converted into SI units.

$$p \cdot \mathrm{V} = n \cdot R \cdot T \tag{1}$$

where p is the pressure, Pa; V is the volume, m^3; n is the amount of substance, mol; R is the universal gas constant ~8.314, J mol^{-1} K^{-1}; and T is the absolute temperature, K. The Dutch chemist and first Nobel Prize laureate J. H. Van't Hoff observed that the chemical reaction rate doubles or triples when the temperature is increased by 10 K, which he expressed with the following equation:

$$Q_{10} = \left(\frac{k_2}{k_1}\right)^{\frac{10}{T_2 - T_1}} \tag{2}$$

This "rule of thumb" for chemical kinetics allows estimations for various phenomena in chemistry, biochemistry, and ecology. He furthermore described the change in the equilibrium constant K of a chemical reaction with respect to the change in temperature at constant pressure with the Van't Hoff Equation (3):

$$\frac{d}{dT} \ln K_{\mathrm{eq}} = \frac{\Delta H}{R \cdot T^2} \tag{3}$$

where K is the dimensionless equilibrium constant; ΔH is the standard enthalpy change, J mol^{-1}; R is the universal gas constant ~8.314, J mol^{-1} K^{-1}; and T is the absolute temperature, K. Van't Hoff's student and the father of temperature models Svante Arrhenius continued the work of his teacher on the description of temperature-dependent specific reaction rate constants in chemical reactions with his essay "On the Reaction Velocity of the Inversion of Cane Sugars by Acids" [4]. Arrhenius observed that the reaction velocity of chemical reactions increased between 10% and 15% for each degree of rising temperature and postulated a semi-empirical model based on the Van't Hoff equation, which is shown in its integrated form in Equation (4).

$$k = A \cdot e^{\frac{-E_a}{R \cdot T}} \tag{4}$$

where k is the rate constant, s^{-1}, for a first-order rate constant; A is called a pre-exponential frequency or collision factor, s^{-1}, for a first-order rate constant; E_a is an empirical parameter, the (Arrhenius) activation energy, J mol^{-1}, characterizing the exponential temperature dependence of k; R is the universal gas constant ~8.314, J mol^{-1} K^{-1}; and T is the absolute temperature, K. In 1935, Henry Eyring formulated a statistical mechanistic equation following the transition state theory (former activated-complex theory) that assumed a transition state complex (‡TC) and a quasi-type equilibrium between educts (e_1; e_2), the transition state, and the product (P) [20,21]. The model has a similar way of describing the variance of the rate of a chemical reaction with temperature as the equation

of Arrhenius. Therefore, it underlined Arrhenius' previous observations and assumptions with a mechanistic approach.

$$e_1 + e_2 \underset{k_2}{\overset{k_1}{\rightleftharpoons}} {}^{\ddagger}TC \xrightarrow{k_3} P \quad (5)$$

According to the transition state theory, the rate constant can be described as follows:

$$k(T) = \frac{k_B \cdot T}{h} \cdot K^{\ddagger} \quad (6)$$

where k_B is the Boltzmann constant ~1.381 $\cdot 10^{-23}$, J K^{-1}; T is the absolute temperature, K; h is the Planck's constant ~6.626$\cdot 10^{-34}$, J s^{-1}; and $K^{\ddagger}$ is the dimensionless equilibrium constant. A different way to express the rate constant is by replacing the equilibrium constant with a term containing the standard molar changes of entropy and enthalpy:

$$k(T) = \frac{k_B \cdot T}{h} \cdot e^{\Delta^{\ddagger}S^{\circ}/R} \cdot e^{-\Delta^{\ddagger}H^{\circ}/(R \cdot T)} \quad (7)$$

where the entropy and enthalpy of activation are the standard molar change of entropy $\Delta^{\ddagger}S^{\circ}$, J K^{-1} mol^{-1}, when reactants form the transition state (activated) complex and standard molar change of enthalpy $\Delta^{\ddagger}H^{\circ}$, respectively, J mol^{-1}. R is the universal gas constant ~8.314, J mol^{-1} K^{-1}. The (Arrhenius) activation energy (E_a) and enthalpy of activation are not the same, but approximately equal, as they are convertible, depending on the molecularity [22].

2.1. Temperature in Biological Systems—The History Began with Arrhenius

Microbiologists have noticed a major effect of temperature on the growth rate of microbial populations and described this effect with the Arrhenius equation by simply replacing the rate constant k in Equation (4) with the growth rate (μ), meaning the reciprocal of the generation time. The so-called Arrhenius plot, where ln(μ) is plotted against the reciprocal temperature, was used in the past and is still applied today to describe a relation between the temperature and growth of different bacteria and molds [23–26]. From this plot, Arrhenius parameters can easily be derived. Their plots show a good fit for lower temperatures. The Arrhenius model does not represent cell death, so a decrease of the growth curve at non-physiological temperatures. The lack of fit of the Arrhenius model for some temperature-dependent biological processes gave rise to the development of improved models describing growth as a function of temperature. Most of these models are based on Arrhenius' parental model and evolved over time.

2.2. Biological Mechanisms Involved in Temperature Responses

Microorganisms have developed molecular traits to respond to changing environmental temperatures. These traits have been extensively reviewed [2,27,28]. The principles of microbial thermo responses range from changing DNA topology, e.g., supercoiling caused by heat stress, stalled ribosomes, or stable RNA preventing translation during cold stress to proper folding of proteins, working optima of enzymes, or lipid membrane stability and fluidity. Biomolecules are generally thermos-sensitive. Therefore, various options for direct molecular thermosensing are possible. Molecular thermosensors may consist of DNA, RNA, proteins, or lipids [2]. The accessibility of DNA for the transcriptional machinery is crucial for transferring genetic information via RNA into a protein and is influenced by DNA topology [29]. DNA supercoiling, and thus accessibility, is altered in response to a shifting temperature, as has been reported for the plasmic DNA of meso- and thermophiles [30]. Mesophiles have negatively supercoiled plasmic DNA and hyperthermophilic archaea with a growth optimum ≥80 °C have relaxed or positively supercoiled plasmic DNA [30–32]. Proteins such as the histone-like structuring proteins (H-NS) work as temperature-dependent regulators,

governing >200 temperature-regulated genes in *Salmonella* sp. and more than two third of *E. coli* K-12 temperature-regulated genes, respectively [33,34]. The inhibition of gene expression by H-NS is caused by trapping RNA polymerase and mediating DNA looping, thereby disturbing the progression of RNA polymerase [35–38]. Temperature-dependent gene expression is also influenced on the RNA level, where RNA can form inhibitory loop structures called RNA-thermometers (RNAT). Here, base pairing blocks the Shine-Dalgarno-sequence (SD) and AUG start codons, inhibiting ribosomal binding and translation initiation. By raising the temperature to a threshold (melting temperature), the hairpin structure opens and permits the access of ribosomes to the translation initiation site [2,39]. The secondary structure and thereby functionality of RNAT is characterized by canonical or non-canonical base paring, internal loops or mismatches, and the total number of loop structures. Based on these characteristics, RNA thermometers may be subdivided into three categories: (i) ROSE-like RNATs (repression of heat shock gene expression), (ii) FourU RNATs, and (iii) additional types of RNATs [40]. Most RNATs have been identified in the 5′-UTR of mRNA. The ROSE-like RNAT family is probably the most abundant temperature-sensing mRNA structure. ROSE-like RNATs usually control the repression of heat shock gene expression, but have also been reported to control expression of the rhamnosyl transferase, which is associated with *Pseudomonas aeruginosa* virulence [41]. ROSE-RNATs are located in the 5′UTR, are between 60 and 100 nt in length, and consist of 2–4 loop structures [41–43]. The majority of described RNATs of the second family, the FourU RNATs, govern the gene expression of virulence genes, and only two FourU RNAT's are known to control heat shock protein formation. FourU RNATs contain a sequence of four Uridines that occlude the SD sequence by canonical A-U and/or non-canonical G-U base pairing [40]. The virulence gene *lcrF* (*virF*) of *Yersina pestis* and the *agsA* small heat shock gene of *Salmonella enterica* were among the first genes described to be governed by a FourU RNAT [44]. Furthermore, attempts have been made to design synthetic RNATs with tailor-made characteristics to differ in up to 10-fold sensitivity- and around 3-fold threshold changes compared to a starting thermometer sequence [45]. On the protein level, global repressors, sensor kinases, methyl-accepting chemotaxis proteins (MCPs), M-like proteins, chaperones, and proteases are involved in microbial temperature responses [2]. The global transcriptional repressor CtsR has been termed a "protein thermosensor", and liberates DNA upon an up-shift in temperature connected to the expression of heat shock proteins. Due to a glycine-rich loop structure, CtsR exhibits intrinsic heat-sensing characteristics [46]. MCPs function as transmembrane receptors and consist of a periplasmic ligand-binding domain and a signaling domain in the cytosol that can interact with cytosolic sensor kinases [47]. The Tar MCP, for example, is convertible from a heat to a cold sensor in the presence of aspartate and consequent methylation at up to four sites [48]. The surface M and M-like proteins of the human pathogens group A streptococci bind to a variety of human plasma proteins in a temperature-dependent manner. The affinity of the M-like coild-coil protein Arp4 to IgA, is high at 10 and 20 °C, but low at 37 °C, due to a conformational change of Arp4 and consequent loss of the coild-coil conformation and binding activity [49]. The diverse class of small heat shock proteins (sHsp) can act as molecular chaperones upon heat shock. They are temperature sensors with different molecular mechanisms. For example, the sHsp Hsp26 of *Saccharomyces cerevisiae* consists of 24 subunits and changes its affinity state towards unfolded proteins at high temperatures by undergoing a conformational change [50,51].

2.3. Characteristic Graph for Growth as a Function of Temperature

Representative curvature of a model depicting the specific growth rate as a function of temperature, called the thermal growth curve, is shown in Figure 2. The simulated optimal specific growth rate (μ_{opt}) with the maximum turning point at the temperature optimum (T_{opt}) and growth rate at half of μ_{opt} ($\mu_{50\%opt}$) are marked in the model of a thermal growth curve. It has been pointed out that the term "optimal temperature" may need further specification to distinguish between the temperature for the optimal growth rate and the optimal temperature of the maximum biomass yield [52]. The minimum and maximum temperatures (T_{min} and T_{max}, respectively) for growth flank the asymmetric function

and mark the thermal tolerance or thermal niche of an organism [53,54]. These three temperatures (T_{min}, T_{opt}, and T_{max}) are commonly referred to as cardinal temperatures. Bacteria can adapt to changing temperatures in the short run by producing cold- or heat-shock proteins. Furthermore, it was reported that the performance optimum of *E. coli* can be shifted when exposed to suboptimal temperatures for ~2000 generations. Conversely, the thermal niche breadth remained constant in that case [54]. The result is a reshaped thermal growth curve with the same upper and lower limits. The asymmetry of the thermal growth curve indicates that bacteria, which may be adapted to high temperatures, can survive in lower temperatures quite well. In contrary, fitness decreases sharply when temperatures exceed the optimum, resulting in thermal shock [55,56]. In one of the most recent approaches, the growth of psychrophiles, mesophiles, thermophiles, and hyperthermophiles was modeled, covering a temperature range of 124 °C, from −2 to +122 °C. The model was applied to 230 different strains of uni- and multicellular organisms with growth temperatures below freezing and the highest known temperature for biological growth so far [57,58].

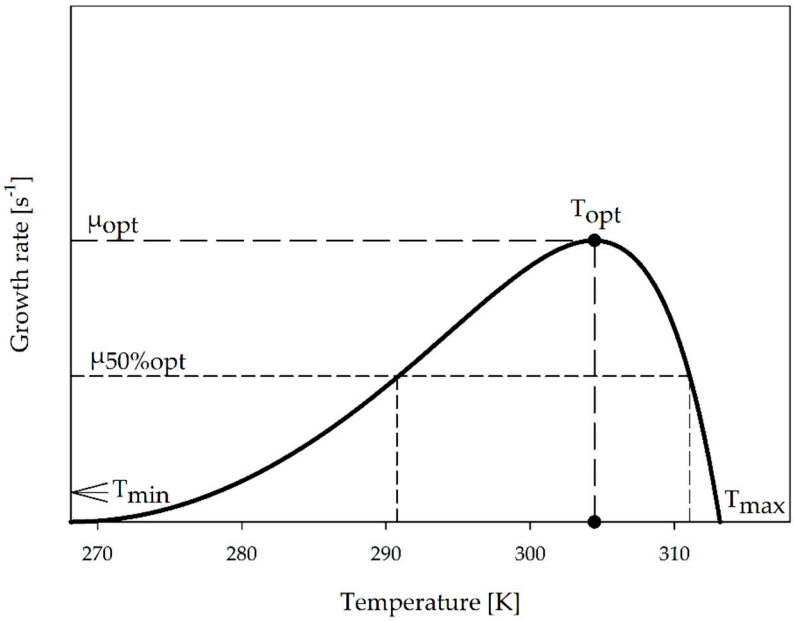

Figure 2. Scheme of the thermal growth curve where the temperature (K) is plotted against the growth rate (s^{-1}). Cardinal temperatures (T_{min}, T_{opt}, and T_{max}) with their corresponding growth rates (μ_{opt} and $\mu_{50\%opt}$) are indicated.

2.4. Mechanistic Versus Empirical Models

An often cited empirical approach for modeling the thermal growth curve of microorganisms is the approach of Ratkowsky et al. [59] (Scopus: cited by 615, 6 November 2019) and the semi-empirical model of Arrhenius. The development of mechanistic approaches for modeling the thermal growth curve of microorganisms started with the master reaction model of Johnson et al. in 1946 [60] (Scopus: cited by 80, 6 November 2019). The mechanistic models consider the description of single essential protein thermal stability (master reaction model) or the thermal stability of the whole proteome (the proteome model) as key for modeling the thermal growth curve. The transition of the native to an active and/or inactive state of the protein is considered. Grimaud et al. have extensively reviewed temperature growth models and concluded that empirical models display a better fit for balanced growth in non-limiting conditions than mechanistic models. Conversely, mechanistic models offer a complementary point of view for modeling thermal growth and can accurately represent temperature responses for growth under non-balanced conditions [61].

3. Temperature Modeling—From the 20th Century until Today

3.1. The Model of Hinshelwood (1946)

Hinshelwood expanded Arrhenius' model by adding a temperature-dependent term describing a "rate of degeneration" that becomes relevant at temperatures above T_{opt} [62]. Hinshelwood assumes a balanced growth for his model, saying that the total amount of compounds in a cell is constant. The model is based on the assumptions that just one enzymatic reaction is rate-controlling and the product of this reaction is a thermosensitive essential biomolecule which denatures irreversibly when temperatures are raised beyond the optimum. Temperature dependency and denaturation at high temperatures are of zero order and exhibit a temperature dependency similar to the Arrhenius model. The model represents the rate of synthesis in the minuend and degeneration in the subtrahend. At low temperatures, the subtrahend term is insignificantly small; in a small temperature region, both terms are almost equal, canceling each other out; and at high temperatures, the subtrahend term mostly accounts for the rapid decrease of the rate to zero.

$$u(T) = A_1 \cdot e^{-\frac{E_1}{R \cdot T}} - A_2 \cdot e^{-\frac{E_2}{R \cdot T}} \tag{8}$$

where A_1, and A_2 are referred to as pre/non-exponential, collision, or frequency actors, s^{-1}, related to entropy [62]; E_1 and E_2 are related to enthalpy [22], representing activation energies, J mol^{-1}, of the rate-determining enzyme reaction and high-temperature denaturation, respectively; R is the universal gas constant ~8.314, J mol^{-1} K^{-1}; and T is the temperature, K.

3.2. The Model of Johnson (1946)

In the same year, Johnson and Lewin [60] proposed another mechanistic model, which also assumes a simple case of a single reaction controlling growth, and called it their "master reaction model". In contrast to Hinshelwood, they assumed that a reversibly denaturable "master enzyme" E_0 controls an essential reaction for growth (assuming no substrate limitation). They reported their observation that *E. coli* stopped growing at non-viable 45 °C, but started growing exponentially again when transferred back to 37 °C. Increasing the exposition time of *E. coli* to non-viable temperatures led to lowered growth rates at 37 °C compared to the control. Hence, they assumed and described reversible protein denaturation damage as part of their model by integrating an equilibrium constant (K_1). The constant accounts for the equilibrium of reversibly denatured inactive (E_d) to native active enzymes (E_n).

$$K_1 = \frac{E_d}{E_n} \tag{9}$$

Hence, the amount of native active enzyme is given by Equation (10), with E_0 being the total amount of enzyme (native and denatured, mol).

$$E_n = \frac{E_0}{1 + K_1} = \frac{E_0}{1 + e^{\frac{-\Delta H}{R \cdot T}} \cdot e^{\frac{\Delta S}{R}}} \tag{10}$$

Johnson and Lewin then referred to Equation (7) proposed by Eyring, adding Equation (10) to account for the amount of active enzyme and substrate concentration and yielding Equation (11) for the temperature-dependent specific reaction rate (k).

$$k(T) = \frac{k_B \cdot T}{h} \cdot e^{\Delta^{\ddagger} S^{\circ} / R} \cdot e^{-\Delta^{\ddagger} H^{\circ} / (R \cdot T)} \cdot [S] \cdot [E_n] \tag{11}$$

By assuming that one single enzymatic reaction governs temperature-dependent growth at a constant substrate concentration and by substituting E_n in Equation (11) with rearranged Equation (10), temperature-dependent growth can be described as Equation (12):

$$u(T) = c \cdot T \cdot E_0 \cdot e^{\Delta^{\ddagger}S^{\circ}/R} \cdot e^{-\Delta^{\ddagger}H^{\circ}/(R \cdot T)} \cdot \frac{1}{1 + e^{-(\Delta H - T \cdot \Delta S)/(R \cdot T)}} \quad (12)$$

where c is a derived Boltzmann/Plancks constant, s K^{-1}, from the Eyring model of Equation (7); $\Delta^{\ddagger}H^{\circ}$ and $\Delta^{\ddagger}S^{\circ}$ are the standard molar change of enthalpy and entropy of activation, respectively (as described for Equation (7)); ΔH and ΔS are the enthalpy, J, and entropy change, J K^{-1}, respectively, between native and denatured enzymes; R is the universal gas constant ~8.314, J mol^{-1} K^{-1}; and T is the absolute temperature, K. The equation can then be shortened to the model in Equation (14) using the expression for Gibbs free energy change (between a catalytically active and reversibly denatured inactive state) at a constant temperature (Equation (13)):

$$\Delta G = \Delta H - T \cdot \Delta S \quad (13)$$

$$u(T) = C \cdot T \cdot e^{-\Delta^{\ddagger}H^{\circ}/(R \cdot T)} \cdot \frac{1}{1 + e^{-\Delta G/(R \cdot T)}} \quad (14)$$

where E_0 is assumed to be constant and $c \cdot e^{\Delta^{\ddagger}S^{\circ}/R} \cdot E_0$ is compressed to C. The fraction term containing the Gibbs free energy change can be assumed as the probability that the enzyme is in its native, and not its inactive, state. In the temperature region for a catalytically active enzyme, ΔG, J, has high positive values, yielding almost zero for the exponential term in the denominator of the probability term, and thus one for the probability for a catalytically active enzyme.

3.3. The Model of Sharpe (1977)

In 1977, Sharpe et al. [63,64] merged the models of Johnson and Lewin with the model of Hultin, which were both founded on Eyring's theory and modeled on the activated complex in chemical reactions [20,60,65,66]. The result was a unified rate model for the description of biological processes at physiological temperatures. Sharpe's model was originally developed for poikilotherms. Sharpe assumed balanced growth with a constant total amount of compounds per cell and just a single rate-controlling enzyme determining the development rate at all temperatures. Its reaction rate is of a zero order. The total concentration of enzyme (active + inactive) is assumed to be constant at all temperatures. Three enzyme states are considered and described: an inactivation state at low and high temperatures, as well as an active development state. Sharpe described transition between the states by his model, which depicts the thermal growth curve with the following equation:

$$u(T) = \frac{T \cdot e^{(\Phi - \Delta^{\ddagger}H^{\circ}/T)/R}}{1 + e^{(\Delta S_L - \Delta H_L/T)/R} + e^{(\Delta S_H - \Delta H_H/T)/R}} \quad (15)$$

where T is the temperature, K; is the universal gas constant ~8.314, J mol^{-1} K^{-1}; and the other parameters describe the rate-controlling enzyme reaction, where Φ is a dimensionless conversion factor; $\Delta^{\ddagger}H^{\circ}$ is the enthalpy of activation of the reaction catalyzed by the rate-controlling enzyme, J mol^{-1}; the subscript L accounts for low-temperature inactivation and the subscript H for high-temperature inactivation; and ΔS^*, J K^{-1} mol^{-1}, and ΔH^*, J mol^{-1}, mark the entropic and enthalpic change, respectively, upon high- or low-temperature inactivation specified by the subscript. In 1991, Zwietering et al. [8] rewrote the model of Sharpe exhibiting an Arrhenius-type of temperature dependency using activation energies rather than changes in enthalpy to describe growth. As described by the International Union of Pure

and Applied Chemistry, IUPAC, the (Arrhenius) activation energy (E_a) and enthalpy of activation are not the same, but approximately equal, as they are convertible, depending on the molecularity [22].

$$u(T) = \frac{k_a \cdot e^{\frac{-E_a}{R \cdot T}}}{1 + k_l \cdot e^{-\frac{E_l}{R \cdot T}} + k_h \cdot e^{-\frac{E_h}{R \cdot T}}} \tag{16}$$

where k_a (s^{-1}), k_l (-), and k_h (-) are collision factors that are dimensionless in the denominator, as described by Zwietering et al. [8]; E, J mol^{-1}, represents the activation energy; subscript a accounts for the rate-determining enzyme reaction; subscripts h and l describe high- and low-temperature inactivation, respectively; R is the gas constant ~8.314, J mol^{-1} K^{-1}; and T is the temperature, K.

3.4. The Model of Mohr (1980)

Mohr and Krawiec [24] analyzed the thermal growth curves for 12 bacterial species. Among them were thermophiles, mesophiles, and psychrophiles. They used the Arrhenius plot for their data, where $\ln(\mu)$ is plotted against the reciprocal temperature in Kelvin. They reported two different slopes for the Arrhenius profiles for some mesophiles and thermophiles at suboptimal temperatures. The temperature at the interception point were both slopes meet is referred to as the "critical temperature" (T_{crit}) [24,67]. This point marks the turning point where the organization of an organism, and hence it growth behavior, changes. In order to describe the two different slopes, they proposed two equations, which they reduced to one with the assumption that "[...] a balance of organizations exists at any temperature":

$$u(T) = A_1 \cdot e^{-E_1/R \cdot T} - A_2 \cdot e^{-E_2/R \cdot T} \; T_{crit} < T < T_{\max} \tag{17}$$

$$u(T) = A_1' \cdot e^{E_1'/R \cdot T} \quad T_{\min} < T < T_{crit} \tag{18}$$

$$u(T) = \frac{1}{A_1^* \cdot e^{E_1'/R \cdot T} + A_1^{**} \cdot e^{E_1/R \cdot T}} - A_2 \cdot e^{-E_2/R \cdot T} \tag{19}$$

where A_1, A_1', and A_2 are referred to as pre/non-exponential, collision, or frequency actors, s^{-1}; E_1, E_1', and E_2 are referred to as temperature characteristics, J mol^{-1}; R is the gas constant ~8.314, J mol^{-1} K^{-1}; and T is the temperature, K. The parameters marked with a " ' " are used to describe temperature-dependent growth for $T_{\min} < T < T_{crit}$, whereas parameters without " ' " are used to describe temperature-dependent growth for $T_{crit} < T < T_{\max}$, $A_1^* = 1/A_1'$, and $A_1^{**} = 1/A_1$.

3.5. The Model of Schoolfield (1981)

Schoolfield developed a non-linear regression model [68] based on the model proposed by Sharpe. His group reformulated the model of Sharpe and eliminated the high correlations of Sharpe's parameters (e.g., 0.9996). Furthermore, Schoolfield et al. argued that there is no "readily apparent" initial guess for beginning iterations for parameter estimation. Hence, they also aimed to facilitate the regression process and parameter estimation.

$$u(T) = \frac{u_{25} \cdot \frac{T}{298} \cdot e^{[\frac{\Delta^{\ddagger}H^{\circ}}{R} \cdot (\frac{1}{298} - \frac{1}{T})]}}{1 + e^{[\frac{\Delta H_L}{R} \cdot (\frac{1}{T_{1/2_L}} - \frac{1}{T})]} + e^{[\frac{\Delta H_H}{R} \cdot (\frac{1}{T_{1/2_H}} - \frac{1}{T})]}} \tag{20}$$

Schoolfield et al. chose 25 °C (298 K) and the respective specific growth rate u_{25}, s^{-1}, as a reference because enzyme inactivation would be low or not present at that temperature in most biological systems. $\Delta^{\ddagger}H^{\circ}$ is the enthalpy of activation of the reaction catalyzed by the rate-controlling enzyme, J mol^{-1}; the subscript L accounts for low-temperature inactivation and the subscript H for high-temperature inactivation of the enzyme; and ΔH_* marks the enthalpic change upon high- or low-temperature inactivation specified by the subscript, J mol^{-1}. With an increasing or decreasing temperature, 50%

of the rate-controlling enzyme is inactivated by either a high $T_{1/2_H}$, K or low temperature $T_{1/2_L}$, K, as previously described by Hultin [66] and adopted by Schoolfield et al. [68].

3.6. The Models of Ratkowsky and Zwietering (1982–1991)

As extensively reviewed by Grimaud et al. [61], several models for temperature-dependent growth in biological systems have been developed. Most of these models were developed to describe food spoilage and medical applications. One often cited (802, Scopus, 8 August 2019) empirical model is the square root model proposed by Ratkowsky et al., as an alternative to the widely used Arrhenius model, to describe growth as a function of temperature [26]:

$$u(T) = [b_1 \cdot (T - T_{\min})]^2 \tag{21}$$

where b_1 is a Ratkowsky parameter, K^{-1} $s^{-0.5}$, and T_{min} is the minimum temperature of growth, K. This model was extended to the complete bio-kinetic range in 1983 by the same author [59]:

$$u(T) = \left(b_2 \cdot (T - T_{\min}) \cdot \left\{1 - e^{[c_2 \cdot (T - T_{\max})]}\right\}\right)^2 \tag{22}$$

where c is a Ratkowsky parameter, K^{-1}, and T_{max} is the maximum temperature, K, at which growth is observed. Zwietering et al. [8] argued that Ratkowsky's model could not be used for temperatures above T_{max} because the model predicted positive values for growth rates beyond the high-temperature end of the thermal niche. They therefore adapted the model accordingly and the result is shown in Equation (23).

$$u(T) = [b_3 \cdot (T - T_{\min})]^2 \cdot \left\{1 - e^{[c_3 \cdot (T - T_{\max})]}\right\} \tag{23}$$

3.7. The Model of Roels (1983)

In 1983, Roels et al. [69] developed a model to describe the growth rate as a function of temperature. The numerator has an Arrhenius-type appearance and the energy for activation was replaced by the Gibbs free energy change upon denaturation of a rate-controlling enzyme in the denumerator.

$$u(T) = \frac{A \cdot e^{\left(\frac{-E_G}{RT}\right)}}{1 + B \cdot e^{\left(\frac{-\Delta G_d}{RT}\right)}} \tag{24}$$

where A and B are pre-exponential factors, s^{-1}; R is the gas constant ~8.314, J mol^{-1} K^{-1}; and T is the temperature, K.

3.8. The Model of Davey (1989)

Davey proposed an empirical generalized predictive model based on a modified linear-Arrhenius equation, which combined the influence of temperature and water activity to describe microbial growth [70]. The activation energy parameter from the original Arrhenius model was replaced in Davey's model by two coefficients of inverse temperature. In his work, Davey provided and evaluated models for the influence of environmental factors like the a_w value or pH in combination with temperature, as well as temperature as the sole influencing factor, on growth [70–72]. The model describing temperature as the sole environmental factor is shown in Equation (25):

$$u(T) = e^{C_0 + C_1/T + C_2/T^2} \tag{25}$$

where C_0–C_2 are dimensionless Davey coefficients, - and the energy of activation given in the Arrhenius equation is replaced by two parameters of reciprocal temperature, K. Two years later, in 1991, Davey used the model for predicting the temperature-dependent lag time [72].

3.9. The Models of Lobry and Rosso (1991–1993)

In 1991, Lobry [73] developed an empirical model that includes the three cardinal temperatures (T_{min}, T_{opt}, and T_{max}) as parameters. The cardinal temperature model (CTM) estimates positive values for growth rates at temperatures between the low temperature and high temperature end (T_{min} and T_{max}), with the highest growth rate (u_{opt} (s^{-1})) at T_{opt}. Outside the thermal niche ($T < T_{min}$; $T > T_{max}$), negative values are predicted. Each microbial species exhibits these three characteristic cardinal temperatures, which permits direct biological interpretation of the model parameters and facilitates parameter estimation using experimental data for Lobry's CTM-model Equation (26). The authors emphasize the "absence of high structural correlations" between parameters of their model. In 1991, Rosso et al. [74] further elaborated Lobry's empirical model by including the point of inflection in the suboptimal range of temperatures, which was experimentally determined. Following this, the so-called cardinal temperature model with inflection (CTMI; Equation (27)) could be used to accurately predict growth in the suboptimal range of temperature. Rosso's group noted an "unexpected" high linear correlation between cardinal temperatures, especially between T_{max} and T_{opt}, with r = 0.991. They then argued that due to the correlations found, one instead of three cardinal temperatures could sufficiently describe the permissive temperature range for growth. They also mentioned an exception for the stated relationships between the cardinal temperatures for the growth behavior of *Vibrio* sp. In total, they analyzed 47 different data sets describing the growth of psychrophilic, mesophilic, and thermophilic strains.

$$u(T) = u_{opt} \cdot \left[1 - \frac{\left(T - T_{opt}\right)^2}{\left(T - T_{opt}\right)^2 + T \cdot (T_{\max} + T_{\min} - T) - T_{\max} \cdot T_{\min}} \right] \tag{26}$$

$$u(T) = u_{opt} \cdot \frac{(T - T_{\max}) \cdot (T - T_{\min})^2}{\left(T_{opt} - T_{\min}\right) \cdot \left[\left(T_{opt} - T_{\min}\right) \cdot \left(T - T_{opt}\right) - \left(T_{opt} - T_{\max}\right) \cdot \left(T_{opt} + T_{\min} - 2 \cdot T\right)\right]} \tag{27}$$

3.10. The Model of Blanchard (1996)

Blanchard et al. [75] originally developed their model to quantify the short-term temperature effect on natural assemblages of microphytobenthos' photosynthetic capacity. Blanchard described a progressive increase in photosynthetic capacity during a temperature increase up to an optimum temperature, with a rapid decrease when the temperature was raised beyond the optimum. For the model, cardinal temperatures (T_{min}, T_{opt}, and T_{max}) with a biological meaning are used to facilitate a reasonable initial guess for parameter estimation. Grimaud et al. [61] rewrote the Blanchard model to represent growth as a function of temperature instead of photosynthetic capacity, as shown in Equation (28):

$$u(T) = u_{opt} \left(\frac{T_{\max} - T}{T_{\max} - T_{opt}} \right)^{\beta} \cdot e^{-\beta \cdot (T_{opt} - T) / (T_{\max} - T_{opt})} \tag{28}$$

where μ_{opt}, s^{-1}, is the maximal specific growth rate at optimal temperature T_{opt}, K; T_{max}, K, is the maximum temperature where growth is observed; and β is a dimensionless Blanchard parameter.

3.11. The Models of Eppley and Norberg (2004)

Eppley [76] proposed a simple function with a positive exponential correlation between temperature and maximum expected growth, as shown in Equation (29). He stated that this model may be used for a generalized estimate for μ_{max} in unicellular algae for temperatures <40 °C.

$$u(T) \; = \; 0.851 \cdot 1.066^{T} \tag{29}$$

The proposed Eppley curve or envelope function of Equation (29) shows the evolutionary interspecific upper limit for the maximum specific growth rate at any temperature up to 40 °C. The limit for the maximum growth rate increases exponentially until 40 °C in Eppley's function. For model assembly, Eppley used almost 200 data points of different species of unicellular algae [76]. Based on Eppley's findings, Jon Norberg developed a model for temperature-dependent growth in 2004 [77], shown in Equation (30).

$$u(T) = \left[1 - \left(\frac{T - Z}{w}\right)^2\right] \cdot 0.59 \cdot e^{0.0633 \cdot T} \tag{30}$$

An envelope function $0.59 \times e^{0.0633T}$ according to Eppley is contained in Norberg's model for temperature-dependent growth, where T, K, is the ambient temperature and Z, K, is the temperature with the maximum specific growth rate derived from the envelope function representing T_{opt} respectively. The width of the temperature response function is determined by the parameter w, K, meaning the width of the thermal niche. A generalized form of the Eppley–Norberg model Equation (31) would add a and b as dimensionless parameters, -, generalizing the Eppley envelope function.

$$u(T) = \left[1 - \left(\frac{T - Z}{w}\right)^2\right] \cdot a \cdot e^{b \cdot T} \tag{31}$$

3.12. The Modified Master Reaction Model (2005)

In 1967, Brandts recognized that the master reaction model proposed by Johnson and Lewin (see Equation (12)) failed to describe enzymatic reactions adequately when applied to the full bio kinetic temperature range [78,79]. Arguably, the limitations of the model arise from the assumed temperature independence of ΔG in the master reaction model upon protein denaturation. Therefore, Brandts et al. attributed the temperature dependency to ΔG by simply using an empirical polynomial expression relating ΔG to T. In 1974, Privalov et al. [80] reported a linear relation between enthalpy and entropy and temperature upon protein unfolding when assuming a specific constant heat capacity change for a specific protein. Almost 20 years later, it was reported that the change in enthalpy upon denaturation (ΔH_d) normalized to the number of amino acid residues (or molecular weight, respectively) at a specific temperature (T^*_H ~373 K) converged to a common value (ΔH^*). Likewise, the same convergence behavior to one common value (ΔS^*) at a specific temperature (T^*_S ~385 K) for entropy upon denaturation (ΔS_d) normalized to the number of amino acid residues was described for a number of homologous compounds [80–83]. The so-called convergence temperatures (T^*_H and T^*_S) were obtained as the temperatures where the apolar contributions (apolar hydrogen atoms CH) to the corresponding changes in entropy or enthalpy, respectively, upon denaturation approach zero [81,82,84]. Therefore, ΔH^* describes only polar and van der Waals interactions and ΔS^* primarily accounts for configurational entropy [83]. In 1990, Murphy et al. [81] analyzed the convergence behavior by plotting ΔH_d or ΔS_d normalized to mol amino acid residue against the normalized heat capacity change (ΔC_p) upon denaturation and obtained the following correlations:

$$\Delta S_d = \Delta S^* + \Delta C_p \cdot ln\left(\frac{T}{T^*_S}\right) \tag{32}$$

$$\Delta H_d = \Delta H^* + \Delta C_p \cdot \left(T - T^*_H\right) \tag{33}$$

The above-mentioned equations describe a temperature-dependent enthalpic and entropic change upon denaturation normalized to the number of amino acid residues in a protein (n). From Murphy's findings [81], the change in Gibbs free energy upon protein denaturation (~protein thermal stability) is given by

$$\Delta G_d(T) = n \cdot \left[\Delta H^* - T \cdot \Delta S^* + \Delta C_p \cdot \left[\left(T - T^*_H\right) - T \cdot ln\left(\frac{T}{T^*_S}\right)\right]\right] \tag{34}$$

where $\Delta C_p \cdot \left[\left(T - T_H^*\right) - T \cdot ln\left(\frac{T}{T_S^*}\right)\right]$ accounts for the hydrophobic contribution of the Gibbs free energy change upon denaturation of the rate-determining "master enzyme". Ross connected Murphy's findings with the rewritten master reaction model of Johnson and Lewis, where the change in enthalpy between the catalytically active and inactive state of the rate-limiting enzyme was replaced by the temperature-dependent Gibbs free energy change [79,85].

$$u(T) = \frac{c \cdot T \cdot e^{(-\Delta^{\ddagger}H^{\circ}/R \cdot T)}}{1 + e^{(-\Delta G_d/R \cdot T)}} \tag{35}$$

Replacing the description of the Gibbs free energy in the denominator of Equation (35) with the term in Equation (34) resulted in a modified master reaction model:

$$u(T) = \frac{c \cdot T \cdot e^{(-\Delta^{\ddagger}H^{\circ}/R \cdot T)}}{1 + e^{(-n \cdot \{\Delta H^* - T \cdot \Delta S^* + \Delta C_p \cdot [(T - T_H^*) - T \cdot ln(T/T_S^*)]\}/R \cdot T)}}. \tag{36}$$

In the denominator of Equation (36), the thermodynamic parameters ΔH^*, ΔS^*, and ΔC_p are normalized to mol amino acid residue. In 2005, Ratkowsky et al. [79] reduced the eight-parameter model given in Equation (36) to a five-parameter model by simply applying the universal constants for globular proteins T_H^* = 373.6 K, T_S^* = 385.2 K, and ΔS^* = 18.1 J K^{-1} found by Murphy et al. [81,82] to the model. Ratkowsky's group fitted the reduced five-parameter modified master reaction model to data from 35 bacterial strains. The universal constant ΔH^* suggested by Murphy's group with 5640 J mol^{-1} amino acid residue was found to be unsuitable for representing bacterial growth when applied to five data sets of Ross [86]. The reduced modified master reaction model with applied universal constants evaluated in the work of Ratkowsky et al. [79] is given in Equation (37).

$$u(T) = \frac{c \cdot T \cdot e^{(-\Delta^{\ddagger}H^{\circ}/8.314 \cdot T)}}{1 + e^{(-n \cdot \{\Delta H^* - T \cdot 18.1 + \Delta C_p \cdot [(T - 373.6) - T \cdot ln(T/385.2)]\}/8.314 \cdot T)}} \tag{37}$$

3.13. The Model of Zeldovich (2007–2016)

The group of Zeldovich [87] argued that the whole proteome has to be considered when describing the temperature response and sensitivity of an organism. Ghosh and Dill [88] continued the work of Zeldovich et al. and proposed a model that considers the folding stabilities across an organisms' proteome to describe temperature-dependent growth rates of bacteria. They assumed that the growth rate was a function of temperature composed of a product of two factors: First, Arrhenius-type low-temperature activation for one or more activated metabolic processes controlling the increase of growth rate at low temperatures, and second, a term accounting for the folded part of the proteome at any temperature, which also depicts the "denaturation catastrophe" when reaching high temperatures.

$$u(T) = u_0 \cdot e^{\left(\frac{-\Delta^{\ddagger}H^{\circ}}{k \cdot T}\right)} \prod_{i=1}^{\Gamma} \frac{1}{1 + e^{(-\Delta G_{\mathrm{un}}(N_i, T)/R \cdot T)}}, \tag{38}$$

where μ_0 is a growth rate reference, s^{-1}. The parameter $\Delta^{\ddagger}H^{\circ}$, J mol^{-1}, describes the activation barrier for growth (e.g., an essential growth-limiting metabolic rate). The authors found that the activation barrier for growth (~68.2 kJ mol^{-1}) in *E. coli* approximately corresponds to the energy needed by ribosomes to form a peptide bond. Hence, the authors identified ribosomal action to grow protein chains as one of the key growth rate-limiting factors, along with protein motions necessary for enzymatic reactions. Γ describes the amount of essential proteins required for growth. The product

term accounts for the probability that the *i*th essential protein composed of N_i amino acids is in its native state, which is expressed by ΔG_{un} in Equation (39):

$$\Delta G_{un} = -k_B \cdot T_0 \cdot n \cdot \left[\begin{array}{c} \frac{g_0 + m_1 \cdot c}{k_B \cdot T_0} + \frac{\Delta C_p}{k_B \cdot T_0} \cdot \left(T - T_H^*\right) + \frac{T}{T_0} \cdot ln(z) - \frac{T}{T_0} \cdot \Delta C_p \cdot ln\left(\frac{T}{T_S^*}\right) + \frac{l_b}{2 \cdot n} \cdot \\ \left(\frac{{Q_n}^2}{R_n \cdot (1 + \kappa \cdot R_n)} - \frac{{Q_d}^2}{R_d \cdot (1 + \kappa \cdot R_d)}\right) \end{array} \right] \quad (39)$$

where k_B is the Boltzmann constant ~$1.381 \cdot 10^{-23}$, J K^{-1}; T_0 = 300 K; n is the number of amino acids with respective to the chain length of a protein; g_0 is the free energy upon amino acid desolvation and upon contact; c is the concentration of denaturant; ΔC_p is the heat capacity change upon denaturation, J K^{-1} mol-residue^{-1}; T is the absolute temperature, K; T_H^* = 373 K and T_S^* = 385 K are the enthalpic and entropic convergence temperatures, respectively; z is defined as the loss of average conformational freedom per backbone bond; l_b is the average Bjerrum length; Q_n and Q_d are the total net charge of native and denatured protein, respectively; R_n and R_d account for the radii of native and denatured protein, respectively; κ is the reciprocal of the Debye length (for further details, see [89,90]). To obtain the probability distribution for protein stabilities of a proteome p(ΔG), Equation (39) can be used. The equation accounts for the stability of an average single protein of length n and may be used in combination with the distribution of protein chain lengths (P(n)) of a cell available for various cell types from genomic/proteomic data in order to calculate temperature-dependent proteome stability.

3.14. The Model of Daniel (2010)

In 2010, Daniel et al. [91] proposed the equilibrium model to describe temperature-dependent catalytic activity of enzymes in non-limiting conditions. The group reported that the decrease of the catalytic rate constant (k_{cat}) of tested enzymatic reactions above the optimal temperature (T_{opt}) does not entirely correspond to thermal stability data and irreversible denaturation. Furthermore, they found that part of the activity loss above T_{opt} was reversible and probably associated with a "conformational, dynamic and solvent-based effect" altering the active site of the enzyme. To explain the higher than expected decrease of k_{cat} at a certain temperature, they suggested that an enzyme may be present in three states: (i) catalytically active (E_{act}); (ii) catalytically inactive, but not (significantly) unfolded (E_{inact}); and (iii) irreversibly denatured (X). They rapid changes of the Michaelis constant (K_m), describing an enzyme's affinity towards a substrate, that occur with temperature support their hypothesis of an "E_{inact} state", where the active site is altered. They argue that the active site may need a certain degree of flexibility to function properly and is therefore more prone to changes in temperature affecting conformation and dynamics.

$$E_{act} \overset{K_{eq}}{\rightleftharpoons} E_{inact} \overset{k_{inact}}{\rightarrow} X \quad (40)$$

Daniel's group assumed a rapid equilibrium between E_{act} and E_{inact} and time-dependent denaturation at a certain temperature. The conversion rate of E_{act} to E_{inact} is thereby assumed to be faster than the rate of denaturation and catalytic reaction rate, respectively. The authors investigated the applicability of the model for >50 datasets of >30 enzymes of different reaction classes and structures (monomeric to hexameric) and concluded that their model is universally applicable and independent of the reaction type and enzymatic structure [91]. The model may therefore be suitable for describing a thermal growth curve, where a rate-controlling enzymatic reaction is often assumed to describe temperature-dependent growth (e.g., master reaction model, [60]).

$$u(T) = \frac{k_B}{h} \cdot T \cdot E_0 \cdot e^{-\left(\frac{\Delta G_{cat}^*}{R \cdot T}\right)} \cdot e^{\left[-\frac{k_B}{h} \cdot T \cdot \frac{e^{-\left(\frac{\Delta G_{inact}^*}{R \cdot T}\right)} \cdot e^{\left(\Delta H_{eq} \cdot \left(\frac{1}{T_{eq}} - \frac{1}{T}\right)/R\right) \cdot t}}{1 + e^{\left(\Delta H_{eq} \cdot \left(\frac{1}{T_{eq}} - \frac{1}{T}\right)/R\right)}}\right]} \cdot \left[1 + e^{\left(\Delta H_{eq} \cdot \left(\frac{1}{T_{eq}} - \frac{1}{T}\right)/R\right)}\right]^{-1} \quad (41)$$

where k_B is the Boltzmann constant ~1.381 · 10^{-23}, J K^{-1}; h is the Planck's constant ~6.626·10^{-34}, J s^{-1}; T is the absolute temperature, K; E_0 is the total enzyme concentration composed of the sum of E_{act}, E_{inact}, and X, mol m^{-3}; ΔG^*_{cat} is the Gibbs free energy of activation of the enzymatic reaction; R is the universal gas constant ~8.314, J mol^{-1} K^{-1}; ΔG^*_{inact} is the Gibbs free energy of activation for the irreversible denaturation of the rate-controlling enzyme; ΔH_{eq} is the enthalpic change between E_{act} and E_{inact}; T_{eq} is the equilibrium temperature where the rate-controlling enzyme is present as 50:50 E_{act} and E_{inact}, K; and t is the time, s.

3.15. The Model of Kooijman (2010)

The DEB or Dynamic Energy Budget theory deals with the description of rates for physiological processes. Assimilation, growth, respiration, maintenance, or reproduction in individual, not further specified, "organisms" are analyzed and described by the generalized theory. The rates are described as a function of the environment, like the temperature or nutrient availability, and the state of the organism like size or age, for example. S.A.L.M. Kooijman, whose early concepts on energy budgets were published in 1986 [92], summarized his work in "DEB theory for Metabolic Organization" in 2010 [93]. In DEB theory, temperature-dependent growth is described by a reformulated Arrhenius equation in the numerator and complemented by a term inspired by Sharpe's model [63] for reduced rates at the high- and low-temperature end in the denominator. The equation therefore accounts for the amount of enzyme in its native state and considers a possible transition to an inactive state via hot and cold denaturation. Kooijman argues that Eyring's thermodynamic interpretation of the Arrhenius type of temperature dependence might only be understood as an approximation. It is an enormous step from Eyring's model, considering bimolecular reactions in the gas phase, to physiological rates with many compounds [94].

$$u(T) = \frac{k_1 \cdot e^{T_A/T_1 - T_A/T}}{1 + e^{T_{Al}/T - T_{Al}/T_l} + e^{T_{Ah}/T_h - T_{Ah}/T}} \tag{42}$$

where T_1 is a reference temperature, K, with the corresponding rate k_1, s^{-1}; T_A is the Arrhenius temperature (i.e., linear slope of the Arrhenius plot), K; T_l and T_h mark the cardinal temperatures flanking the thermal niche (low- and high-temperature denaturation, respectively), K; and T_{Al} and T_{Ah} account for Arrhenius temperatures at temperature boundaries of the thermal niche, K.

3.16. The Model of Huang (2011)

The group of Huang [95] developed a model by modifying and combining the Arrhenius equation with the theory and model of Eyring et al. [4,20,65].

$$u(T) = A \cdot T \cdot e^{-\left(\frac{\Delta G'}{R \cdot T}\right)^{\alpha}} \tag{43}$$

where $\Delta G'$, J mol^{-1}, accounts for an energy term; R is the universal gas constant ~8.314, J mol^{-1} K^{-1}; T is the absolute temperature, K; α is a Huang parameter, K^{-1}; and A describes the collision or frequency factor, s^{-1}. Huang reports that their model can only sufficiently describe growth behavior at a suboptimal temperature. To extend their model to the entire physiological temperature range, they used an expression known from Ratkowsky et al. [59]:

$$u(T) = A \cdot T \cdot e^{-\left(\frac{\Delta G'}{R \cdot T}\right)^{\alpha}} \cdot \left[1 - e^{c_2 \cdot (T - T_{max})}\right] \tag{44}$$

where c_2 is a Ratkowsky parameter, K^{-1}, and T_{max} is the maximum growth temperature, K. Huang's group reported good fits (R^2 = 0.985) for their model using data for thermal growth rates from five different bacteria.

3.17. The Model of Corkrey (2014)

In 2014, Corkrey et al. attempted to build a universal mechanistic model [58]. It was used to model the growth of 230 different strains of unicellular and multicellular organisms ranging from psychrophilic to hyperthermophilic, covering a temperature range of 124 °C, from −2 °C to +122 °C. They therefore argued that their findings might be used to model the dependence of the growth rate on temperature for all unicellular and multicellular life forms. Being able to find a good fit for their universal model to the thermal growth curves of various life forms, they concluded that there might be evidence for the presence of a single highly conserved reaction in the last universal common ancestor. Under all limiting conditions, a single-enzyme-catalyzed reaction rate, which controls the growth rate, is described in the numerator of the Corkrey model by an Arrhenius type of temperature dependency. The denominator accounts for the effects of temperature on protein conformation, which causes alterations in catalytic activity of the putative enzyme and therefore a change in the expected rate.

$$u(T) = \frac{T \cdot e^{(c - \frac{\Delta^{\ddagger}H^{\circ}}{R \cdot T})}}{1 + e^{(-n \cdot \frac{\Delta H^{*} - T \cdot \Delta S^{*} + \Delta Cp \cdot (T - T_{H}^{*} - T \cdot ln(T/T_{S}^{*}))}{R \cdot T})}} \tag{45}$$

where $\Delta^{\ddagger}H^{\circ}$ is the enthalpy of activation, J/mol; R is the universal gas constant ~8.314, J mol^{-1} K^{-1}; c is a dimensionless scaling factor; T is the temperature, K; ΔC_p is the heat capacity change, J K^{-1} mol^{-1} -amino acid residue, upon denaturation of the putative enzyme; ΔH^{*} is the change of enthalpy, J mol^{-1} amino acid residue, at the convergence temperature T_H^{*}, K, for enthalpy of protein unfolding; and ΔS^{*} is the change of entropy, J K^{-1}, at the convergence temperature T_S^{*}, K, for the entropy of protein unfolding.

3.18. The Model of Hobbs (2014)

The heat capacity model or macromolecular rate theory was proposed by Hobbs et al. [96] and applied by Schipper et al. [97]. They state that enzymatic rates show Arrhenius behavior when increasing with temperature, until an optimum (T_{opt}), but argue that decreasing rates above T_{opt} cannot sufficiently be explained only by denaturation of the enzymes. They have reported the effect of a heat capacity change upon activation (between the ground state and transition state of a rate-limiting enzyme) that shapes the thermal growth curve. The change in heat capacity affects the temperature dependency of $\Delta^{\ddagger}G^{\circ}$ (Gibbs free energy difference, between a ground state and transition state) that is in turn responsible for determining the temperature dependency of enzymatic activity. They state that the change in heat capacity influencing enzymatic rates implicates temperature dependence for various biological rates, ranging from "enzymes to ecosystems". Hobbs et al. formulated their findings using Eying's Equation (46) as a scaffold and a term to describe the degree of temperature dependence of $\Delta^{\ddagger}G^{\circ}$ with $\Delta^{\ddagger}C_p^{\circ}$ Equation (47). Assuming $\Delta^{\ddagger}C_p^{\circ}$ to be zero, $\Delta^{\ddagger}G^{\circ}$ would be independent from temperature and the reaction behavior of the growth rate-limiting enzyme would follow an Arrhenius type of temperature dependence. Large negative values for $\Delta^{\ddagger}C_p^{\circ}$ would lead to a significant temperature dependence of $\Delta^{\ddagger}G^{\circ}$, leading to a non-Arrhenius behavior and explaining a decrease in reaction rate above T_{opt}, independent of denaturation. Compared to the master reaction model, heat capacity theory takes into account that enzymes are in fast equilibrium with the transition state and denaturation does not easily occur [61,96,97].

$$u(T) = \frac{k_B}{h} \cdot T \cdot e^{(-\Delta^{\ddagger}G^{\circ}(T)/R \cdot T)} \tag{46}$$

$$\Delta^{\ddagger}G^{\circ}(T) = \Delta^{\ddagger}H_{T_0}^{\circ} + \Delta^{\ddagger}C_p^{\circ} \cdot (T - T_0) + T \cdot \left(\Delta^{\ddagger}S_{T_0}^{\circ} + \Delta^{\ddagger}C_p^{\circ} \cdot ln\left(\frac{T}{T_0} \right) \right) \tag{47}$$

where k_B is the Boltzmann constant ~1.381 · 10^{-23}, J K^{-1}; h is the Planck's constant ~6.626·10^{-34}, J s^{-1}; $\Delta^{\ddagger}G^{\circ}$ is the Gibbs free energy difference, between a ground state and transition state, J mol^{-1}; R is the universal gas constant ~8.314, J mol^{-1} K^{-1}; T is the absolute temperature, K; T_0 is a reference temperature, K; $\Delta^{\ddagger}H^{\circ}_{T_0}$ and $\Delta^{\ddagger}S^{\circ}_{T_0}$ are enthalpic and entropic change between reactants and the transition state at the reference temperature T_0; $\Delta^{\ddagger}C^{\circ}_{p}$ is the heat capacity change between reactants and the transition state, J mol^{-1} K^{-1}.

3.19. The Model of DeLong (2017)

In 2017, DeLong et al. [98] argued that models describing the thermal growth curve lack the assumption that the catalyzing enzyme lowers the activation energy of the rate-determining reaction. They therefore introduced a model that describes the reduction of required activation energy for the rate-determining reaction as a function of free energy (enzyme stability) of the catalyzing enzyme. This term was incorporated into the dividend of the exponential term of the Arrhenius function. The Arrhenius activation energy (E_a; see Equation (4)) was replaced with the difference of a baseline energy (E_b, J), describing kinetic requirements as if the reaction would take place outside an organism, lowered by the enzymatic contribution (E_c, J) inside an organism, yielding Equation (48):

$$u(T) = A \cdot e^{\frac{-(E_b - E_c)}{k_B \cdot T}} \tag{48}$$

where the authors used the Boltzmann constant k_B ~1.381 · 10^{-23}, J K^{-1}, instead of the universal gas constant in the divisor of the exponential term and T is the absolute temperature, K. The dividend of the exponential term then accounts for the activation energy lowered by the enzymatic action. The extent of enzymatic contribution (E_c) depends on the activity status of the enzyme, which is given by probability terms of protein stability. The temperature-dependent protein stability is given by ΔG (Equation (49)), where ΔH, J, is the change of enthalpy and ΔC_p, J mol^{-1} K^{-1}, the change in heat capacity, both relative to the melting temperature T_m, K, between the folded and unfolded state. At T_m, ΔH is by definition zero and increases for temperatures below T_m. ΔC_p reflects the extent of free energy that can be kept by the enzyme without changing the temperature, which increases below T_m with a decreasing temperature. The authors assumed that the probability of the maximum contribution of the enzyme to reduce the activation energy by the amount E_L approaches 1 at $\Delta G_{\max}$. Hence, the probability function Equation (50) is composed of the maximum amount (E_L) by which an active enzyme can lower the activation energy and the probability of the enzyme being correctly folded and active, given by the ratio of ΔG to $\Delta G_{\max}$. This transformation yields probability terms for each parameter in Equation (49), as presented in Equations (51) and (52). Therefore, Equation (49) can be rewritten as Equation (53).

$$\Delta G = \Delta H \cdot \left(1 - \frac{T}{T_m}\right) + \Delta C_p \cdot \left(T - T_m - T \cdot ln\left(\frac{T}{T_m}\right)\right) \tag{49}$$

$$E_c = E_L \cdot \frac{\Delta G}{\Delta G_{\max}} \tag{50}$$

$$E_{\Delta H} = E_L \cdot \frac{\Delta H}{\Delta G_{\max}} \tag{51}$$

$$E_{\Delta C_p} = E_L \cdot \frac{\Delta C_p}{\Delta G_{\max}} \tag{52}$$

$$E_c = E_{\Delta H} \cdot \left(1 - \frac{T}{T_m}\right) + E_{\Delta C_p} \cdot \left(T - T_m - T \cdot ln\left(\frac{T}{T_m}\right)\right) \tag{53}$$

Combining the probability function Equation (53) for the degree of enzymatic contribution to lowering the baseline energy E_b of the rate-determining reaction with the Arrhenius-type Equation (48) yields the enzyme-assisted Arrhenius model in Equation (54).

$$u(T) = A \cdot e^{\frac{-(E_b - (E_{\Delta H} \cdot (1 - \frac{T}{Tm}) + E_{\Delta Cp} \cdot (T - Tm - T \cdot ln(\frac{T}{Tm}))))}{k_B \cdot T}} \quad (54)$$

3.20. Additional Temperature Models

In Table 1 further models describing a hunchback-shaped curve for temperature-dependent rates are summarized.

Table 1. Models describing a hunchback-shaped curve of temperature-dependent rates (not explained in the text).

Model	Equation	Source
Lehman et al.	$u(T) = \begin{cases} e^{-2.3 \cdot [\frac{(T - T_{opt})}{(T\max - T_{opt})}]^2}, & T > T_{opt} \\ e^{-2.3 \cdot [\frac{(T - T_{opt})}{(T\min - T_{opt})}]^2}, & T \leq T_{opt} \end{cases}$	[99]
Moison et al.	$u(T) = \begin{cases} \log(2) \cdot 0.851 \cdot \left(1.066^T\right) \cdot e^{-\lvert T - T_{opt} \rvert \cdot \frac{3}{T_{low}}}, & T \leq T_{opt} \\ \log(2) \cdot 0.851 \cdot \left(1.066^T\right) \cdot e^{-\lvert T - T_{opt} \rvert \cdot \frac{3}{T_{high}}}, & T > T_{opt} \end{cases}$	[100]
Bitaube Pérez et al.	$u(T) = A_1 \cdot e^{(\frac{E_1}{R \cdot T} \cdot \frac{T - T_{ref}}{T_{ref}})} - A_2 \cdot e^{(\frac{E_2}{R \cdot T} \cdot \frac{T - T_{ref}}{T_{ref}})}$	[101]
Alexandrov et al.	$u(T) = \frac{2 \cdot e^{(\frac{E_a}{R \cdot T_{opt}} - \frac{E_a}{R \cdot T})}}{\left(1 + \left(e^{(\frac{E_a}{R \cdot T_{opt}} - \frac{E_a}{R \cdot T})}\right)^2\right)}$	[102, 103]
Tevatia et al.	$u(T) = u_{opt} \cdot \frac{e^{(\frac{-E_a}{R \cdot T})}}{1 + K \cdot e^{(\frac{-E_d}{R \cdot T})}}$	[104]

T is the absolute temperature, K; T_{opt} is the optimal growth temperature, K; T_{max} and T_{min} are the upper and lower limit of the thermal curve, respectively; T_{low} and T_{high} are shaping parameters that determine asymmetry of the growth curve, -; A_i represents frequency factors, s^{-1}; E_i represents activation energies, J mol^{-1}; R is the universal gas constant ~8.314, J mol^{-1} K^{-1}; T_{ref} is a reference temperature, K; μ_{opt} is the optimal specific growth rate, s^{-1}; E_d is the activation energy for enzyme denaturation, J mol^{-1}; K is a dimensionless inactivation constant.

4. Biotechnological Applications for Targeted Temperature Variation Assisted by Temperature Models

4.1. Temperature with Potential for Bioprocess Design

Temperature is an easily measurable (continuously, in situ, and in real-time) and controllable process variable. In most cases, temperature is controlled at constant values to maintain suitable physiological conditions at a given optimum value. Besides temperature, these requirements are also common for other basic physico-chemical characteristics, including dissolved oxygen and the pH value, which are routinely controlled in most bioreactor cultivations. For bioprocess design and optimization, very few correcting variables (e.g., the addition of fresh feed media) are available to direct a bioprocess towards a desired outcome. There are two strategies for efficiently using the temperature to influence the process outcome. First, alterations in the process temperature may be used to target metabolism, deliberately trigger stress responses, modify enzymatic turnover, or activate existing regulatory mechanisms. Secondly, natural or synthetic regulation mechanisms may be introduced to engineer host microorganisms (see Section 2.2). As such, processes can be designed to include these regulatory mechanisms as an effective tool to influence the process. Even though several systems inducible by temperature have been discovered and made available to biotechnologists in the last decades, only very few have been applied for process design or optimization [12].

4.2. Application of Temperature Models and Temperature for Bioprocesses Design

Mukhtar et al. modeled the temperature-dependent soil nitrification potential rate with the square root model of Ratkowsky et al. and estimated the optimum temperature for the nitrification potential rate with the heat capacity model. The authors suggest that the knowledge of thermodynamic

properties of the soil nitrification response may be used to improve the application of large-scale fertilization, while reducing eutrophication and connected negative environmental impacts [105]. For cleaning purposes of contaminated water with excess nitrogen, denitrifying fixed-bed bioreactors can be used for NO_3^- removal [106]. The group of Nordström et al. used the Eyring equation to simulate the temperature dependency of NO_3^- removal rates in a denitrifying fixed-bad wood chip bioreactor [107]. They used the heat capacity model of Hobbs et al. [96] to derive the optimum temperature for NO_3^- removal by their bioreactor. Nordström et al. reported that NO_3^- removal rates of reducing microbial consortium change over time, while the temperature optimum is shifted towards lower temperatures (from 24.2 to 16.0 °C) [107]. Downshifts in temperature may somewhat be beneficial for a bioprocess, depending on the intended outcome. Seel et al. were able to increase biomass yields to optimize nutrient assimilation at suboptimal temperatures (10 °C) for mesophilic isolates from chilled foods and refrigerators in defined medium compared to their reference strains [52]. They emphasized the importance of defining the "optimum temperature". Seel et al. distinguish between the optimum temperature for the maximum growth rate and the optimum for the maximum biomass yield. At 10 °C, which was around 15–25 °C below the optimum for the maximum growth rate of isolates, they reported an increase of 20%–110% of biomass formation. They argue that the generally assumed optimum growth temperature at μ_{max} may not be the optimum for all biological processes in the host. This has been described for protein production, membrane permeability, and cellular stress [108–112]. The works of Corkrey et al. [58,113] thermodynamically justified the applied findings of Seel et al. Corkrey's model described the connection between the temperature stability of proteins and the growth rate governed by an assumed essential enzymatic reaction, with the temperature for optimal enzyme stability being 10–15 °C below the temperature of μ_{max}. Seel et al. state that due to correct protein folding and protein turnover, energy can be conserved and the biomass yield improved. Perhaps the most popular example for altering temperature as a means of an optimized process outcome can be found during the production of recombinant protein, such as by using *E. coli* as a heterologous expression system [12]. During the process, typically at the stage of the induction of protein expression, a temperature shift is performed, lowering the process temperature by several °C. This temperature shift does not benefit overall transcription or translation activity, but instead, results in an increased amount of correctly folded protein. This is due to lower amounts of recombinant protein being less likely to form inactive, insoluble aggregates (inclusion bodies), and allowing more time for correct folding after translation due to lower protein production rates. In the case of enzyme production, correctly folded protein is a prerequisite of enzymatic activity, and therefore, in most cases, temperature shifts are applied [114]. Another possibility for using temperature as a method for optimizing protein production is the application of thermo-inducible promoter systems. Considering the perspective of bioprocess engineering, it is of high interest to combine strain engineering and process development approaches to maximize overall productivity and yields. Strong chemically inducible promoters and expression systems that are commonly used in laboratory-scale protein expression [115] cause a high degree of metabolic burden to the microorganisms, and as such, protein production results in a simultaneous reduction of growth. It is therefore beneficial for optimized process design to be able to uncouple biomass growth from protein biosynthesis. Furthermore, production of recombinant proteins at early stages of cultivation often results in reduced overall yields, as many proteins are sensitive to degradation by proteases [114,116]. To counteract this instability of recombinant proteins, inducible promoter systems are a possible tool. Thermo-inducible promoter systems have the advantage of not requiring intrusion into the process, as chemical inductors are not required. As such, the risk of contamination, as well as the costs of the process, may be reduced. Nalley et al. evaluated the effect of temperature on growth, fatty acid production, and the fatty acid profile for algae suitable for mass cultivation and biofuel production [117]. They assessed the effect of temperature on microalgae with the model of Norberg [77]. Nalley et al. report temperature-specific fatty acid production, which is mostly controlled by the temperature-dependent growth rate. Furthermore, they found that temperature dramatically influences the fatty acid profile, with an increase in polyunsaturated

fatty acids and decrease in monounsaturated and short fatty acids when increasing the temperature. The thermostable phosphotriesterase-like lactonases (PLLs) from hyperthermophilic *Sulfolobus* genera present an industrially relevant molecule for bioremediation processes, such as in the degradation of highly toxic pesticides like organophosphates [118]. Thermostable PLLs are of particular interest due to their wide temperature and pH working range, as well as resistance to organic solvents. In contrast to mesophilic enzyme isolates, the application of extremozymes is not prone to low stability in solution or an elevated temperature (>30 °C) [119,120]. In the work of Restaino et al., a high-yield pre-industrial-scale process with an optimized purification method for PLLs was developed [11]. The authors exploited the thermostability of PLLs in their downstream and recombinant PLL production in fast-growing mesophilic *E. coli* for their upstream and bioproduction strategy. Impurities were removed by a thermo-precipitation step (65–75 °C), which was optimized using a statistical response surface method to compute optimal precipitation temperatures. The solubility of proteins can be altered by different variables, like the pH, protein concentration, ionic strength, or temperature. Ethanol may be used as a solvent for precipitation, but exhibits the tendency to denature proteins at temperatures above 0 °C. Therefore, cold EtOH is often used for protein fractionation [121]. The authors Cimini et al. investigated the influence of temperature on the industrially relevant capsular polysaccharide (CPS) of *E. coli*, K4 [122]. It exhibits a high similarity to the economically valuable but only expensively extractable chondroitin from animal tissue. Chondroitin is, for example, used in the pharmaceutical sector to prevent osteoarthritis [123]. Cimini et al. found a positive correlation between CPS production and temperature. As stated before, CPS production is thermoregulated and *E. coli* CPS are not expressed at temperatures <20 °C [124]. Another pharmaceutically relevant product and precursor for the commonly used anti-inflammatory drug desfluorotriamcinolone, is 16α-hydroxy hydrocortisone. Hydrocortisone is converted in a temperature-dependent manor by *Streptomyces roseochromogenes* to 16α-hydroxy hydrocortisone. The group of Restaino et al. was able to maximize the bioconversion of hydrocortisone to 16α-hydroxy hydrocortisone, while lowering side-product formation. By adjusting the process temperature to 26 °C and pH to 6, they were able to almost entirely (95%) convert hydrocortisone into the desired product 16α-hydroxy hydrocortisone [125]. Another example for lowering the temperature to obtain optimal expression, correctly folded, and working recombinant enzymes is the mammalian enzyme 6-*O*-sulfotransferase (6-OST). It can be recombinantly produced in *E. coli*. 6-OST is of particular interest as it is required for the industrial and biotechnological production of heparin. So far, the blood anticoagulant heparin has only been derived from animals. 6-OST side-specifically sulfonates a heparin precursor and marks a key step in heparin bioproduction. The group of Restaino et al. reported high cell density cultivation of *E. coli* in which recombinant mammalian 6-OST was produced using an induction strategy optimized for yield and productivity. The strategy involved lowering the temperature (37 to 25 °C) upon induction and using a combination of two inducer molecules to balance the metabolic burden. The combination of balanced biomass growth and the induction strategy resulted in an optimal recombinant enzyme expression and enhanced biomass productivity [126].

An interesting application involving measuring and controlling the temperature during bioprocesses is the estimation of metabolic activity by heat balancing. In a partially isolated bioreactor system, heat generation by metabolic processes can be calculated by measuring heat transfer from or to the bioreactor [5]. This calorimetric technique typically involves the calculation of a heat balance by calculating transfer from or to the heat exchanger, enthalpy balancing in exhaust gas, energy dissipation by stirring, and monitoring the temperature of added liquids [6]. A calorimetric control strategy for the growth rate of *Escherichia coli* [13] and *Saccharomyces cerevisiae* [14] by adjusting feed rates was developed. The authors report the successful establishment and control of a high-cell density cultivation, with the feed rate solely relying on heat balancing. Furthermore, besides applications in process control, recently, a calorimetric approach for the detection of prophage activation and release was proposed. The authors report that by evaluating differences in metabolic heat, reactivation of dormant infected bacterial cells can be detected [127]. In general, however, the development of

calorimetric control strategies at a laboratory scale is difficult, as sufficient isolation and sensitive equipment to detect heat generated at a small-scale is required [128]. Even though, at a larger scale, increasing ratios of volume to surface favor the sensitivity of calorimetric approaches, calorimetric approaches are only scarcely applied in industrial biotechnology. Table 2 provides an overview of biological traits, and temperature models and/or temperature adjustments used to achieve a desired process outcome.

Table 2. Biological traits associated with modeling techniques and/or targeted temperature adjustments for the control, monitoring, and optimization of biotechnological processes.

Purpose	Process	Biological Basis	Applied Model/Temperature Adjustment	Outcome	Source
Control	Rec. protein production	Lower protein production rates	Downshift in *T*	Correctly folded proteins	[114,116,126]
Control	Rec. protein production	Thermo-inducible promotor	Upshift in *T*	Induced promoter	[12]
Monitoring	Antibiotic biosynthesis	Metabolic heat ≈ metabolic state	Calorimetry	Estimation of metabolic activity	[5]
Monitoring and control	Insecticidal crystal proteins production	Metabolic heat ≈ metabolic state	Calorimetry	Estimation of metabolic state, control of nutrient feed	[6]
Control	Biomass production	Metabolic heat ≈ metabolic state	Calorimetry	Calorimetric control of nutrient feed	[13,14]
Monitoring	Evaluating prophage activating chemicals	Metabolic heat difference ≈ activity state of prophage	Calorimetry	Detection of prophage activation + release	[127]
Optimization	Denitrification of wastewaters	Reducing microbial consortia	Eyring model (Equation (7))	Derive (shifts of) T_{opt} for NO_3^- removal rate	[106,107]
Control	Biomass production	Arguably more stable RNA + correctly folded protein + lower degradation rates at low *T*	Downshift in *T*, ~Assumptions of Corkrey's model (see 3.17)	Increased biomass yield, improved nutrient assimilation	[52,129]
Control	Fatty acid production for biofuel	Shorter und more unsaturated fatty acids at low *T* ~modulate membrane fluidity	Norberg model (Equation (31))	Temperature-specific fatty acid production (profile)	[117]
Optimization	Downstream processing	Thermostable extremozyme	RSM/Thermo precipitation	Purified phosphotriesterase-like lactonases	[11]

5. Summary and Conclusions

In bioprocess engineering, very few process variables are usually available online. Therefore, exploiting existing control variables to their full extent is a reasonable strategy for broadening existing toolsets of monitoring and control. Both underlying biological mechanisms of temperature sensing and adaptation and mathematical models for temperature effects have been well-described. However, temperature as a control variable is only scarcely applied in bioprocess engineering, so an exploitation strategy merging both in context has not yet been established.

This review presents and discusses the most important models for physiological, biochemical, and physical properties governed by temperature, along with application perspectives. As such, this review provides a toolset for the future exploitation of temperature as a control variable for optimization, monitoring, and control applications in bioprocess engineering.

Author Contributions: Conceptualization, P.N. and M.H.; Formal Analysis, P.N., L.L., R.H. and M.H.; Investigation P.N., L.L., R.H. and M.H.; Writing-Original Draft Preparation, P.N.; Writing-Review & Editing, P.N., L.L., R.H. and M.H.; Supervision, M.H. All authors have read and agreed to the published version of the manuscript.

Funding: P.N. is a member of the "BBW ForWerts" graduate program and receives a scholarship within the frame of the Baden-Wuerttemberg Landesgraduiertenfoerderung (LGF) awarded by the Ministry of Science, Research and the Arts (MWK) of Baden-Wuerttemberg, Germany.

Conflicts of Interest: The authors declare no conflicts of interest.

References

1. Hausmann, R.; Henkel, M.; Hecker, F.; Hitzmann, B. *Present Status of Automation for Industrial Bioprocesses*; Elsevier, B.V., Ed.; Elsevier: Amsterdam, The Netherlands, 2016; ISBN 9780444636744.
2. Klinkert, B.; Narberhaus, F. Microbial thermosensors. *Cell. Mol. Life Sci.* **2009**, *66*, 2661–2676. [CrossRef] [PubMed]
3. Noll, P.; Treinen, C.; Müller, S.; Senkalla, S.; Lilge, L.; Hausmann, R.; Henkel, M. Evaluating temperature-induced regulation of a ROSE-like RNA-thermometer for heterologous rhamnolipid production in *Pseudomonas putida* KT2440. *AMB Express* **2019**, *9*, 154. [CrossRef] [PubMed]
4. Arrhenius, S. Über die Reaktionsgeschwindigkeit bei der Inversion von Rohrzucker durch Säuren. *Z. Phys. Chem.* **1889**, *4*, 226–248. [CrossRef]
5. Von Stockar, U.; Duboc, P.; Menoud, L.; Marison, I.W. On-line calorimetry as a technique for process monitoring and control in biotechnology. *Thermochim. Acta* **1997**, *300*, 225–236. [CrossRef]
6. Voisard, D.; Von Stockar, U.; Marison, I.W. Quantitative calorimetric investigation of fed-batch cultures of *Bacillus sphaericus* 1593M. *Thermochim. Acta* **2002**, *394*, 99–111. [CrossRef]
7. Schaepe, S.; Kuprijanov, A.; Aehle, M.; Simutis, R.; Lübbert, A. Simple control of fed-batch processes for recombinant protein production with *E. coli*. *Biotechnol. Lett.* **2011**, *33*, 1781–1788. [CrossRef]
8. Zwietering, M.H.; De Koos, J.T.; Hasenack, B.E.; De Witt, J.C.; Van't Riet, K. Modeling of bacterial growth as a function of temperature. *Appl. Environ. Microbiol.* **1991**, *57*, 1094–1101. [CrossRef]
9. De Oliveira Filho, P.B.; Nascimento, M.L.F.; Pontes, K.V. *Optimal Design of a Dividing Wall Column for the Separation of Aromatic Mixtures Using the Response Surface Method*; Elsevier Masson SAS: Paris, France, 2018; Volume 43, ISBN 9780444642356.
10. MathWorks, Inc. Matlab-Documentation. 2019. Available online: https://de.mathworks.com/help/stats/response-surface-designs.html (accessed on 5 January 2020).
11. Restaino, O.F.; Borzacchiello, M.G.; Scognamiglio, I.; Fedele, L.; Alfano, A.; Porzio, E.; Manco, G.; De Rosa, M.; Schiraldi, C. High yield production and purification of two recombinant thermostable phosphotriesterase-like lactonases from *Sulfolobus acidocaldarius* and *Sulfolobus solfataricus* useful as bioremediation tools and bioscavengers. *BMC Biotechnol.* **2018**, *18*, 18. [CrossRef]
12. Aucoin, M.G.; McMurray-Beaulieu, V.; Poulin, F.; Boivin, E.B.; Chen, J.; Ardelean, F.M.; Cloutier, M.; Choi, Y.J.; Miguez, C.B.; Jolicoeur, M. Identifying conditions for inducible protein production in *E. coli*: Combining a fed-batch and multiple induction approach. *Microb. Cell Fact.* **2006**, *5*, 27. [CrossRef]
13. Biener, R.; Steinkämper, A.; Hofmann, J. Calorimetric control for high cell density cultivation of a recombinant *Escherichia coli* strain. *J. Biotechnol.* **2010**, *146*, 45–53. [CrossRef]
14. Biener, R.; Steinkämper, A.; Horn, T. Calorimetric control of the specific growth rate during fed-batch cultures of *Saccharomyces cerevisiae*. *J. Biotechnol.* **2012**, *160*, 195–201. [CrossRef] [PubMed]
15. Jensen, W.B.; Kuhlmann, J.; Brush, S.G.; Tyndall, J. Leopold Pfaundler and the origins of the kinetic theory of chemical reactions. *Bull. Hist. Chem.* **2012**, *37*, 29–41.
16. Bernoulli, D. *Hydrodynamica, Sive de Viribus et Motibus Fluidorum Commentarii*; Johannis Reinholdi Dulseckeri: Strasbourg, France, 1738.
17. Mikhailov, G.K. Daniel Bernoulli, Hydrodynamica (1738). In *Landmark Writings in Western Mathematics 1640–1940*; Grattan-Guinness, I., Corry, L., Guicciardini, N., Cooke, R., Crépel, P., Eds.; Elsevier: Amsterdam, The Netherlands, 2005; pp. 131–142. ISBN 9780444508713.
18. Clapeyron, P.E. Puissance motrice de la chaleur. *J. l'École Polytech.* **1834**, *14*, 153–190.
19. Jensen, W.B. The universal gas constant R. *J. Chem. Educ.* **2003**, *80*, 731–732. [CrossRef]
20. Eyring, H. The Activated Complex in Chemical Reactions. *J. Chem. Phys.* **1935**, *3*, 107–115. [CrossRef]

21. Laidler, K.J. A glossary of terms used in chemical kinetics, including reaction dynamics (IUPAC recommendations 1996). *Pure Appl. Chem.* **1996**, *68*, 149–192. [CrossRef]
22. Chalk, S.J. Enthalpy of activation, Δ‡H°. In *IUPAC Compendium of Chemical Terminology*; Nič, M., Jirát, J., Košata, B., Jenkins, A., McNaught, A., Eds.; IUPAC: Research Triagle Park, NC, USA, 2009; ISBN 0-9678550-9-8.
23. Johnson, F.H.; Eyring, H.; Stover, B.J. *The Theory of Rate Processes in Biology and Medicine*; John Wiley & Sons: New York, NY, USA, 1974; ISBN 9780471444855.
24. Mohr, P.W.; Krawiec, S. Temperature characteristics and Arrhenius plots for nominal psychrophiles, mesophiles and thermophiles. *J. Gen. Microbiol.* **1980**, *121*, 311–317. [CrossRef]
25. Smith, T.P.; Thomas, T.J.H.; Garcia-Carreras, B.; Sal, S.; Yvon-Durocher, G.; Bell, T.; Pawar, S. Metabolic rates of prokaryotic microbes may inevitably rise with global warming. *BioRxiv* **2019**, 524264. [CrossRef]
26. Ratkowsky, D.A.; Olley, J.; McMeekin, T.A.; Ball, A. Relationship between temperature and growth rate of bacterial cultures. *J. Bacteriol.* **1982**, *149*, 1–5. [CrossRef]
27. Shapiro, R.S.; Cowen, L.E. Thermal Control of Microbial Development and Virulence: Molecular Mechanisms of Microbial Temperature Sensing. *MBio* **2012**, *3*, e00238-12. [CrossRef]
28. Sengupta, P.; Garrity, P. Sensing temperature. *Curr. Biol.* **2013**, *23*, R304–R307. [CrossRef]
29. Pruss, G.J.; Drlica, K. DNA supercoiling and prokaryotic transcription. *Cell* **1989**, *56*, 521–523. [CrossRef]
30. López-García, P.; Forterre, P. DNA topology and the thermal stress response, a tale from mesophiles and hyperthermophiles. *BioEssays* **2000**, *22*, 738–746. [CrossRef]
31. Forterre, P.; Bergerat, A.; Lopez-Garcia, P. The unique DNA topology and DNA topoisomerases of hyperthermophilic archaea. *FEMS Microbiol. Rev.* **1996**, *18*, 237–248. [CrossRef]
32. López-García, P.; Forterre, P. DNA topology in hyperthermophilic archaea: Reference states and their variation with growth phase, growth temperature, and temperature stresses. *Mol. Microbiol.* **1997**, *23*, 1267–1279. [CrossRef] [PubMed]
33. Ono, S.; Goldberg, M.D.; Olsson, T.; Esposito, D.; Hinton, J.C.D.; Ladbury, J.E. H-NS is a part of a thermally controlled mechanism for bacterial gene regulation. *Biochem. J.* **2005**, *391*, 203–213. [CrossRef]
34. White-Ziegler, C.A.; Davis, T.R. Genome-wide identification of H-NS-controlled, temperature-regulated genes in *Escherichia coli* K-12. *J. Bacteriol.* **2009**, *191*, 1106–1110. [CrossRef] [PubMed]
35. Schröder, O.; Wagner, R. The bacterial DNA-binding protein H-NS represses ribosomal RNA transcription by trapping RNA polymerase in the initiation complex. *J. Mol. Biol.* **2000**, *298*, 737–748. [CrossRef] [PubMed]
36. Shin, M.; Song, M.; Joon, H.R.; Hong, Y.; Kim, Y.J.; Seok, Y.J.; Ha, K.S.; Jung, S.H.; Choy, H.E. DNA looping-mediated repression by histone-like protein H-NS: Specific requirement of Eσ70 as a cofactor for looping. *Genes Dev.* **2005**, *19*, 2388–2398. [CrossRef] [PubMed]
37. Lim, C.J.; Lee, S.Y.; Kenney, L.J.; Yan, J. Nucleoprotein filament formation is the structural basis for bacterial protein H-NS gene silencing. *Sci. Rep.* **2012**, *2*, 509. [CrossRef]
38. Kotlajich, M.V.; Hron, D.R.; Boudreau, B.A.; Sun, Z.; Lyubchenko, Y.L.; Landick, R. Bridged filaments of histone-like nucleoid structuring protein pause RNA polymerase and aid termination in bacteria. *Elife* **2015**, *4*, e04970. [CrossRef] [PubMed]
39. Chowdhury, S.; Maris, C.; Allain, F.H.T.; Narberhaus, F. Molecular basis for temperature sensing by an RNA thermometer. *EMBO J.* **2006**, *25*, 2487–2497. [CrossRef] [PubMed]
40. Wei, Y.; Murphy, E.R. Temperature-Dependent Regulation of Bacterial Gene Expression by RNA Thermometers. In *Nucleic Acids: From Basic Aspects to Laboratory Tools*; IntechOpen: London, UK, 2016; pp. 157–181.
41. Grosso-Becerra, M.V.; Croda-Garcia, G.; Merino, E.; Servin-Gonzalez, L.; Mojica-Espinosa, R.; Soberon-Chavez, G. Regulation of *Pseudomonas aeruginosa* virulence factors by two novel RNA thermometers. *Proc. Natl. Acad. Sci. USA* **2014**, *111*, 15562–15567. [CrossRef] [PubMed]
42. Waldminghaus, T.; Fippinger, A.; Alfsmann, J.; Narberhaus, F. RNA thermometers are common in α- and γ-proteobacteria. *Biol. Chem.* **2005**, *386*, 1279–1286. [CrossRef] [PubMed]
43. Narberhaus, F.; Waldminghaus, T.; Chowdhury, S. RNA thermometers. *FEMS Microbiol. Rev.* **2006**, *30*, 3–16. [CrossRef] [PubMed]
44. Waldminghaus, T.; Heidrich, N.; Brantl, S.; Narberhaus, F. FourU: A novel type of RNA thermometer in *Salmonella*. *Mol. Microbiol.* **2007**, *65*, 413–424. [CrossRef] [PubMed]
45. Sen, S.; Apurva, D.; Satija, R.; Siegal, D.; Murray, R.M. Design of a Toolbox of RNA Thermometers. *ACS Synth. Biol.* **2017**, *6*, 1461–1470. [CrossRef]

46. Elsholz, A.K.W.; Michalik, S.; Zühlke, D.; Hecker, M.; Gerth, U. CtsR, the Gram-positive master regulator of protein quality control, feels the heat. *EMBO J.* **2010**, *29*, 3621–3629. [CrossRef]
47. Krell, T.; Lacal, J.; Busch, A.; Silva-Jiménez, H.; Guazzaroni, M.-E.; Ramos, J.L. Bacterial Sensor Kinases: Diversity in the Recognition of Environmental Signals. *Annu. Rev. Microbiol.* **2010**, *64*, 539–559. [CrossRef]
48. Nishiyama, S.I.; Umemura, T.; Nara, T.; Homma, M.; Kawagishi, I. Conversion of a bacterial warm sensor to a cold sensor by methylation of a single residue in the presence of an attractant. *Mol. Microbiol.* **1999**, *32*, 357–365. [CrossRef]
49. Cedervall, T.; Johansson, M.U.; Åkerström, B. Coiled-coil structure of group A streptococcal M proteins. Different temperature stability of class A and C proteins by hydrophobic-nonhydrophobic amino acid substitutions at heptad positions a and d. *Biochemistry* **1997**, *36*, 4987–4994. [CrossRef] [PubMed]
50. Franzmann, T.M.; Menhorn, P.; Walter, S.; Buchner, J. Activation of the Chaperone Hsp26 Is Controlled by the Rearrangement of Its Thermosensor Domain. *Mol. Cell* **2008**, *29*, 207–216. [CrossRef] [PubMed]
51. Haslbeck, M.; Walke, S.; Stromer, T.; Ehrnsperger, M.; White, H.E.; Chen, S.; Saibil, H.R.; Buchner, J. Hsp26: A temperature-regulated chaperone. *EMBO J.* **1999**, *18*, 6744–6751. [CrossRef] [PubMed]
52. Seel, W.; Derichs, J.; Lipski, A. Increased biomass production by mesophilic food-associated bacteria through lowering the growth temperature from 30 °C to 10 °C. *Appl. Environ. Microbiol.* **2016**, *82*, 3754–3764. [CrossRef] [PubMed]
53. Huey, R.B.; Stevenson, R.D. Integrating Thermal Physiology and Ecology of Ectothenns: A Discussion of Approaches Department. *Am. Zool.* **1979**, *19*, 357–366. [CrossRef]
54. Bennett, A.F.; Lenski, R.E. Evolutionary Adaptation to Temperature II. Thermal Niches of Experimental Lines of *Escherichia coli*. *Evolution* **1993**, *47*, 1–12. [CrossRef] [PubMed]
55. Travisano, M.; Lenski, R.E. Long-term experimental evolution in *Escherichia coli*. IV. Targets of selection and the specificity of adaptation. *Genetics* **1996**, *143*, 15–26.
56. Cullum, A.J.; Bennett, A.F.; Lenski, R.E. Evolutionary adaptation to temperature. IX. Preadaptation to novel stressful environments of *Escherichia coli* adapted to high temperature. *Evolution* **2001**, *55*, 2194–2202. [CrossRef]
57. Takai, K.; Nakamura, K.; Toki, T.; Tsunogai, U.; Miyazaki, M.; Miyazaki, J.; Hirayama, H.; Nakagawa, S.; Nunoura, T.; Horikoshi, K. Cell proliferation at 122 °C and isotopically heavy CH_4 production by a hyperthermophilic methanogen under high-pressure cultivation. *Proc. Natl. Acad. Sci. USA* **2008**, *105*, 10949–10954. [CrossRef]
58. Corkrey, R.; McMeekin, T.A.; Bowman, J.P.; Ratkowsky, D.A.; Olley, J.; Ross, T. Protein thermodynamics can be predicted directly from biological growth rates. *PLoS ONE* **2014**, *9*, e96100. [CrossRef]
59. Ratkowsky, D.A.; Lowry, R.K.; McMeekin, T.A.; Stokes, A.N.; Chandler, R.E. Model for bacterial culture growth rate throughout the entire biokinetic temperature range. *J. Bacteriol.* **1983**, *154*, 1222–1226. [CrossRef] [PubMed]
60. Johnson, F.H.; Lewin, I. The growth rate of *E. coli* in relation to temperature, quinine and coenzyme. *J. Cell. Comp. Physiol.* **1946**, *28*, 47–75. [CrossRef] [PubMed]
61. Grimaud, G.M.; Mairet, F.; Sciandra, A.; Bernard, O. Modeling the temperature effect on the specific growth rate of phytoplankton: A review. *Rev. Environ. Sci. Biotechnol.* **2017**, *16*, 625–645. [CrossRef]
62. Hinshelwood, C.N. Influence of temperature on the growth of bacteria. In *The Chemical Kinetics of the Bacterial Cell*; Clarendon Press: Oxford, UK, 1946; pp. 254–257.
63. Sharpe, P.J.H.; Curry, G.L.; DeMichele, D.W.; Cole, C.L. Distribution model of organism development times. *J. Theor. Biol.* **1977**, *66*, 21–38. [CrossRef]
64. Sharpe, P.J.H.; DeMichele, D.W. Reaction kinetics of poikilotherm development. *J. Theor. Biol.* **1977**, *64*, 649–670. [CrossRef]
65. Eyring, H.; Stearn, A.E. The application of the theory of absolute reaction rates to proteins. *Chem. Rev.* **1939**, *24*, 253–270. [CrossRef]
66. Hultin, E. The influence of temperature on the rate of enzymic processes. *Acta Chem. Scand.* **1955**, *9*, 1700–1710. [CrossRef]
67. Lamanna, C.; Mallette, M.F.; Zimmermann, L.N. *Basic Bacteriology*, 4th ed.; Williams & Wilkins: Baltimore, MD, USA, 1973.
68. Schoolfield, R.M.; Sharpe, P.J.H.; Magnuson, C.E. Non-linear regression of biological temperature-dependent rate models based on absolute reaction-rate theory. *J. Theor. Biol.* **1981**, *88*, 719–731. [CrossRef]

69. Roels, J. *Energetics and Kinetics in Biotechnology*; Elsevier Biomedical Press: Amsterdam, The Netherlands, 1983; ISBN 0444804420.
70. Davey, K.R. A predictive model for combined temperature and water activity on microbial growth during the growth phase. *J. Appl. Bacteriol.* **1989**, *67*, 483–488. [CrossRef]
71. Davey, K.R. Modelling the combined effect of temperature and pH on the rate coefficient for bacterial growth. *Int. J. Food Microbiol.* **1994**, *23*, 295–303. [CrossRef]
72. Davey, K.R. Applicability of the Davey (linear Arrhenius) predictive model to the lag phase of microbial growth. *J. Appl. Bacteriol.* **1991**, *70*, 253–257. [CrossRef]
73. Lobry, J.R.; Rosso, L.; Flandrois, J.-P. A FORTRAN Subroutine for the Determination of Parameter Confidence Limits in non-linear models. *Binary* **1991**, *3*, 86–93.
74. Rosso, L.; Lobry, J.R.; Flandrois, J.P. An Unexpected Correlation between Cardinal Temperatures of Microbial Growth Highlighted by a New Model. *J. Theor. Biol.* **1993**, *162*, 447–463. [CrossRef] [PubMed]
75. Blanchard, G.F.; Guarini, J.M.; Richard, P.; Gros, P.; Mornet, F. Quantifying the short-term temperature effect on light- saturated photosynthesis of intertidal microphytobenthos. *Mar. Ecol. Prog. Ser.* **1996**, *134*, 309–313. [CrossRef]
76. Eppley, R.W. Temperature and phytoplankton growth in the sea. *Fish Bull.* **1972**, *70*, 1063–1085.
77. Norberg, J. Biodiversity and ecosystem functioning: A complex adaptive systems approach. *Limnol. Oceanogr.* **2004**, *49*, 1269–1277. [CrossRef]
78. Brandts, J.F. Heat effects on proteins and enzymes. In *Thermobiology*; Academic Press: London, UK, 1967; pp. 25–72.
79. Ratkowsky, D.A.; Olley, J.; Ross, T. Unifying temperature effects on the growth rate of bacteria and the stability of globular proteins. *J. Theor. Biol.* **2005**, *233*, 351–362. [CrossRef]
80. Privalov, P.L.; Khechinashvili, N.N. A thermodynamic approach to the problem of stabilization of globular protein structure: A calorimetric study. *J. Mol. Biol.* **1974**, *86*, 665–684. [CrossRef]
81. Murphy, K.P.; Privalov, P.L.; Gill, S.J. Common features of protein unfolding and dissolution of hydrophobic compounds. *Science* **1990**, *247*, 559–561. [CrossRef]
82. Murphy, K.P.; Gill, S.J. Solid model compounds and the thermodynamics of protein unfolding. *J. Mol. Biol.* **1991**, *222*, 699–709. [CrossRef]
83. Robertson, A.D.; Murphy, K.P. Protein structure and the energetics of protein stability. *Chem. Rev.* **1997**, *97*, 1251–1267. [CrossRef]
84. Baldwin, R.L. Temperature dependence of the hydrophobic interaction in protein folding. *Proc. Natl. Acad. Sci. USA* **1986**, *83*, 8069–8072. [CrossRef]
85. Ross, T. Assessment of a theoretical model for the effects of temperature on bacterial growth rate. In Proceedings of the Refrigeration Science and Technology Proceedings, Quimper, France, 16–18 June 1997; pp. 64–71.
86. Ross, T. A Philosophy for the Development of Kinetic Models in Predictive Microbiology. Ph.D. Thesis, University of Tasmania, Hobart, Australia, 1993.
87. Zeldovich, K.B.; Chen, P.; Shakhnovich, E.I. Protein stability imposes limits on organism complexity and speed of molecular evolution. *Proc. Natl. Acad. Sci. USA* **2007**, *104*, 16152–16157. [CrossRef] [PubMed]
88. Ghosh, K.; De Graff, A.M.R.; Sawle, L.; Dill, K.A. Role of Proteome Physical Chemistry in Cell Behavior. *J. Phys. Chem. B* **2016**, *120*, 9549–9563. [CrossRef] [PubMed]
89. Sawle, L.; Ghosh, K. How do thermophilic proteins and proteomes withstand high temperature? *Biophys. J.* **2011**, *101*, 217–227. [CrossRef] [PubMed]
90. Ghosh, K.; Dill, K.A. Computing protein stabilities from their chain lengths. *Proc. Natl. Acad. Sci. USA* **2009**, *106*, 10649–10654. [CrossRef] [PubMed]
91. Daniel, R.M.; Danson, M.J. A new understanding of how temperature affects the catalytic activity of enzymes. *Trends Biochem. Sci.* **2010**, *35*, 584–591. [CrossRef]
92. Kooijman, S.A.L.M. Energy budgets can explain body size relations. *J. Theor. Biol.* **1986**, *121*, 269–282. [CrossRef]
93. Kooijman, S.A.L.M. Dynamic Energy Budget theory for metabolic organisation: Summary of concepts of the third edition. *Water* **2010**, *365*, 68.
94. Kooijman, S.A.L.M. *Dynamic Energy Budgets in Biological Systems: Theory and Applications in Ecotoxicology*; Cambridge University Press: Cambridge, UK, 1993; ISBN 0-521-45223-6.

95. Huang, L.; Hwang, A.; Phillips, J. Effect of Temperature on Microbial Growth Rate-Mathematical Analysis: The Arrhenius and Eyring-Polanyi Connections. *J. Food Sci.* **2011**, *76*, 553–560. [CrossRef]
96. Hobbs, J.K.; Jiao, W.; Easter, A.D.; Parker, E.J.; Schipper, L.A.; Arcus, V.L. Change in heat capacity for enzyme catalysis determines temperature dependence of enzyme catalyzed rates. *ACS Chem. Biol.* **2013**, *8*, 2388–2393. [CrossRef] [PubMed]
97. Schipper, L.A.; Hobbs, J.K.; Rutledge, S.; Arcus, V.L. Thermodynamic theory explains the temperature optima of soil microbial processes and high Q10 values at low temperatures. *Glob. Chang. Biol.* **2014**, *20*, 3578–3586. [CrossRef] [PubMed]
98. DeLong, J.P.; Gibert, J.P.; Luhring, T.M.; Bachman, G.; Reed, B.; Neyer, A.; Montooth, K.L. The combined effects of reactant kinetics and enzyme stability explain the temperature dependence of metabolic rates. *Ecol. Evol.* **2017**, *7*, 3940–3950. [CrossRef] [PubMed]
99. Lehman, J.T.; Botkin, D.B.; Likens, G.E. The assumptions and rationales of a computer model of phytoplankton population dynamics. *Limnol. Oceanogr.* **1975**, *20*, 343–364. [CrossRef]
100. Moisan, J.R.; Moisan, T.A.; Abbott, M.R. Modelling the effect of temperature on the maximum growth rates of phytoplankton populations. *Ecol. Model.* **2002**, *153*, 197–215. [CrossRef]
101. Bitaubé Pérez, E.; Caro Pina, I.; Pérez Rodríguez, L. Kinetic model for growth of *Phaeodactylum tricornutum* in intensive culture photobioreactor. *Biochem. Eng. J.* **2008**, *40*, 520–525. [CrossRef]
102. Alexandrov, G.A.; Yamagata, Y. A peaked function for modeling temperature dependence of plant productivity. *Ecol. Model.* **2007**, *200*, 189–192. [CrossRef]
103. Quinn, J.; de Winter, L.; Bradley, T. Microalgae bulk growth model with application to industrial scale systems. *Bioresour. Technol.* **2011**, *102*, 5083–5092. [CrossRef]
104. Tevatia, R.; Demirel, Y.; Rudrappa, D.; Blum, P. Effects of thermodynamically coupled reaction diffusion in microalgae growth and lipid accumulation: Model development and stability analysis. *Comput. Chem. Eng.* **2015**, *75*, 28–39. [CrossRef]
105. Mukhtar, H.; Lin, Y.-P.; Lin, C.-M.; Petway, J.R. Assessing thermodynamic parameter sensitivity for simulating temperature responses of soil nitrification. *Environ. Sci. Process. Impacts* **2019**, *21*, 1596–1608. [CrossRef]
106. Schipper, L.A.; Robertson, W.D.; Gold, A.J.; Jaynes, D.B.; Cameron, S.C. Denitrifying bioreactors-An approach for reducing nitrate loads to receiving waters. *Ecol. Eng.* **2010**, *36*, 1532–1543. [CrossRef]
107. Nordström, A.; Herbert, R.B. Identification of the temporal control on nitrate removal rate variability in a denitrifying woodchip bioreactor. *Ecol. Eng.* **2019**, *127*, 88–95. [CrossRef]
108. Feller, G.; Gerday, C. Psychrophilic enzymes: Hot topics in cold adaptation. *Nat. Rev. Microbiol.* **2003**, *1*, 200–208. [CrossRef] [PubMed]
109. Feller, G. Life at low temperatures: Is disorder the driving force? *Extremophiles* **2007**, *11*, 211–216. [CrossRef] [PubMed]
110. Jaouen, T.; Dé, E.; Chevalier, S.; Orange, N. Pore size dependence on growth temperature is a common characteristic of the major outer membrane protein OprF in psychrotrophic and mesophilic *Pseudomonas* species. *Appl. Environ. Microbiol.* **2004**, *70*, 6665–6669. [CrossRef] [PubMed]
111. D'Amico, S.; Collins, T.; Marx, J.C.; Feller, G.; Gerday, C. Psychrophilic microorganisms: Challenges for life. *EMBO Rep.* **2006**, *7*, 385–389. [CrossRef]
112. Margesin, R.; Fonteyne, P.A.; Redl, B. Low-temperature biodegradation of high amounts of phenol by *Rhodococcus* spp. and basidiomycetous yeasts. *Res. Microbiol.* **2005**, *156*, 68–75. [CrossRef]
113. Corkrey, R.; Olley, J.; Ratkowsky, D.; McMeekin, T.; Ross, T. Universality of thermodynamic constants governing biological growth rates. *PLoS ONE* **2012**, *7*, e32003. [CrossRef]
114. Hannig, G.; Makrides, S.C. Strategies for optimizing heterologous protein expression in *Escherichia coli*. *Stud. Health Technol. Inform.* **1998**, *16*, 54–60. [CrossRef]
115. Gombert, A.K.; Kilikian, B.V. Recombinant gene expression in *Escherichia coli* cultivation using lactose as inducer. *J. Biotechnol.* **1998**, *60*, 47–54. [CrossRef]
116. Schmidt, M.; Babu, K.R.; Khanna, N.; Marten, S.; Rinas, U. Temperature-induced production of recombinant human insulin in high-cell density cultures of recombinant *Escherichia coli*. *J. Biotechnol.* **1999**, *68*, 71–83. [CrossRef]
117. Nalley, J.O.; O'Donnell, D.R.; Litchman, E. Temperature effects on growth rates and fatty acid content in freshwater algae and cyanobacteria. *Algal Res.* **2018**, *35*, 500–507. [CrossRef]

118. Jacquet, P.; Daudé, D.; Bzdrenga, J.; Masson, P.; Elias, M.; Chabrière, E. Current and emerging strategies for organophosphate decontamination: Special focus on hyperstable enzymes. *Environ. Sci. Pollut. Res.* **2016**, *23*, 8200–8218. [CrossRef] [PubMed]
119. Singh, B.K. Organophosphorus-degrading bacteria: Ecology and industrial applications. *Nat. Rev. Microbiol.* **2009**, *7*, 156–164. [CrossRef] [PubMed]
120. Horne, I.; Qiu, X.; Russell, R.J.; Oakeshott, J.G. The phosphotriesterase gene opdA in *Agrobacterium radiobacter* P230 is transposable. *FEMS Microbiol. Lett.* **2003**, *222*, 1–8. [CrossRef]
121. Zellner, M.; Winkler, W.; Hayden, H.; Diestinger, M.; Eliasen, M.; Gesslbauer, B.; Miller, I.; Chang, M.; Kungl, A.; Roth, E.; et al. Quantitative validation of different protein precipitation methods in proteome analysis of blood platelets. *Electrophoresis* **2005**, *26*, 2481–2489. [CrossRef]
122. Cimini, D.; Restaino, O.F.; Catapano, A.; De Rosa, M.; Schiraldi, C. Production of capsular polysaccharide from *Escherichia coli* K4 for biotechnological applications. *Appl. Microbiol. Biotechnol.* **2010**, *85*, 1779–1787. [CrossRef]
123. McAlindon, T.E.; LaValley, M.P.; Gulin, J.P.; Felson, D.T. Glucosamine and chondroitin for treatment of osteoarthritis: A systematic quality assessment and meta-analysis. *JAMA* **2000**, *283*, 1469–1475. [CrossRef]
124. Whitfield, C.; Roberts, I.S. Structure, assembly and regulation of expression of capsules in *Escherichia coli*. *Mol. Microbiol.* **1999**, *31*, 1307–1319. [CrossRef]
125. Restaino, O.F.; Marseglia, M.; Diana, P.; Borzacchiello, M.G.; Finamore, R.; Vitiello, M.; D'Agostino, A.; De Rosa, M.; Schiraldi, C. Advances in the 16α-hydroxy transformation of hydrocortisone by *Streptomyces roseochromogenes*. *Process Biochem.* **2016**, *51*, 1–8. [CrossRef]
126. Restaino, O.F.; Bhaskar, U.; Paul, P.; Li, L.; De Rosa, M.; Dordick, J.S.; Linhardt, R.J. High cell density cultivation of a recombinant *E. coli* strain expressing a key enzyme in bioengineered heparin production. *Appl. Microbiol. Biotechnol.* **2013**, *97*, 3893–3900. [CrossRef]
127. Xu, J.; Jiang, F.L.; Liu, Y.; Kiesel, B.; Maskow, T. An enhanced bioindicator for calorimetric monitoring of prophage-activating chemicals in the trace concentration range. *Eng. Life Sci.* **2018**, *18*, 475–483. [CrossRef]
128. Schubert, T.; Breuer, U.; Harms, H.; Maskow, T. Calorimetric bioprocess monitoring by small modifications to a standard bench-scale bioreactor. *J. Biotechnol.* **2007**, *130*, 24–31. [CrossRef] [PubMed]
129. Bakermans, C.; Nealson, K.H. Relationship of Critical Temperature to Macromolecular Synthesis and Growth Yield in *Psychrobacter cryopegella*. *J. Bacteriol.* **2004**, *186*, 2340–2345. [CrossRef] [PubMed]

The following article was published in 2021 in *Scientific Reports*, 11 as

- Exploiting RNA thermometer-driven molecular bioprocess control as a concept for heterologous rhamnolipid production -

Philipp Noll, Chantal Treinen, Sven Müller, Lars Lilge,
Rudolf Hausmann and Marius Henkel

DOI: 10.1038/s41598-021-94400-4

scientific reports

Check for updates

OPEN

Exploiting RNA thermometer-driven molecular bioprocess control as a concept for heterologous rhamnolipid production

Philipp Noll, Chantal Treinen, Sven Müller, Lars Lilge, Rudolf Hausmann & Marius Henkel✉

A key challenge to advance the efficiency of bioprocesses is the uncoupling of biomass from product formation, as biomass represents a by-product that is in most cases difficult to recycle efficiently. Using the example of rhamnolipid biosurfactants, a temperature-sensitive heterologous production system under translation control of a fourU RNA thermometer from *Salmonella* was established to allow separating phases of preferred growth from product formation. Rhamnolipids as bulk chemicals represent a model system for future processes of industrial biotechnology and are therefore tied to the efficiency requirements in competition with the chemical industry. Experimental data confirms function of the RNA thermometer and suggests a major effect of temperature on specific rhamnolipid production rates with an increase of the average production rate by a factor of 11 between 25 and 38 °C, while the major part of this increase is attributable to the regulatory effect of the RNA thermometer rather than an unspecific overall increase in bacterial metabolism. The production capacity of the developed temperature sensitive-system was evaluated in a simple batch process driven by a temperature switch. Product formation was evaluated by efficiency parameters and yields, confirming increased product formation rates and product-per-biomass yields compared to a high titer heterologous rhamnolipid production process from literature.

A major part of a future bioeconomy-driven industrial biotechnology is based on sustainable bulk products with typically low added-value. Formerly mainly focused on products that are difficult to synthesize by chemical means, such as proteins or chiral molecules etc., industrial biotechnology will include typical low-molecular weight products that were exclusively produced by chemical means. As such, the efficiency of substrate conversion is of particular importance, as future processes of industrial biotechnology are therefore tied to efficiency requirements in competition with the chemical industry. A key challenge to advance the efficiency of bioprocesses is the uncoupling of biomass from product formation, as biomass represents a by-product that is in most cases difficult to recycle efficiently.

Rhamnolipids. Microbial rhamnolipid biosurfactants (RL) as bulk chemicals represent a model system for future industrial biotechnology in the context of a bio-based economy. Biosurfactants are based on renewable substrates, whereas many conventional surfactants are derived from petrochemical sources[1]. Biosurfactants exhibit beneficial properties like low toxicity, biodegradability, high surfactant efficiencies and high stability at extreme pH, temperature and salinity when compared to many chemical surfactants[2]. The fields of application for surfactants range from the cosmetic sector (personal care products), the food sector (emulsifiers or stabilizers) and the pharmaceutical sector (antimicrobial and antifungal activities) to enhanced oil recovery and cleaning agents (household detergents)[2–6]. Unsurprisingly, an increase in research interest on microbial biosurfactants could be observed over the past decade[7]. However, production of biosurfactants is still cost intensive, especially the downstream processing[8]. Furthermore, the use of the model organism *P. aeruginosa*, even though it is reported to produce the highest RL titers (39 g/L)[9], bares two disadvantages for a commercial production of the biosurfactant RL. First, *P. aeruginosa* is a human pathogen[10] and second, RL production is controlled by

Institute of Food Science and Biotechnology, Department of Bioprocess Engineering (150K), University of Hohenheim, Fruwirthstr. 12, 70599 Stuttgart, Germany. ✉email: Marius.Henkel@uni-hohenheim.de

a complex regulatory cell density-dependent mechanism called quorum sensing. To overcome these obstacles, heterologous RL production was first described by *Pseudomonas putida*[11,12]. In 2016, the *rhlAB* genes were transferred from *P. aeruginosa* with the pBBR1MCS-3 based plasmid pSynPro8oT_*rhlAB* into the nonpathogenic host *P. putida* KT2440 resulting in heterologous constitutive expression of rhamnosyltransferase genes needed for mono-RL production[13]. A maximum concentration of 14.9 g/L RL could be reached in a fed batch process with a two-phase glucose feeding profile. However, this approach for heterologous RL production suffers from considerable biomass production which represents a major carbon sink (roughly 50% more biomass than product)[14]. This challenge is addressed with the presented study.

RNA thermometer. Temperature fluctuations can be detected by different molecular thermosensors made of DNA, RNA, proteins or lipids. The different principles of temperature sensing have been extensively reviewed[15–17]. The thermosensors of interest for this study are molecular structures mostly found in the 5'-UTR of the mRNA that enable thermosensing. Due to the physical properties of RNA, so-called hairpin structures can be formed. In these hairpin structures, base pairing blocks the Shine-Dalgarno sequence, and the AUG start codon, which are part of the ribosomal binding and translation initiation site. A certain amount of thermal energy, depending on the composition of base pairs, is required to melt the H-bridges in the hairpin structure. By raising the temperature, the hairpin structure gradually opens and allows ribosomes to access the translation initiation site[16]. In 1989, the first *cis* encoded regulatory RNA element determining temperature-dependent translation initiation was discovered in the *cIII* gene of bacteriophage λ[18]. Up until today several temperature-sensitive RNA structures, governing mainly the expression of heat shock and virulence genes have been reported[19–23] but to our knowledge not leveraged for industrial applications. This study aims to provide a proof-of-concept process exploiting a temperature responsive RNA thermometer (RNAT) for bioprocess control.

ROSE-like RNA thermometer. In *P. aeruginosa* RL production is governed by an RNA-based temperature-sensing element an RNAT. RNATs are instrumental in an adequate response to the decisive signal of a temperature-shift from low environmental to elevated temperatures e.g. of 37 °C in a host system. The consequence after successful invasion of a host by a pathogen is the upregulation of its virulence factor production. To respond to elevated host temperatures, the pathogen *P. aeruginosa*, has a so termed ROSE (Repression Of heat-Shock gene Expression)-like RNAT. The RNAT is located in the 5' UTR (untranslated region) of the *rhlA* mRNA, thermo-regulates the translation of the mRNA and therefore indirectly the production of the virulence factor RL. Almost all known ROSE-like RNATs govern heat shock gene expression with the exception of the ROSE-like element found to control the formation of the virulence factor RL in *P. aeruginosa* and in the heterologous system *P. putida* KT2440 pSynPro8oT_*rhlAB*[24,25]. It was argued that at non-permissive environmental temperatures (≤ 30 °C) translation of *rhlA* is inhibited by the RNAT, which in turn interferes with the transcription of the *rhlB* gene. This phenomenon is known as polar effect[24]. In 2019, a ROSE-like RNAT structure was evaluated for temperature-responsivity and its ability to govern a temperature dependent expression of the *rhlAB* genes[25]. The latter study showed the potential to use RNATs as regulatory elements; however, the evaluated ROSE-like RNAT showed a limited regulatory effect on RL production. Consequently, a different temperature responsive element with a more pronounced regulatory effect on translation was investigated in this study.

FourU RNA thermometer. Another family of RNATs are the fourU-type RNATs. FourU RNATs located mostly in the 5'UTR, are between 40 and > 270 nucleotides in length (*htrA*; *E. coli* and *shuA*; *Shigella dysenteriae*) and consist of 1–5 hairpin structures[26–28]. The temperature responsive "hairpin 2" of the 57 nucleotides *Salmonella* fourU-type RNAT was used in this study. In *Salmonella enterica* the fourU RNAT governs the expression of the heat shock gene *agsA*. In vivo experiments showed that the temperature responsive wild type fourU RNAT mostly prevents translation of a subsequent *bgaB* gene at 30 °C but is upregulated at common mammalian host temperatures of 37 °C and above. Previous studies reported that a destabilized variant of the wild type fourU RNAT can be obtained by introducing a single point mutation into the hairpin structure. This structure is destabilized at the temperature range investigated here allowing for an earlier onset of translation initiation (at lower temperatures) than the wild type RNAT (Fig. 1)[29].

Aim of this study. The presented study was meant to be a case study on the applicability of RNAT in combination with temperature changes to govern an exemplary bulk chemical production process within the framework of an industrial biotechnology, in this case microbial RLs. A temperature-sensitive heterologous RL production system under translation control of a fourU RNAT from *Salmonella*[29] (Fig. 1) was established. The characteristics of this system are assessed in comparison to a destabilized structure used as a control that allows translation already at lower temperatures. The use of RNATs for molecular control through partial decoupling of biomass and product formation in bioprocesses is illustrated using RL biosurfactants as an example and presented by growth respectively product formation rates and yields. Furthermore, a proof-of-concept of a bioreactor cultivation with a temperature switch was carried out to elucidate the production capacity and potential of the molecular temperature switch for bioprocess control. Hence, this work marks a fundamental step for temperature-based (molecular) process design and control by exploiting temperature responsive elements.

Results

To demonstrate the effect of temperature on RL production and cell growth, a set of experiments, comparing shake flask cultivations at different temperatures (20—42.5 °C), was conducted.

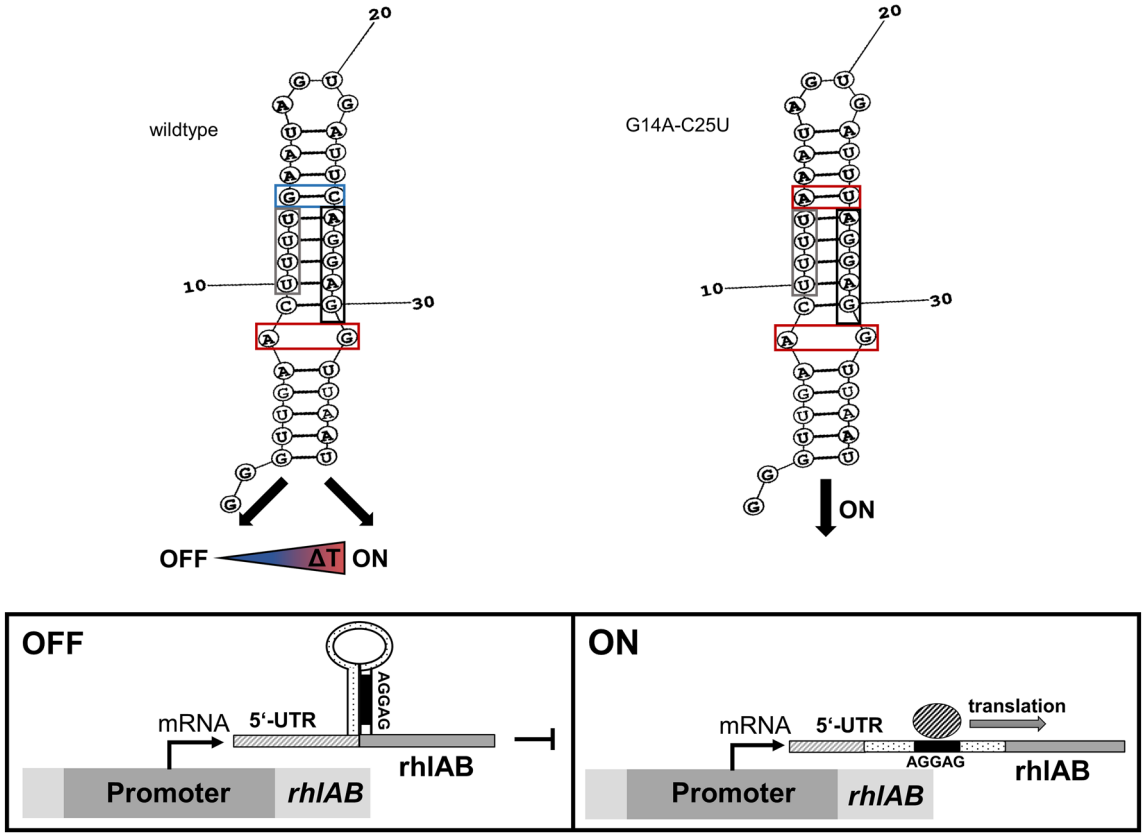

Figure 1. Working principal, hairpin structure and RNA sequence of *Salmonella* wild type fourU RNAT and destabilized (G14A-C25U) mutant used in this study. Base pairs framed in red are less stable than base pairs framed in blue, grey frames indicate the fourU motive and black frames the Shine-Dalgarno sequence. (Adapted from[29]).

Heterologous fourU RNA thermometer thermo-regulates RL production. When cultivating *P. putida* KT2440 pSynPro8oT_4U_*rhlAB* with the functional wild type fourU RNAT a lower biomass concentration was obtained at 38 °C (1.43 g/L), compared to 20 °C (5.71 g/L). However, the lower amount of biomass at 38 °C yielded a maximum concentration of RLs (1.84 g/L) approximately 10 times higher than the maximum RL concentration (0.19 g/L) measured at 20 °C. Compared to that the cultivation of the control strain with the destabilized fourU RNAT yielded 4.55 g/L biomass with 1.64 g/L RL at 20 °C and 0.49 g/L biomass with 0.48 g/L RL at 38 °C. At 42.5 °C almost no cell growth could be observed (0.10 g/L (inoculation)—maximum of 0.15 g/L (after 6 h)). In Fig. 2 selected time courses of shake flask cultivations of *P. putida* KT2440 pSynPro8oT_4U_*rhlAB* and *P. putida* KT2440 pSynPro8oT_4U(G14A-C25U)_*rhlAB* using ModR medium with 10 g/L glucose are shown. To visualize the effect of the different temperatures tested on the strains under investigation, maximum (q_{max}) and mean (q_{avg}) specific RL production rates were plotted against temperature (Fig. 3). Whereas q_{max} was chosen to illustrate and compare the highest rate recorded of each cultivation temperature tested and q_{avg} to display an average rate over the cultivation period for each cultivation temperature tested. A 15-fold increase of q_{max} from 9 mg/(g·h) at 20 °C to 133 mg/(g·h) at 38 °C was calculated. A model describing q_{max} as a function of temperature (Eq. (1)) according to the group of Schoolfield[30] was fitted to the experimentally determined values of q_{max} for the *P. putida* strain harboring the functional fourU RNAT (Fig. 3). The experimentally determined values for q_{avg} respectively q_{max} increased from roughly 0 almost exponentially to a maximum of 67 mg/(g·h) (q_{avg}) respectively 133 mg/(g·h) (q_{max}) at 38 °C. The temperature at which the highest specific RL productivity could be observed (highest q_{max} from model) was calculated to be 38.4 °C when using the model of Schoolfield et al. At temperatures higher than 38 °C, experimentally determined RL production rates decreased rapidly. A mathematical artifact arising from a low biomass concentration at 42.5 °C, distorts the calculated value for q_{max} causing a high specific production rate at that temperature. Summarizing, the temperature responsive fourU element shows a pronounced thermo regulatory effect on RL production.

Increased RL-per-glucose and RL-per-biomass yields at elevated temperatures. RL-per-glucose yields ($Y_{P|S}$) and total RL-per-biomass yields ($Y_{P|X}$) are shown for different temperatures for the functional fourU RNAT in Fig. 4a. An apparent correlation of $Y_{P|S}$ respectively $Y_{P|X}$, and temperature can be derived (Fig. 4a). The $Y_{P|S}$ increased with the temperature by around 10-fold from 0.02 g/g (20 °C) to 0.20 g/g (38 °C). The $Y_{P|X}$ value showed a similar trend with an even stronger increase when raising temperature. An almost 50-fold increase of the $Y_{P|X}$ value between 20 °C and 38 °C from 0.03 g/g to 1.43 g/g was calculated. When temperature was

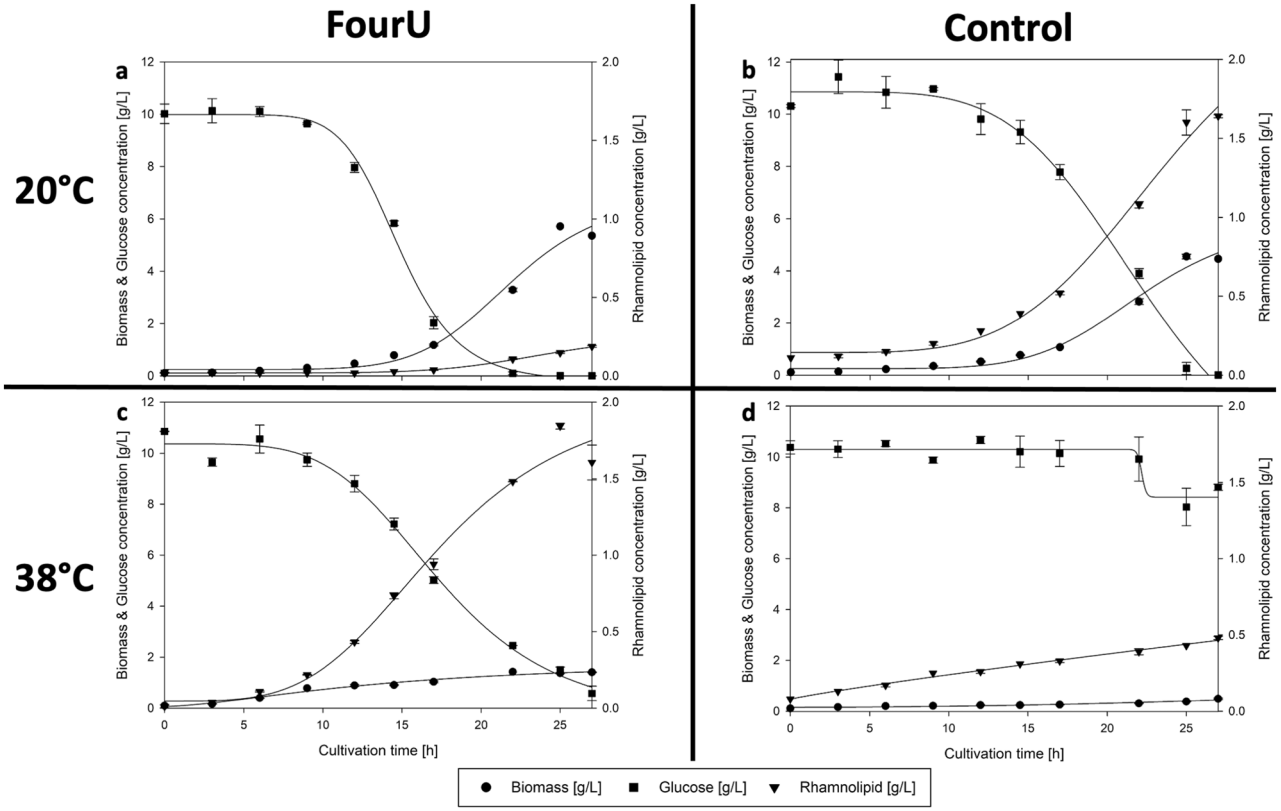

Figure 2. Time course of biomass- (circles), rhamnolipid- (triangles) and glucose concentration (squares) during shake flask cultivation of *P. putida* KT2440 pSynPro8oT_4U_*rhlAB* and pSynPro8oT_4U(G14A-C25U)_*rhlAB* control strain on ModR medium with 10 g/L glucose at 20 °C (**a**,**b**) and 38 °C (**c**,**d**).

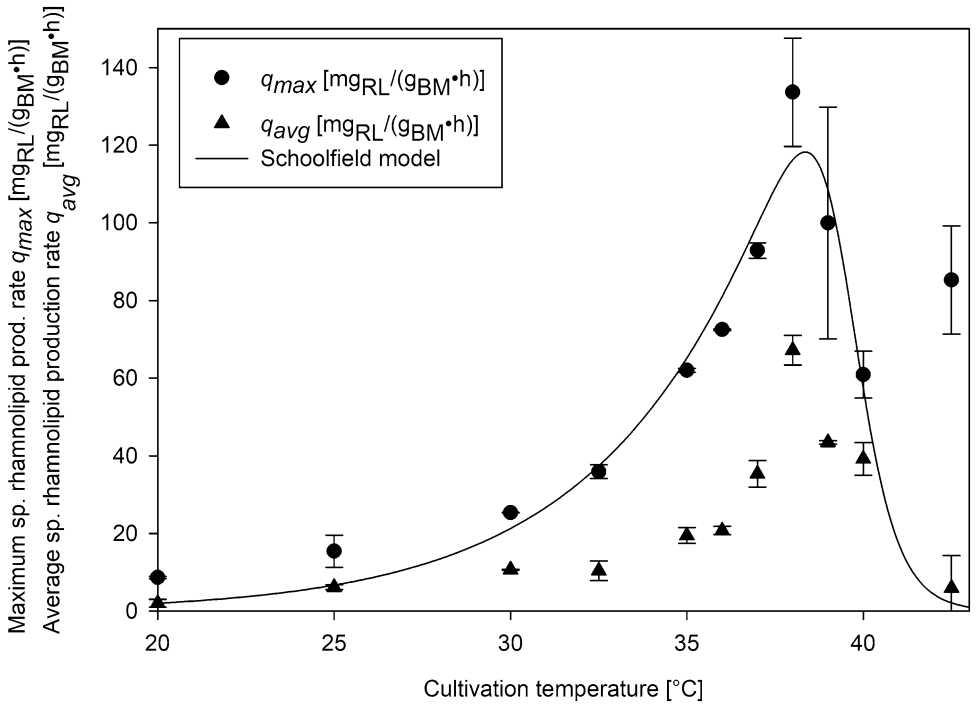

Figure 3. Experimentally determined maximum (q_{max}; black circles) and mean (q_{avg}; black triangles) specific rhamnolipid production rates plotted against temperatures tested for *Pseudomonas putida* KT2440 pSynPro8oT_4U_*rhlAB*. Maximum specific rhamnolipid production rates were described as a function of temperature by fitting a temperature model (Schoolfield et al.[30]; Eq. (1); black line) to the obtained data of q_{max}.

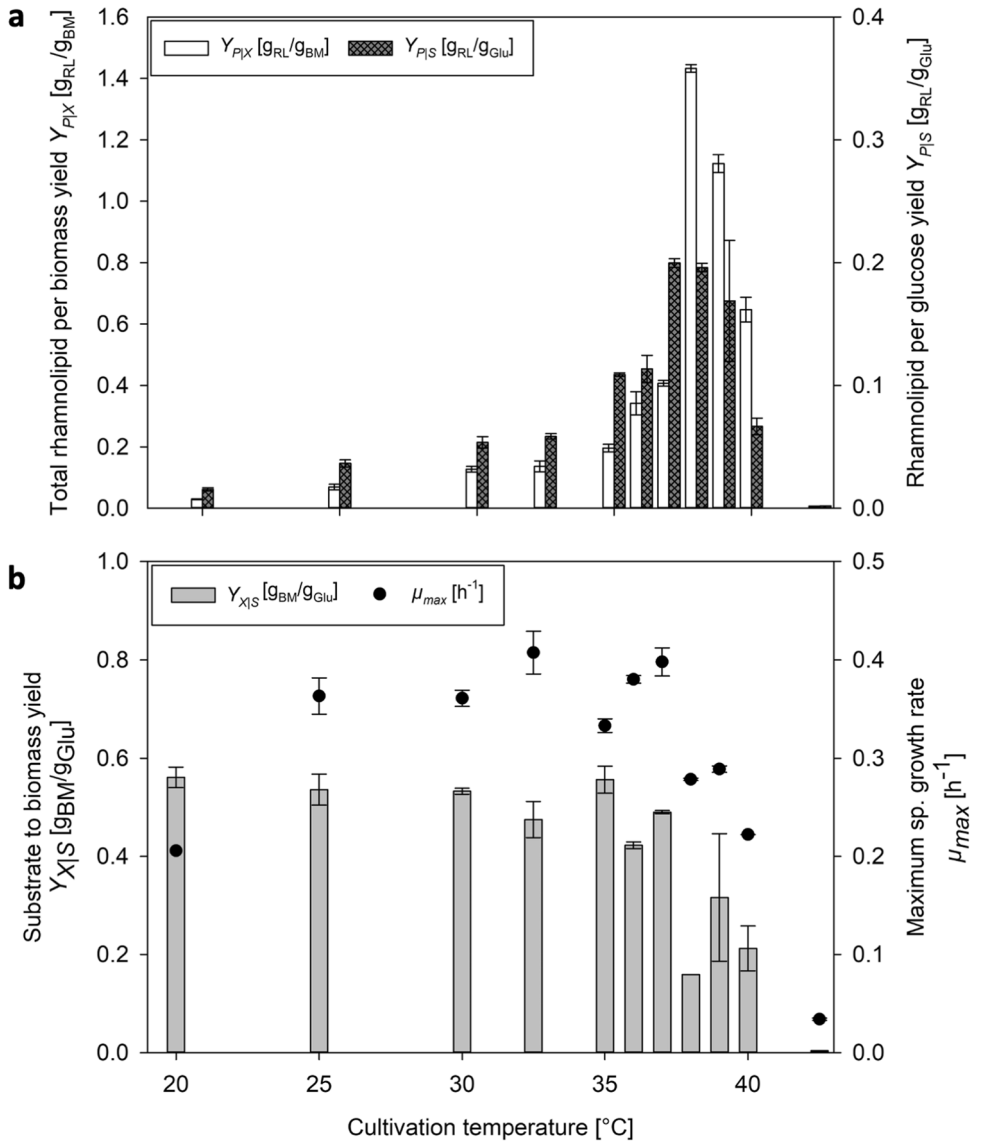

Figure 4. Effect of temperature on (**a**) rhamnolipid-per-glucose yields ($Y_{P|S}$; dark grey bars) and total rhamnolipid-per-biomass yields ($Y_{P|X}$; white bars) and on (**b**) biomass-per-glucose yields ($Y_{X|S}$; grey bars) and maximum specific growth rates (μ_{max}; circles) for *Pseudomonas putida* KT2440 pSynPro8oT_4U_*rhlAB*.

raised higher than 38 °C both yield-values decreased approaching 0 at 42.5 °C. In addition to the performance parameters shown above, growth rates (μ) and biomass-to-glucose yields ($Y_{X|S}$) were furthermore calculated (Fig. 4b). The highest maximum specific growth rates (μ_{max}) were reached at 32.5 °C for the strain carrying the functional fourU RNAT with a μ_{max} of 0.41 h^{-1} respectively 0.33 h^{-1} at 35 °C for the control. $Y_{X|S}$ remained relatively constant below and around the growth optimum (20–35 °C) with values around 0.50 g/g. Yields decreased at temperatures above 35 °C to 0.16 g/g at 38 °C before approaching almost 0 at 42.5 °C (Fig. 4b). As stated in the introduction, heterologous RL production suffers from considerable biomass production which represents a major carbon sink (roughly 50% more biomass than product)[14]. It is shown here that elevated temperatures, shift the RL-per-biomass yield in favor of RLs and simultaneously improve RL-per-glucose yields.

Proof-of-concept temperature switch process. To benchmark the regulatory capabilities of the investigated fourU RNAT and to assess the production capacities of the applied biological system on a technical scale, a temperature switch process was carried out in a bioreactor. To achieve a separation of growth and product formation, cells were initially grown at 25 °C for biomass generation. At this temperature, RL formation rates were low, while biomass growth was high, as indicated in Figs. 3 + 4b. Subsequently, temperature was switched to 38 °C, which represents the experimental optimum of specific RL production rates. Switching the temperature from 25 to 38 °C was performed at t = 9 h, and a stable temperature could be reached within 15 min, with an error of less than 0.05 °C. The results are shown in the figure below. As expected, RL titers were lower than 0.10 g/L at

Strain	q_{max} [$mg_{RL}/(g_{BM} \cdot h)$]	q_{avg} [$mg_{RL}/(g_{BM} \cdot h)$]	$Y_{P\|X}$ [g/g]	c_{RL}^{max} [g/L]	References
P. putida KT2440 pSynPro8oT_4U_*rhlAB*	92–145	25–32	0.66–0.85	2.15–2.42	This study
P. putida KT2440 pSynPro8oT_*rhlAB*	72	42	0.61	0.83	[31]
P. putida KT2440 pSynPro8oT_*rhlAB*	89–113	18–24	0.66–0.77	14.9	[13,14]
P. putida KT2440 SK4	N/A	N/A	0.35–0.37	0.68–0.74	[32]
P. putida KT2440 E1.1_RL	N/A	N/A	0.41–0.43	1.01–1.03	
P. aeruginosa wt, various strains	N/A	12–54	0.3–2.3	0.2–39	[9,33]

Table 1. Comparison of rhamnolipid production processes from literature using glucose as carbon source with the presented switch process (Fig. 5). N/A = Information not available; c_{RL}^{max} = Maximum rhamnolipid concentration.

25 °C before induction and reached around 2.28 g/L after switching the temperature to 38 °C and 48 h of total cultivation time.

For the process shown above, maximum specific RL production rates of up to 145 mg/(g h) and average specific production rates of up to 32 mg/(g h) were reached. To put this simple batch process in context, a comparison was drawn with a literature high titer heterologous RL production process. The authors used the same strain, *P. putida* KT2440 pSynPro8oT_*rhlAB* without the fourU RNAT. Their cultivation was carried out in ModR medium with glucose as carbon source as well and at constant 30 °C (table below). The following table shows further reports on (heterologous) RL production processes using *Pseudomonas*.

The highest titer reported to date for mono-RL production, using a heterologous host, was reached in 2016 with a two phase feeding strategy at constant 30 °C[14]. For the switch process shown in this study average specific RL production rates (q_{avg}) of up to 32 mg/(g h)) were reached. This result was around 25% higher compared to the highest average specific RL production rate (q_{avg}: 24 mg/(g h)) reported in the literature reference process for heterologous RL production using *P. putida* KT2440 pSynpro8oT_*rhlAB*[14] (Table 1; Fig. 5). This finding supports the potential of temperature to be exploited as control variable in combination with a functional RNAT. However, a suitable feeding strategy would still be required in conjunction with the RNAT-driven molecular control system to allow for higher titers and achieve reduced side product formation. The presented switch process in this study is a proof-of-concept for exploiting a temperature responsive RNAT for bioprocess control on a pre-industrial scale. To our knowledge the process is the first of its kind to leverage a fourU RNAT in combination with a temperature shift to control RL production.

Discussion

When comparing time courses of biomass and RL concentration during shake flask cultivations of *P. putida* KT2440 pSynPro8oT_4U_*rhlAB* at 20 °C and 38 °C, the final biomass concentration at 38 °C was lower while the maximum RL concentration was almost 10-times higher than what was obtained at 20 °C (Fig. 2). Consequentially a higher biomass specific productivity was reached when cultivations were performed at elevated temperatures (Fig. 3). The temperature-dependency of RL production rates using fourU RNAT was investigated in a range between 20 and 42.5 °C (Fig. 3). An almost exponential increase of RL productivity between 20 °C to an optimum at 38 °C could be observed. In the absence of limitations and by assuming that RL production rate is proportional to rhamnosyl transferase concentration, this correlation mirrors what is known for RNAT regulation behavior. It has been reported before that the opening of the RNA hairpin structure exhibits a gradual temperature-response profile and typically never entirely prevents translation[34,35]. The rapid decrease in productivity when the optimal temperature for RL production is exceeded could be attributed to various effects of elevated temperatures on the bacterial cell. High temperatures are for example connected to aggregation and denaturation of proteins. This may lead to deactivation of enzymes needed for RL biosynthesis. Indirect effects arising from an altered bacterial metabolism may also be considered, such as the availability of precursors necessary for RL production. A lower availability of the RL precursors HAA and dTDP-rhamnose may then present a bottleneck for RL synthesis. Low temperature results in low growth which then leads to a reduced demand for dTDP because less DNA needs to be synthesized. This would mean that more dTDP nucleotide sugars (activated sugars) for RL biosynthesis may be available, thus resulting in higher RL production rates at the respective temperature. Furthermore, the substrate binding capacity of RhlA respectively RhlB towards the previously mentioned precursors may also be negatively affected by temperatures beyond the production optimum. The total productivity of the process may be evaluated according to the average specific RL production rate which can then ultimately be used as target for process optimization as has been suggested previously[25]. The observed increase of average specific RL production rate over temperature may differ in prolonged processes, for example in a bioreactor cultivation with a higher initial glucose concentration. For bulk chemical production, total $Y_{P|X}$ respectively $Y_{P|S}$ mark important parameters for process optimization and are therefore suitable targets to assess the production capacity of the applied biological system under control of the fourU RNAT. In this study, these yields were observed to be increasing alongside with increasing maximum respectively average RL production rates when raising temperature (Figs. 3 + 4). Translating this to the design of a more efficient production process at heightened temperatures would mean both a shortening of process time (increased RL production rates q) and higher efficiency (increased product per biomass respectively per substrate yields over temperature) of RL production. The higher efficiency of RL production at elevated temperatures may be assigned to different overlapping effects. To estimate the influence of a functional

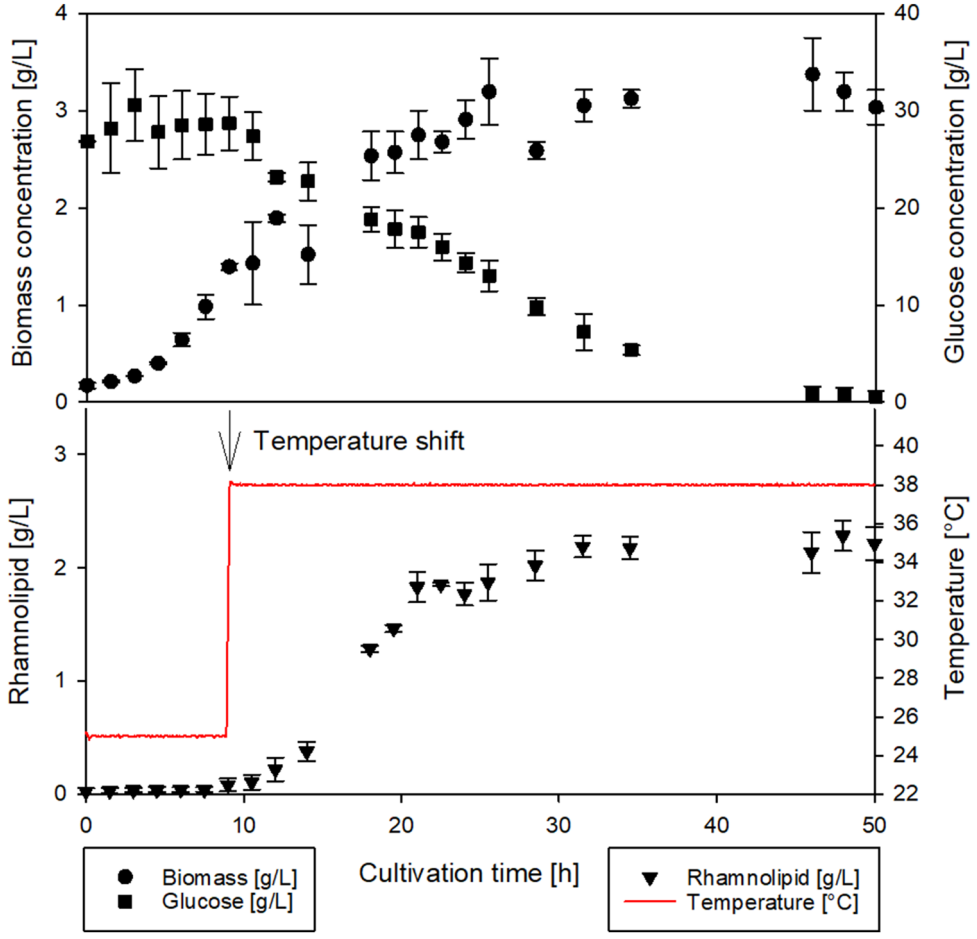

Figure 5. Bioreactor batch cultivation of *Pseudomonas putida* KT2440 pSynPro8oT_4U_*rhlAB* in ModR medium with 30 g/L glucose. Time courses of measured biomass- (circles), and glucose concentration (squares) are shown in the upper plot as well as rhamnolipid concentration (triangles) and measured temperature (red line) in the bottom plot. Biomass was grown at 25 °C until reaching an OD_{600} of 4 (approx. 1.4 g/L, after ~ 9 h). Then temperature was switched to 38 °C to induce rhamnolipid production as indicated by an arrow at the bottom plot.

fourU RNAT on the observed increase of RL productivity over temperature, the G14A-C25U mutant was used as comparison. As has been reported previously, the RNA structure of the G14A-C25U mutant is destabilized already at a lower temperatures than the wild type RNA structure[29]. The increase of q_{max} and q_{avg} between 25 and 38 °C for the *P. putida* strain harboring the functional fourU RNAT was determined to be 9.3-fold respectively 11.1-fold compared to 1.4-fold for both rate changes of the G14A-C25U mutant (Fig. 3). Assuming on the one hand that the functional fourU RNAT has no significant regulatory effect on RL production rates, the increase of the rate over temperature for the G14A-C25U mutant should have been approximately the same. On the other hand, if an absence of unspecific or metabolic effects is assumed, the increase in production rate over temperature were to be solely caused by the RNATs regulatory effect. This would mean that the increase in production rate of the G14A-C25U mutant should have been close to 0. The here presented experiments revealed that besides the discussed metabolic effect, a major part of the total increase in RL production rate is to be attributed to the regulatory effect of the RNAT. The specific production rate between 25 and 38 °C for the G14A-C25U mutant increased 1.4-fold and may be due to unspecific metabolic effects (Fig. 3). Compared to that the specific production rate of the strain with the functional fourU RNAT increased by more than 9-fold on average between 25 and 38 °C, which confirms the regulatory action of the deployed fourU RNAT element in the heterologous host *P. putida* KT2440 (Figs. 3 + 6). The effect could be mainly assigned to the presence and regulatory effect of a functional fourU RNAT (RE, Fig. 6). The regulatory effect is derived by comparing specific productivities and time courses of cultivations with the strain carrying the functional fourU RNAT (e.g., 9.3-fold change of q_{max} comparing 25 to 38 °C, Fig. 6) with the control strain. In case of the control, only a slight increase in maximum specific productivity (e.g., 1.4-fold change of q_{max} comparing 25 to 38 °C, Fig. 6) was obtained. The observed increase in q_{max} for the control may be assigned to an unspecific metabolic effect (UME, Fig. 6) caused by the temperature increase itself along with elevated biochemical reaction rates. The UME accounts for 12 – 15% of the total change in average respectively maximum specific production rate over temperature as is shown below.

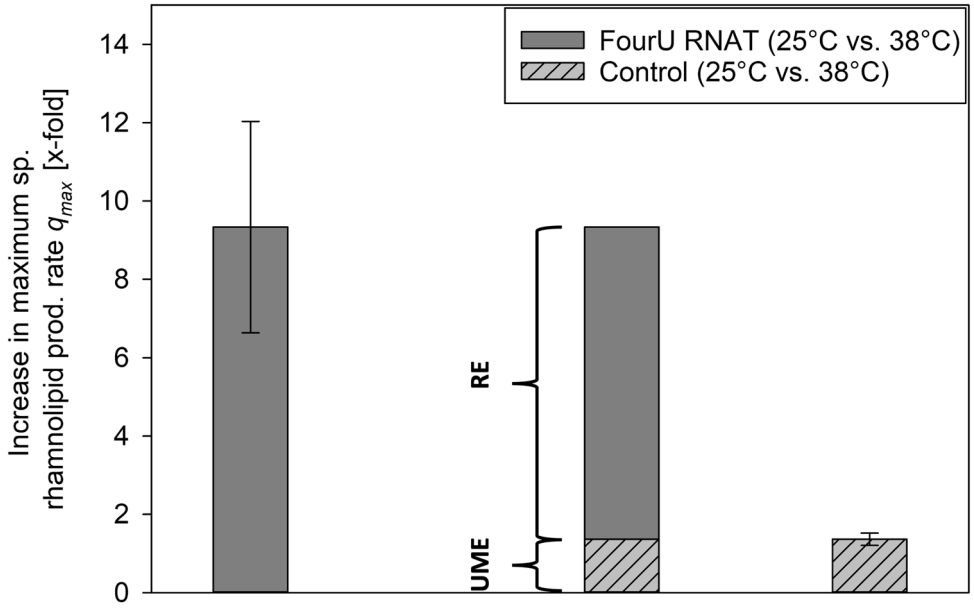

Figure 6. Comparison of increase in maximum specific rhamnolipid production rate (q_{max}) of *Pseudomonas putida* KT2440 pSynPro8oT_4U_*rhlAB* and control strain when grown at 25 °C and 38 °C respectively. Average differences in production rate calculated from individual biological data are shown with derived regulatory effect (RE) and unspecific metabolic effect (UME).

Different overlapping effects reported in connection to the RNATs, and their regulatory abilities have to be mentioned and considered. RNATs are often reported to have a high degree of "leakiness" respectively inefficiency when it comes to inhibition of translation[36]. Moreover, the regulatory potential of RNATs can only be harnessed by changing the temperature. In addition, temperature influences also the entire metabolism and individual metabolic conversion reaction rates can change by altered enzyme activity or even result in inactive enzymes due to denaturation of proteins at elevated temperatures[37]. This could consequently lead to an increase of substrate usage required in metabolic maintenance. An altered temperature also causes different levels of solubilized oxygen in the growth medium, with higher temperatures generally leading to a reduction in oxygen solubility. In this study, a plasmid with the *rhlAB* genes governed by the fourU RNAT was designed and used. The strong increase of RL production rates (> 9-fold) and yields (up to 10 respectively 50-fold for $Y_{P|S}$ respectively $Y_{P|X}$) with increasing temperature indicates a high potential for dynamic temperature adjustments to be used in process control during a RL production process. Figure 6 summarizes the effect of higher biomass specific productivity at elevated temperatures and elucidates its potential for a bioreactor switch process. In the batch reactor set-up, the applicability of the molecular RNAT combined with a switch in temperature (25 °C to 38 °C) for a RL production process (Fig. 5) was shown and compared to previous results for (high titer heterologous) RL production processes (Table 1). The initial temperature of 25 °C was chosen instead of 20 °C to ensure growth at a sufficiently high growth rate while still having low RL production rates (Figs. 3 + 4b) to separate growth and production phase. In this simple batch set-up incorporating a switch from 25 °C to 38 °C after reaching an OD_{600} of 4, the average specific RL production rate could be increased by up to 25% compared to the literature process[14] (Table 1). As such, this batch process outlines the potential of using a RNAT based temperature switch for molecular bioprocess control. Furthermore, RNAT hold several advantages over conventional chemical induction systems such as no use of chemical inducers, (reversible) induction by temperature, possible autoinduction of the system by metabolic heat and earlier onset of the induction response (mRNA is already produced). In a large-scale industrial setup, that would potentially reduce overall costs for chemical inducers, enable tighter control of product-per-biomass ratios and allow for greater flexibility of process control. Furthermore, to track metabolic changes, future studies may also include transcriptome and metabolome analysis, which could point to bottlenecks in the bacterial metabolism and provide additional key factors for optimization approaches using metabolic engineering. Future investigations should aim for a gradual adjustment of temperature over time using tailor made temperature profiles along with an optimized feeding strategy to allow for higher product titers and reduce side product formation. Process modeling may be used to facilitate the completion of this challenging task, because temperature adjustments bring about a wide range of metabolic changes and an optimum temperature profile may therefore not be apparently conceivable. A suitable modeling tool to capture the complexity of a changing temperature during a bioprocess may be an artificial neural network. The combination of a trained artificial neural network and a genetic algorithm may be a powerful strategy to compute an optimized temperature profile to achieve high RL titers. By using temperature sensitive control elements in combination with a well-directed shift in temperature a key challenge in bioprocesses can be met. Substrate carbon can be more efficiently used by reducing by-product formation in form of biomass while substrate carbon is directed into the product. As such this step contributes to the development of sustainable and efficient bioprocesses for a future bioeconomy.

Name	Sequence (5′ → 3′)
FourU	GTTGAACTTTTGAATAGTGATTCAGGAGGTTAATG
G14A-C25U	GTTGAACTTTTAAATAGTGATTTAGGAGGTTAATG
Flank A; *BglII*	TCGCAGTCGGCCTATTGGTTAAGATCTTAACGCGCCAGCTCTTG ACAAGGTCGGAAAATTGAAGTATAATATCAGTCATCGGCTACGC GTGAACACGGACGCCAATCGTTTGCGCAGGCCGATCTGCAAGAC CCACACAAGCCCCTCGCCTGAAGGGGTACGCATCCGCCGTGGCT GGTCCGCGCGGATGGCCGCTGAGTT
Flank B; partial *rhlA*; *PciI*	ATGCGGCGCGAAAGTCTGTTGGTATCGGTTTGCAAGGGCCTGCG GGTACATGTCGAGCGCGTTGGGCAGGAT

Table 2. Sequences used for construction of pSynpro8oT plasmid carrying a fourU RNA thermometer from *Salmonella* along with the control (G14A-C25U).

Methods

Chemicals and reference substances. The chemicals used in this study were purchased from Carl Roth GmbH (Karlsruhe, Germany) if not stated otherwise. The chemicals for analytic procedures were of analytical or mass spectrometry grade. Former Hoechst AG (Frankfurt-Hoechst, Germany) kindly provided the di-RL (Rha-Rha-C10-C10) standard used for HPTLC analysis. The mono-RL (Rha-C_{10}-C_{10}) standard was purchased from Sigma-Aldrich Laborchemikalien GmbH (Seelze, Germany). Derivatization of RLs was carried out as described previously[38] using the derivatization agents 4-bromophenacylbromide and triethylamine which were obtained from Sigma-Aldrich Laborchemikalien GmbH (Seelze, Germany).

Microorganism and plasmids. *Pseudomonas putida* KT2440 carrying the pSynPro8oT_*rhlAB* plasmid for heterologous production of mono-RLs was used as described previously[13]. The ROSE-like RNAT sequence on the pSynPro8oT_*rhlAB* plasmid as described previously[25] was exchanged with either the functional fourU RNAT native to *Salmonella* or the destabilized sequence as control (Fig. 1)[29]. The sequences for the wild type fourU RNAT and the destabilized G14A-C25U mutant shown in Table 2 were ordered via Eurofins Genomics (Ebersberg, Germany) as a standard gene synthesis in a standard pEX A128 vector with ampicillin resistance for selection. Each fourU RNAT sequence variant ordered, was flanked by Flank A (Table 2) also present in the pSynPro8oT_*rhlAB* template plasmid containing the pSynPro8oT synthetic promotor as well as the *Bgl*II restriction site and downstream of the fourU RNAT sequence by Flank B (Table 2) coding for a part of the *rhlA* gene as well as the *Pci*I restriction site.

The pEX plasmids containing the sequences described above were transferred into chemically competent *Escherichia coli* DH5α (New England Biolabs, Ipswich, USA) for plasmid propagation and isolation. The isolated pEX plasmids containing the different fourU RNAT variants were cut with *Bgl*II and *Pci*I. The pSynPro8oT_*rhlAB* backbone isolated from *P. putida KT2440* pSynPro8oT_*rhlAB* was cut analogously with *Bgl*II and *Pci*I to remove the ROSE-like RNAT and to produce matching sticky ends. After dephosphorylation of digested pSynPro8oT_*rhlAB* backbone and ligation with digested fourU RNAT fragment from pEX plasmid using T4 DNA ligase, the plasmids pSynPro8oT_4U_*rhlAB* and pSynPro8oT_4U(G14A-C25U)_*rhlAB* containing the different fourU RNAT variants instead of the ROSE-like RNAT were transformed into electrocompetent *Pseudomonas putida* KT2440 wild type cells. Electrocompetent *P. putida* KT2440 wild type cells were prepared according to[39]. Electroporation of electrocompetent cells was carried out with an electroporation device (Eporator, Eppendorf AG, Hamburg, Germany) and voltage set to 2.5 kV. Strains were selected on LB agar plates containing 20 mg/L tetracycline and confirmed with subsequent sequencing (Eurofins Genomics; Ebersberg, Germany). All strains were stored as glycerol stocks at -80 °C. The strains *Pseudomonas putida* KT2440 pSynPro8oT_4U_*rhlAB* and *Pseudomonas putida* KT2440 pSynPro8oT_4U(G14A-C25U)_*rhlAB* respectively are referred to as FourU and control in the following.

Media preparation. All growth media (LB, SupM, ModR) were prepared as described previously[14].

Shake flask cultivation. Cultivations were performed in a shake incubator (New Brunswick/Innova 44, chamber, Eppendorf AG, Hamburg, Germany) using temperatures between 20 and 42.5 °C and 120 rpm. The first preculture was prepared in a 250 mL baffled shake flask, by inoculating 25 mL of LB medium containing 20 mg/L tetracycline with 50 µL from a glycerol stock solution of *P. putida* KT2440 pSynPro8oT_4U_*rhlAB* or *P. putida* KT2440 pSynPro8oT_4U(G14A-C25U)_*rhlAB* respectively. The first preculture was incubated at 120 rpm and 30 °C, grown for 24 h and subsequently 1 mL was used to inoculate 100 mL of SupM medium (seed culture) in 1 L baffled shake flasks as described by[14]. Each seed culture was grown for 15 h at 120 rpm and 30 °C and used to inoculate the main culture in ModR medium to an OD_{600} of 0.3 respectively 0.5 for bioreactor cultivations.

Bioreactor cultivation. The bioreactor cultivation using a 2 L tabletop bioreactor (Minifors 4, Infors HT, Bottmingen, Switzerland) was carried out as described previously[14] with minor changes. The bioreactor cultivation was carried out in duplicates and as a batch cultivation using 30 g/L glucose. Temperature was switched

from 25 °C to 38 °C when reaching an OD_{600} of around 4 after approximately 9 h of cultivation. The antifoam SB590 (Schill + Seilacher, Hamburg, Germany) was added if needed.

Sample processing. Sample processing was carried out as previously described[14]. To extract RLs, culture supernatant was first acidified 1:100 (*v*/*v*) using 85% phosphoric acid. Subsequently extracted two times with 1.25:1 (*v*/*v*) ethyl acetate, then pooled and evaporated in a vacuum centrifuge at 40 °C for 40 min and 10 mbar (RVC 2-25 Cdplus, Martin Christ Gefriertrocknungsanlagen GmbH, Osterode am Harz, Germany).

Quantification of RLs with HPTLC protocol. Detection of RLs was carried out as described previously[38] with a modified protocol for HPTLC[40]. Briefly, RL samples were re-dissolved in acetonitrile after evaporation and derivatized using a 1:1 (*v*/*v*) mixture of 135 mM bromphenacylbromid and 67.5 mM tri-ethyl-ammonium/-amin. The derivatization step was performed for 90 min at 1400 rpm and 60 °C as previously described[41]. Expected RL concentrations exceeding 2 g/L were diluted prior to derivatization. In a next step, derivatized samples were measured on silica gel 60 HPTLC plates with fluorescence marker F^{254} (Merck, Darmstadt, Germany). Measurements were carried out on a HPTLC system for quantitative analysis (CAMAG Chemie-Erzeugnisse & Adsorptionstechnik AG, Muttenz, Switzerland). Samples application was performed with the Automatic TLC Sampler 4 (ATS 4). Plate development was carried out with the Automatic Developing Chamber 2 (ADC 2), which is equipped with a 20 cm × 10 cm twin-trough chamber. Developed plates were subsequently analyzed with the TLC Scanner 4. A HPTLC imaging and data analysis software (winCATS 1.4.7.2018 software, CAMAG, Muttenz, Switzerland) was used to control the HPTLC-system. Filling speed of the syringe for sample application was set to 15 µL/s and dosage speed to 150 nL/s. The syringe was rinsed with methanol in between sample application. Application start was at 15 mm from the left and 8 mm from the lower edge and band width set to 6 mm. For plate development a mobile phase composed of 30:5:2.5:1 isopropyl acetate:ethanol:water:acetic acid was used. Tank saturation was set to 5 min and subsequent drying was carried out for 5 min with a stream of air. For scanning a deuterium (D2) lamp with slit dimensions of 3 mm × 0.3 mm was used. Plates were scanned at 263 nm at which wavelength bromphenacyl-derivatized RL congeners absorb. For data resolution and scanning speed 1 nm/step and 100 nm/s respectively were chosen.

Enzymatic assay. For quantification of glucose content in the culture supernatant of samples, an enzymatic glucose assay kit (R-Biopharm AG, Darmstadt, Germany) was used, according to the manufacturers' instructions and scaled down to 96-well format.

Graphical analysis, regression and replicates. The scientific graphing and data analysis software (SigmaPlot, Systat Software Inc., San Jose, CA) was used to carry out regression analysis of measured data. A four-parameter logistic fit for biomass, glucose and RL concentration, was used to illustrate the time course of these variables[42]. Measurement results and calculated performance parameters (rates and yields) are presented as mean ± standard deviation obtained from data of duplicates from at least two independent biological experiments. To avoid mathematical artifacts caused by low biomass concentrations, specific RL production rates (q) were calculated starting at hour 3.

Parameter optimization, modeling and simulation. MATLAB 2020b (The MathWorks, Natick, MA, USA) was used to perform parameter fitting and simulation for the temperature-dependency model, shown in the results section. The Nelder-Mead numerical algorithm implemented in the embedded function "fminsearch" was used for parameter optimization. Optimization using the functions described above was performed by minimizing the error of simulation data and measured data according to a least-square error function. To demonstrate and describe temperature dependency of specific RL production rates, a mechanistic temperature model (Eq. (1)) was used for a fitting curve[30].

$$q_{max}(T) = \frac{\mu_{25} \cdot \frac{T}{298} \cdot e^{\left[\frac{H_a}{R} \cdot \left(\frac{1}{298} - \frac{1}{T}\right)\right]}}{1 + e^{\left[\frac{H_l}{R} \cdot \left(\frac{1}{T_l} - \frac{1}{T}\right)\right]} + e^{\left[\frac{H_h}{R} \cdot \left(\frac{1}{T_h} - \frac{1}{T}\right)\right]}} \quad (1)$$

Data availability

All obtained data has been included into the manuscript. Please turn to the corresponding author for all other requests.

Received: 13 April 2021; Accepted: 9 July 2021
Published online: 20 July 2021

References

1. Van Bogaert, I. N. A. *et al.* Microbial production and application of sophorolipids. *Appl. Microbiol. Biotechnol.* **76**, 23–34 (2007).
2. Desai, J. D. & Banat, I. M. Microbial production of surfactants and their commercial potential. *Microbiol. Mol. Biol. Rev.* **61**, 47–64 (1997).
3. Schramm, L. L., Stasiuk, E. N. & Marangoni, D. G. 2 Surfactants and their applications. *Annu. Rep. Prog. Chem. Sect. C Phys. Chem.* **99**, 3–48 (2003).
4. Li, Y. *et al.* Surfactin and fengycin contribute to the protection of a *Bacillus subtilis* strain against grape downy mildew by both direct effect and defence stimulation. *Mol. Plant Pathol.* **20**, 1037–1050 (2019).
5. Lourith, N. & Kanlayavattanakul, M. Natural surfactants used in cosmetics: glycolipids. *Int. J. Cosmet. Sci.* **31**, 255–261 (2009).

6. DeSanto, K. Rhamnolipid Mechanism. US Patent 2011 0123623A1 at https://patentimages.storage.googleapis.com/b3/5c/53/42b14278e189b2/US20110123623A1.pdf (2011).
7. Henkel, M., Geissler, M., Weggenmann, F. & Hausmann, R. Production of microbial biosurfactants: Status quo of rhamnolipid and surfactin towards large-scale production. *Biotechnol. J.* **12**, 1600561. https://doi.org/10.1002/biot.201600561 (2017).
8. Najmi, Z., Ebrahimipour, G., Franzetti, A. & Banat, I. M. *In situ* downstream strategies for cost-effective bio/surfactant recovery. *Biotechnol. Appl. Biochem.* **65**, 523–532 (2018).
9. Müller, M. M., Hörmann, B., Syldatk, C. & Hausmann, R. *Pseudomonas aeruginosa* PAO1 as a model for rhamnolipid production in bioreactor systems. *Appl. Microbiol. Biotechnol.* **87**, 167–174 (2010).
10. Nicas, T. I. & Iglewski, B. H. The contribution of exoproducts to virulence of *Pseudomonas aeruginosa*. *Can. J. Microbiol.* **31**, 387–392 (1985).
11. Cha, M., Lee, N., Kim, M., Kim, M. & Lee, S. Heterologous production of *Pseudomonas aeruginosa* EMS1 biosurfactant in *Pseudomonas putida*. *Bioresour. Technol.* **99**, 2192–2199 (2008).
12. Ochsner, U. A., Reiser, J., Fiechter, A. & Witholt, B. Production of *Pseudomonas aeruginosa* rhamnolipid biosurfactants in heterologous hosts. *Appl. Environ. Microbiol.* **61**, 3503–3506 (1995).
13. Beuker, J. *et al.* Integrated foam fractionation for heterologous rhamnolipid production with recombinant *Pseudomonas putida* in a bioreactor. *AMB Express* **6**, 11. https://doi.org/10.1186/s13568-016-0183-2 (2016).
14. Beuker, J. *et al.* High titer heterologous rhamnolipid production. *AMB Express* **6**, 124. https://doi.org/10.1186/s13568-016-0298-5 (2016).
15. Shapiro, R. S. & Cowen, L. E. Thermal control of microbial development and virulence: molecular mechanisms of microbial temperature sensing. *MBio* **3**, e002381-2. https://doi.org/10.1128/mBio.00238-12 (2012).
16. Klinkert, B. & Narberhaus, F. Microbial thermosensors. *Cell. Mol. Life Sci.* **66**, 2661–2676 (2009).
17. Sengupta, P. & Garrity, P. Sensing temperature. *Curr. Biol.* **23**, R304–R307 (2013).
18. Altuvia, S., Kornitzer, D., Teff, D. & Oppenheim, A. B. Alternative mRNA structures of the cIII gene of bacteriophage λ determine the rate of its translation initiation. *J. Mol. Biol.* **210**, 265–280 (1989).
19. Nocker, A. A mRNA-based thermosensor controls expression of rhizobial heat shock genes. *Nucleic Acids Res.* **29**, 4800–4807 (2001).
20. Johansson, J. *et al.* An RNA Thermosensor controls expression of virulence genes in *Listeria monocytogenes*. *Cell* **110**, 551–561 (2002).
21. Waldminghaus, T., Gaubig, L. C. & Narberhaus, F. Genome-wide bioinformatic prediction and experimental evaluation of potential RNA thermometers. *Mol. Genet. Genomics* **278**, 555–564 (2007).
22. Kortmann, J. & Narberhaus, F. Bacterial RNA thermometers: Molecular zippers and switches. *Nat. Rev. Microbiol.* **10**, 255–265 (2012).
23. Wei, Y. & Murphy, E. R. Temperature-dependent regulation of bacterial gene expression by RNA thermometers. In *Nucleic Acids—From Basic Aspects to Laboratory Tools* (eds Larramendy, M. L. & Soloneski, S.) 157–181 (IntechOpen, 2016).
24. Grosso-Becerra, M. V. *et al.* Regulation of *Pseudomonas aeruginosa* virulence factors by two novel RNA thermometers. *Proc. Natl. Acad. Sci.* **111**, 15562–15567 (2014).
25. Noll, P. *et al.* Evaluating temperature-induced regulation of a ROSE-like RNA-thermometer for heterologous rhamnolipid production in *Pseudomonas putida* KT2440. *AMB Express* **9**, 154. https://doi.org/10.1186/s13568-019-0883-5 (2019).
26. Kouse, A. B., Righetti, F., Kortmann, J., Narberhaus, F. & Murphy, E. R. RNA-mediated thermoregulation of iron-acquisition genes in *Shigella dysenteriae* and pathogenic *Escherichia coli*. *PLoS ONE* **8**, e63781. https://doi.org/10.1371/journal.pone.0063781 (2013).
27. Klinkert, B. *et al.* Thermogenetic tools to monitor temperature-dependent gene expression in bacteria. *J. Biotechnol.* **160**, 55–63 (2012).
28. Weber, G. G., Kortmann, J., Narberhaus, F. & Klose, K. E. RNA thermometer controls temperature-dependent virulence factor expression in *Vibrio cholerae*. *Proc. Natl. Acad. Sci.* **111**, 14241–14246 (2014).
29. Rinnenthal, J., Klinkert, B., Narberhaus, F. & Schwalbe, H. Modulation of the stability of the *Salmonella* fourU-type RNA thermometer. *Nucleic Acids Res.* **39**, 8258–8270 (2011).
30. Schoolfield, R. M., Sharpe, P. J. H. & Magnuson, C. E. Non-linear regression of biological temperature-dependent rate models based on absolute reaction-rate theory. *J. Theor. Biol.* **88**, 719–731 (1981).
31. Arnold, S. *et al.* Heterologous rhamnolipid biosynthesis by *P. putida* KT2440 on bio-oil derived small organic acids and fractions. *AMB Express* **9**, 80. https://doi.org/10.1186/s13568-019-0804-7 (2019).
32. Bator, I., Karmainski, T., Tiso, T. & Blank, L. M. Killing two birds with one stone—Strain engineering facilitates the development of a unique rhamnolipid production process. *Front. Bioeng. Biotechnol.* **8**, 899. https://doi.org/10.3389/fbioe.2020.00899 (2020).
33. Henkel, M., Müller, M., Hörmann, B., Syldatk, C. & Hausmann, R. Microbial rhamnolipids. In *Handbook of Carbohydrate-Modifying Biocatalysts* (ed. Grunwald, P.) 697–738 (Pan Stanford Series on Biocatalysis, 2016).
34. Rinnenthal, J., Klinkert, B., Narberhaus, F. & Schwalbe, H. Direct observation of the temperature-induced melting process of the *Salmonella* fourU RNA thermometer at base-pair resolution. *Nucleic Acids Res.* **38**, 3834–3847 (2010).
35. Chowdhury, S., Maris, C., Allain, F. H. T. & Narberhaus, F. Molecular basis for temperature sensing by an RNA thermometer. *EMBO J.* **25**, 2487–2497 (2006).
36. Chowdhury, S., Ragaz, C., Kreuger, E. & Narberhaus, F. Temperature-controlled structural alterations of an RNA thermometer. *J. Biol. Chem.* **278**, 47915–47921 (2003).
37. Ross, T. & Nichols, D. S. Ecology of bacteria and fungi in foods | Influence of Temperature. In *Encyclopedia of Food Microbiology* (eds Batt, C. A. & Tortorello, M. L.) 602–609 (Academic Press, 2014).
38. Schenk, T., Schuphan, I. & Schmidt, B. High-performance liquid chromatographic determination of the rhamnolipids produced by *Pseudomonas aeruginosa*. *J. Chromatogr. A* **693**, 7–13 (1995).
39. Choi, K. H., Kumar, A. & Schweizer, H. P. A 10-min method for preparation of highly electrocompetent *Pseudomonas aeruginosa* cells: Application for DNA fragment transfer between chromosomes and plasmid transformation. *J. Microbiol. Methods* **64**, 391–397 (2006).
40. Horlamus, F. *et al.* One-step bioconversion of hemicellulose polymers to rhamnolipids with *Cellvibrio japonicus* : A proof-of-concept for a potential host strain in future bioeconomy. *GCB Bioenergy* **11**, 260–268 (2019).
41. Cooper, M. J. & Anders, M. W. Determination of long chain fatty acids as 2-naphthacyl esters by high pressure liquid chromatography and mass spectrometry. *Anal. Chem.* **46**, 1849–1852 (1974).
42. Henkel, M. *et al.* Kinetic modeling of rhamnolipid production by *Pseudomonas aeruginosa* PAO1 including cell density-dependent regulation. *Appl. Microbiol. Biotechnol.* **98**, 7013–7025 (2014).

Acknowledgements

The authors would like thank Dr. Frank Rosenau and Dr. Andreas Wittgens (Institute for Pharmaceutical Biotechnology, Ulm University, Germany) for constructive scientific discussion and for providing the initial plasmid pSynPro8.

Author contributions

P.N. planned and executed the experiments, collected data, created the graphs and drafted the manuscript. C.T. and S.M. performed part of the experiments and cloning, collected and evaluated corresponding data. L.L. and R.H. contributed to evaluation of the data, design of the experiments and scientific discussion. M.H. substantially contributed to conception, and design of the conducted experiments, interpretation and evaluation of the results and drafting of the manuscript. All authors read and approved the final version of the manuscript.

Funding

Open Access funding enabled and organized by Projekt DEAL. This study was partially funded by the Ministry of Science, Research and the Arts of Baden-Wuerttemberg (MWK, funding code: 7533-10-5-186 B). PN and CT are members of the "BBW ForWerts" graduate program and PN received a scholarship within the frame of the Baden-Wuerttemberg Landesgraduiertenfoerderung (LGF) awarded by the Ministry of Science, Research and the Arts (MWK) of Baden-Württemberg, Germany.

Competing interests

The authors declare no competing interests.

Additional information

Correspondence and requests for materials should be addressed to M.H.

Reprints and permissions information is available at www.nature.com/reprints.

Publisher's note Springer Nature remains neutral with regard to jurisdictional claims in published maps and institutional affiliations.

Part III

General Discussion

6. Circular economy & rhamnolipids

The production of (bio)chemicals based on renewable resources is one of the goals of a sustainable circular economy [United Nations 2015b]. Rhamnolipids (RLs) are microbially produced surfactants derived from renewable substrates. However, there are few studies to date that ecologically assess the entire life cycle of biosurfactants (BS) such as RLs as recently reported [Kopsahelis *et al.* 2018]. Key challenges of RL synthesis include the production in the native host and human pathogen *Pseudomonas aeruginosa* where RL production is under control of a complex and cell density-dependent mechanism, the quorum sensing. In 2016 these challenges were met with the transfer of the *rhlAB* genes and their constitutive expression in the nonpathogenic relativ *Pseudomonas putida* KT2440 pSynpro8oT_*rhlAB* [Beuker *et al.* 2016b]. Consequently, new challenges arose when using the heterologous host. On the one hand, the comparably low titers of 14.9 g/L for a supposably cheap and abundant bulk chemical [Beuker *et al.* 2016a], and on the other hand, the use of antibiotics for this plasmid-based system. As for the process design, the latter challenge makes it difficult to use the heterologous system in a continuous production process that is often sought by industry. The recyclability of the biomass and the stability of the plasmids are important in a continuous process and may present further hurdles. On the other hand a continuous process would also be difficult for the native host *P. aeruginosa*, since quorum sensing autoinducer molecules that control RL formation may be washed out and RL formation inhibited. In a recent report the strain *P. putida* KT2440 SK4 was introduced in which the *rhlAB* genes were genomically integrated and thus stabilized. However, only titers of 0.7 g/L were achieved and are thus not competitive so far. Furthermore, a low product per substrate yield of only 0.06 g_{RL}/g_{Glc} was achieved [Tiso *et al.* 2020]. Similar issues regarding efficient substrate utilization were also encountered in the plasmid-based system of Beuker et al. [2016]. Here around 250 g of glucose were metabolized to produce around 20 g of RL displaying a poor product to substrate ratio. Thereby biomass generation is a large carbon sink, with roughly 50% more biomass than product formed [Beuker *et al.* 2016a]. The results presented in this thesis showed that the strain *P. putida* KT2440 pSynpro8oT_*rhlAB* with RL synthesis under control of a fourU RNA thermometer (RNAT) could achieve $Y_{P/X}$ values well above 1 (about 1.4 g_{RL}/g_{BM}) and $Y_{P/S}$ values of about 0.2 g_{RL}/g_{Glc} at elevated temperatures of 37–38°C. While these yields showed great potential, they could so far only be achieved in shake flasks [Noll *et al.* 2021]. However, initial attempts have been made to achieve comparable yields in a bioreactor system using a temperature shift as will

be discussed later. The theoretically possible yields for RL formation were calculated by Henkel et al. [2012]. For the RL yield from glucose (from plant starch), a value of 0.52 g_{di-RL}/g_{Glc} was determined. However, this value was calculated for di-RL (Rha_2-C_{10}-C_{10}) [Henkel *et al.* 2012] whereas *P. putida* KT2440 pSynpro8oT_*rhlAB* only forms mono-RL. Using supplementary tables 1–5 of the latter article, the theoretically possible maximum yield for mono-RL (Rha-C_{10}-C_{10}) and glucose catabolism via the Entner-Doudoroff-pathway (ED) can be approximated with 0.48 $g_{mono-RL}/g_{Glc}$ [Henkel *et al.* 2012] (for the calculation of theoretically possible maximum yields it is assumed that all metabolic pathways shown in figure 1 of Henkel *et al.* [2012] are present; the calculations rely on ATP energy balancing; ATP generation from glucose is calculated using the ED pathway [Chavarria *et al.* 2013]). It was assumed for the calculation that energy was limited, cell-growth was absent, and disregarding limitations of e.g. oxygen, carbon, or redox-equivalents. Also, maintenance metabolism was disregarded, and it was assumed that no by-products are formed [Henkel *et al.* 2012]. However in real world processes by-products like exo-(lipo)polysaccharides present a carbon sink as they are build of the monosaccharides, amongst others, glucose and also rhamnose [Kachlany *et al.* 2001]. This may result in a loss of productivity in the RL production process. Exopolysaccharides are also reported to play a role in stable biofilm formation in *P. putida* [Nilsson *et al.* 2011]. Attempts have been made to genetically suppress biofilm formation by manipulating several prominent exopolysaccharide gene clusters e.g., for alginate, bacterial cellulose synthesis, putida exopolysaccharide a and b. However, the biofilm could only be destabilized, its formation whereas could not completely be prevented [Nilsson *et al.* 2011]. The quantification and clear identification of the by-products formed also remains the subject of current research. An alternative to the molecular biological solution of the by-product problem is a process engineering approach. Since by-product formation often occurs at high glucose concentrations, the amount of glucose should be kept at a low level during a fed batch process as has been carried out in the heterologous rhamnolipid production process with the so far highest product titers [Beuker *et al.* 2016a]. Here, the glucose concentration could be maintained between 0.1–0.3 g/L for 20 h due to an optimized 2-phase feeding profile [Beuker *et al.* 2016a]. In classical fed batch developments, where the biomass is forced onto a trajectory through glucose limitation, may also present difficulties since this may result in suboptimal product formation. This means that the lower limit of the glucose control range should be just above 0 g/L. Consequently, there would only be a narrow glucose control corridor (presumably 0 g/L $<$ setpoint $<$ 0.5 g/L), which is a demanding task for bioprocess control. Deviating from this control range may result either in suboptimal product formation due to limited substrat availability or in dominant by-product and biofilm formation with reduced product yields when substrate concentrations are too high. To cope with this difficult control task, model-based soft sensors could be used for glucose monitoring, for example. A summary of different control strategies including soft sensors are presented in the review of Noll & Henkel [Noll *et al.* 2020a]. A more costly alternative to soft sensors are hardware solutions for glucose monitoring e.g. the "Bioreactor Probe Sensor for Glucose and/or Lactate" [KDBIO S.A.S. 2021, Berstett, France] which can be used to monitor glucose in a range of 0—8 g/L and may

be configured for feed pump control. In conclusion, poor $Y_{P/S}$, $Y_{P/X}$ and low titers represent a challenge in heterologous rhamnolipid production. To address these challenges molecular- (RNAT, genes controlling by-product formation) or conventional (feeding strategy) bioprocess control approaches may be used which are discussed in the subsequent section. The effective incorporation of substrate carbon into the product may be hindered by by-product formation. Suitable identification and quantification methods for by-products of *P. putida* remain the subject of current research. As for $Y_{P/S}$ values around 0.2 $g_{mono-RL}/g_{Glc}$ could be achieved during this work which would represent around 40% of the theoretically possible maximum yield (0.48 $g_{mono-RL}/g_{Glc}$ see above). The former poor $Y_{P/X}$ were shown to be shifted in favor of the product in this thesis ($Y_{P/X}$ values well above 1 possible) by using elevated temperatures and the molecular temperature sensors, the RNATs. Whereas the low titers remain a challenge which may be addressed in the future by suitable feeding strategies and improved temperature profiles (see also section 8).

7. Conventional & molecular bioprocess control

The aim of this chapter is to elaborate on the different options to excercise control over a bioprocess either in a conventional way by e.g. substrate limited feeding or by molecular control mechanisms e.g. by RNATs. Thereby the regulatory RNA elements discussed in this thesis are classified and compared to other molecular control units like promoter/regulator systems or riboswitches.

7.1 Conventional bioprocess control

There are several ways to exercise control over a bioprocess and guide it along a beneficial trajectory. In conventional bioprocess engineering, control can be exercised, by limiting the availability of a substrate thus influencing growth and metabolic flux [Klement *et al.* 2013]. A classic example of such an operation would be a carbon limitation achieved by a suitable feeding strategy. A specific growth rate can thereby be set, e.g. by glucose-limited feeding, below the maximum specific growth rate of the organism. This strategy can not only be used to optimize the process and improve reproducibility [Jenzsch *et al.* 2006], but also to obtain a high specific content of product e.g., Histidine [Shioya 1992]. In the latter case the authors simply plotted different μ against specific histidine production rates (q) and reported a proportional increase of q with μ for $\mu < 0.16\ \mathrm{h}^{-1}$ and a sudden decrease of q for $\mu > 0.16\ \mathrm{h}^{-1}$ [Shioya 1992]. There are further examples in other organisms where the formation of a (secondary) metabolite is guided by conventional process control. Classic examples are citric acid or itaconic acid production and the production of the amino acids L-glutamic acid and L-lysine. Citric acid is produced with *Aspergillus niger* with high glucose concentration (approx. ≥ 100 g/L) and biomass growth is controlled by limiting N and P sources while mycelium structure is controlled by low manganese concentration (approx. < 0.05 mg/L) [Kubicek *et al.* 2010]. For industrial itaconic acid production with *Aspergillus terreus*, similar to citric acid production, a high glucose concentration $100 - 150$ g/L and phosphorus limitation are required for improved production [Klement *et al.* 2013]. To produce the amino acids L-glutamic acid and L-lysine, respectively, with *Corynebacterium glutamicum*, a limiting biotin in the first case and a carbon limiting feeding strategy during the production phase in the second case turned

out to be beneficial for the production [Bona *et al.* 1997; Becker *et al.* 2011]. In another approach, the production of the antibiotic, methylenomycin, produced by *Streptomyces coelicolor* could be optimized with a combination of carbon limitation and a pH drop [Hayes *et al.* 1997]. In the case of heterologous RL production a model-optimized 2-phase feeding strategy was used to keep the glucose level low, while optimizing rhamnolipid titer. Here, the highest RL titer in a heterologous process was achieved but also roughly 50% more biomass than RL is produced draining substrate carbon from the process [Beuker *et al.* 2016a]. In contrast to this classical indirect and often complex to conceive control of a bioprocess, considering the manifold interconnected metabolic pathways, it is also possible to influence the formation of products in a more direct way already at the molecular level. Molecular control systems can be introduced that grant direct, fast, and easy access to control product formation.

7.2 Molecular bioprocess control

The aim of this section is to clarify which molecular mechanisms can be exploited for the control of gene expression respectively product formation in a bioprocess and where the regulatory RNA elements discussed in this thesis can be placed. One of the most common methods to control the onset of product formation in microorganisms are inducible promoter systems. There are several studies testing different inducible promoter systems in combination with a reporter (usually x-fluorescent protein) for *P. putida* KT2440 [Schuster *et al.* 2021; Calero *et al.* 2016; Sathesh-Prabu *et al.* 2021; Liang *et al.* 2021]. Only some studies also report a fold-change, i.e. a comparison of basal and induced gene expression normalized to biomass ([Schuster *et al.* 2021; Liang *et al.* 2021], see also table below) and none of the studies evaluated an RNA thermometer based molecular control systems in context of an industrially relevant product like it has been done in this thesis. On the level of DNA-based control systems a T7-like expression system for *P. putida* KT2440 similar to the pET expression system of *E. coli* was constructed and tested measuring an 82-fold change in fluorescence (super-folder GFP) normalized to biomass between basal and induced state [Liang *et al.* 2021]. In a second study, 12 different regulator/promoter/inducer systems were tested in *P. putida* KT2440 revealing a wide range of induction efficiency and promoter leakiness. Detailed information of the promoter – regulator pairs and the used plasmids can be found in the supplementary table 1 elsewhere [Schuster *et al.* 2021]. The fluorescence (monomeric RFP) normalized to biomass of the basal state was compared to the induced state resulting in a wide range of promoter efficiency between 1 – 846-fold change (basal vs. induced; $TtgR^{AM}/P_{Ttg}$/Naringenin – $LuxR/P_{LuxB}$/HSL) [Schuster *et al.* 2021]. Fluorescence was measured at regular intervals after induction up to a maximum of 24 h. This may be problematic in the context of prolonged cultivation processes in industry considering that inducer half-life of the most effective system tested (inducer HSL) is just 9 h in standard media such as M9 medium [Pasotti *et al.* 2014; Schuster *et al.* 2021]. In general, the half-life of inducer molecules should be considered. In a study from 2014, the half-life of 3 common inducers (isopropyl β-D-1-thiogalactopyranoside (IPTG), anhydrotetra-

cycline (ATc) and N-(3-oxohexanoyl)-L-homoserine lactone (HSL)) was tested in sterile LB and M9, respectively, at different temperatures (30, 37°C) and pH values (6, 7) over 32 h. The IPTG concentration remained stable over 32 h in sterile LB and M9 medium. In contrast, the half-life of ATc averaged about 20 h that of HSL in M9 medium at pH 7 was only about 9 h at 30 and 37°C. Induction strength and expression level are normally proportional to the amount of inducer until a saturation concentration of inducer is reached. On the one hand, if inducer concentration falls below this threshold, product expression is slowed [Pasotti *et al.* 2014]. On the other hand, inducer concentrations that are too high can have a toxic effect (e.g. fluoride salts) and inhibit cellular growth [Calero *et al.* 2020; Schuster *et al.* 2021]. The window with the described effects of upper and lower limit of inducer concentration must be considered if the inducer is added over time. In comparison to the chemical induction, physical parameters like temperature can be used to control gene expression as described in the following. The table below shows a summary of different inducible molecular control systems based either on DNA or RNA. All systems were tested in *Pseudomonas putida* KT2440 and compared by the fold-change between basal and induced state. Thereby the fluorescence signal or concentration of a reporter normalized to biomass was used as an indicator for promoter efficiency and leakiness. It should be noted here that RL is listed below as a reporter but in fact the RNAT controlling RL production regulates the expression of *rhlAB* genes encoding a rhamnosyltransferase and thus only indirectly affects the formation of RL.

Table 7.1: Inducible molecular control units in *Pseudomonas putida* KT2440 (if not stated otherwise) based on DNA or RNA inducible via chemical inducer, starvation or temperature. The fluorescence signal or concentration of the reporter were normalized to biomass before calculating the fold-change between basal and induced expression. Detailed information of the regulator/promoter/reporter/inducer combinations depicted and the plasmids used can be found in Noll *et al.* 2019; Noll *et al.* 2021; Chawla *et al.* 2015; Aparicio *et al.* 2019; Liang *et al.* 2021 as well as in the supplementary table 1 of Schuster *et al.* 2021.

Host or vector (reporter)	**Regulator / promoter**	**Inducer**	**Basal vs. induced (x fold-change)**	**Reference**
		Induction by chemical inducer		
T7-like MmP1; (sfGFP)	LacI/P_{MmP1}	IPTG	82	[Liang *et al.* 2021]
pF_R5 (mRFP) [1)]	AraC/P_{BADmin}	Arabinose	243	[Schuster *et al.* 2021]
	$CinR^{AM}$/P_{Cin}	OH-C14-HSL [2)]	597	
	$CymR^{AM}$/P_{CymRC}	Cumate	16	
	LacI/$P_{Llaco-1}$	IPTG	7	
	LuxR/P_{LuxB}	OC6-HSL [3)]	846	
	$NahR^{AM}$/P_{salTTC}	Salicylic acid	540	
	$PcaU^{AM}$/P_{3B5B}	Protocatechuate	5	
	TetR/$P_{LtetO-1}$	Anhydrotetracycline	14	
	RhaSR/P_{RhaBAD}	Rhamnose	41	
	TetR/P_{TetA}	Anhydrotetracycline	4	
	$TetR^{AM}$/P_{Ttg}	Naringenin	1	
	$VanR^{AM}$/P_{VanCC}	Vanillate	15	
		Induction by starvation		
pLAVR3 (N/A) (*P. aeruginosa*)	phoR/P_{PhoA}	Phosphate limitation	N/A	[Filloux *et al.* 1988]

Table 7.1: (continued)

Host or vector (reporter)	Regulator / promoter	Inducer	Basal vs. induced (x fold-change)	Reference
		Riboswitch		
pSEVA441; (msfGFP)	FRS [4]/P_{EM7} or P_{eriC^F}	NaF	1.5 – 3.8	
P. putida KT2440::FRS-T7RNAP	FRS/P_{T7}	NaF	200	[Calero *et al.* 2020]
pS231T7::msfGFP				
		Induction by temperature		
pSEVA2x14 (msfGFP) [5]	*c*I857 system/P_L	30 vs. 37°C	5 – 20	[Aparicio *et al.* 2019]
(*P. putida* EM42)		30 vs. 42°C	300	
pSynpro8oT_4U_*rhlAB*; (RL)	FourU(G14A-C25U)/P_{Syn}	25 vs. 38°C	1.7	[Noll *et al.* 2021]
		20 vs. 38°C	3	
pSynpro8oT_4U_*rhlAB*; (RL)	FourU(wt)/P_{Syn}	25 vs. 38°C	20.4	
		20 vs. 38°C	50	
pSynpro8oT_*rhlAB*; (RL)	ROSE(wt)/P_{Syn}	26 vs. 38.5°C	2.5	[Noll *et al.* 2019]

[1] RSF1010 (incQ) origin of replication, mRFP (monomeric red fluorescent protein), gentamicin marker

[2] Hydroxy-tetradecanoyl-homoserine lactone

[3] N-(3-oxohexanoyl) homoserine lactone

[4] Fluoride ion responsive riboswitch

[5] x = 2: RK2 origin of replication (ORI) (low copy number) / 3: pBBR1 ORI (medium copy number) / 4: RSF1010 ORI (high copy number); (m)sfGFP: (monomeric) superfolder green fluorescent protein

At the DNA level, temperature has been used to induce gene expression. The thermotolerant mutant *P. putida* EM42 and the vectors pSEVA2214, pSEVA2314, pSEVA2514 (based on RK2 low copy number, pBBR1 medium copy number, and RSF1010 high copy number) on which the regulator promoter pair *c*I857/P_L from phage λ regulates the expression of the reporter msfGFP in dependence of temperature, were used [Aparicio *et al.* 2019]. When comparing the basal expression at 30°C with the induced expression at 37°C, a 5 – 20-fold difference in fluorescence was measured. The magnitude of the increase in fluorescence was dependent on the plasmid copy number. The highest fold-change between basal and induced state was measured between 30°C and 42°C, 3 h after induction with a 300-fold difference in fluorescence after which fluorescence decreased again [Aparicio *et al.* 2019]. A drawback of strong expression systems developed to maximize the product formation places a high metabolic burden on an organism, which can possibly even lead to cell death [Striedner *et al.* 2003]. This in turn shortens the time in which production formation can occur and aggravates reaching a higher yield. An approach was developed to counteract this by controlling the transcription rate via conventional limited feeding of chemical inducer, thereby keeping the ratio of inducer to growing biomass constant [Striedner *et al.* 2003]. In this case the biomass must be closely monitored to ensure that the correct amount of inducer is added. On the DNA-level molecular control units are used to control transcription whereas on the RNA-level, translation is adjusted to exercise control on product formation. Riboswitches are a way of modulating gene expression on the RNA-level. Riboswitches regulate gene expression in response to the binding of a low molecular compound by forming secondary structures. Normally, riboswitches consist of 2 domains. One in which the target ligand is bound with high affinity and specificity, and a second domain that, in response to the binding, influences gene expression. In this case, fluorescent proteins are also used as reporter systems to determine the induction efficiency, i.e. the comparison of the basal and induced state normalized to biomass [Hallberg *et al.* 2017]. In a recent study of 2020, a riboswitch for *P. putida* KT2440 was designed and tested [Calero *et al.* 2020]. Originally, the riboswitch used originated from *Pseudomonas syringae*, where it regulates the expression of a putative F^- exporter ($eriC^F$) depending on fluoride ion concentration [Chawla *et al.* 2015]. After optimization of the fluoride ion responsive riboswitch system (FRS) for *P. putida* KT2440, an up to 200-fold (depending on NaF concentration) higher fluorescence per biomass was measured in the induced compared to the basal state [Chawla *et al.* 2015]. RNATs as discussed in this thesis are another RNA-based molecular control tool relying simply on ambient temperature changes, thereby granting easy access to mRNA topography and translation initiation. An RNA-based method to regulate gene expression and thus product formation was investigated in this thesis using RNATs as described in the previous sections. In the first study from 2019, a ROSE RNAT for *P. putida* KT2440 was tested at different temperatures. The cultivation temperature influenced the amount of product, RL (in the context of this section also the reporter) per biomass ($Y_{P/X}$). It should be noted that in fact the RNAT regulates the expression of *rhlAB* genes encoding a rhamnosyltransferase and thus only indirectly affects the formation of RL [Noll *et al.* 2019]. The difference in RL per biomass concentration at the lowest experimental temperature, 26°C, compared with that at the highest

RL to biomass ratio, at 38.5°C, was found to be a 2.5-fold difference [Noll *et al.* 2019]. Comparing the difference in RL per biomass between two similar temperatures (25 vs. 38°C) but for a different RNAT, the fourU(wt) RNAT, a much higher difference of 20.4-fold was found [Noll *et al.* 2021]. If the temperature is lowered further to minimize basal expression, an approximately 50-fold difference of RL per biomass was measured between the lower- (20°C) and the higher temperature (38°C) [Noll *et al.* 2021]. The figure below provides an overview on efficiency of inducible molecular control units described above as regulator/promoter/reporter/inducer combinations. They are either based on DNA or RNA and sorted by fold-change between basal and induced state. The reporter-signal (fluorescence) respectively -concentration normalized to biomass was used to calculate a fold-change between the two states. All systems were tested for *P. putida*. The figure also ranks the RNATs described and tested in this thesis for *P. putida* KT2440. Other temperture-dependent induction systems are also compared.

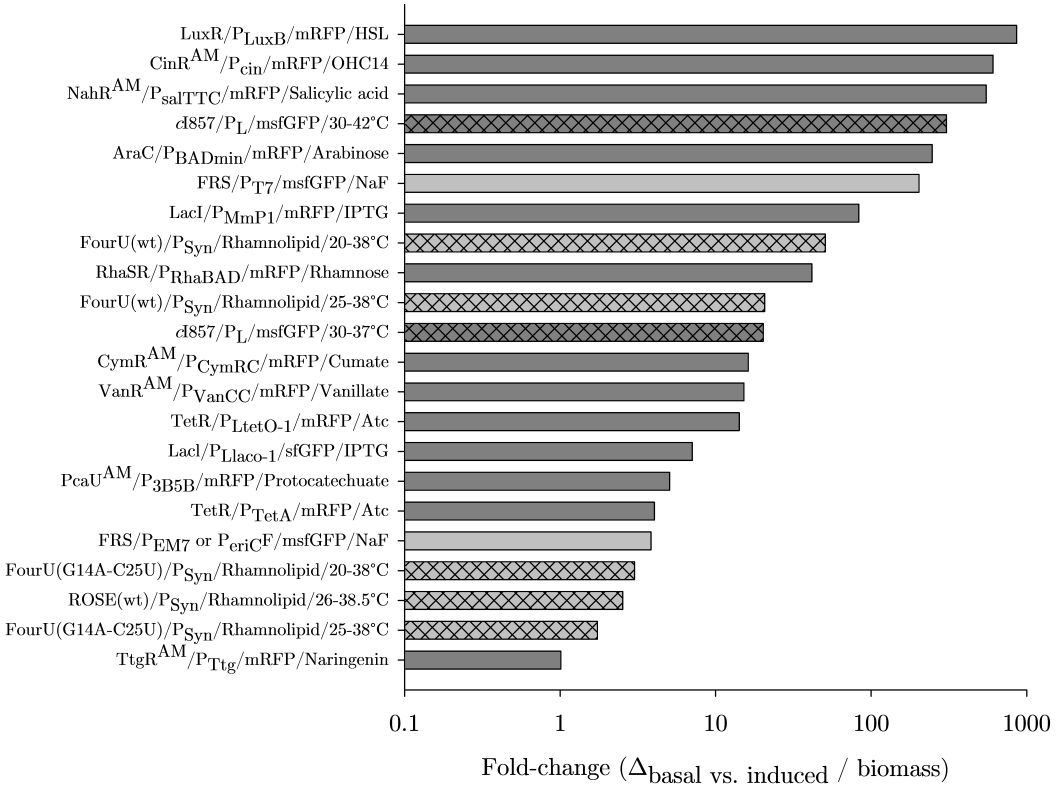

Figure 7.1: Logarithmic plot of fold-change [-] between basal and induced expression of DNA- (dark grey) or RNA (grey) -based systems in *Pseudomonas putida* inducible via a chemical inducer or temperature. Temperature dependent induction is indicated by a black pattern inside the bar. The fluorescence signal or concentration of the reporter was normalized to biomass before calculating the fold-change between basal and induced expression. Detailed information of the regulator/promoter/reporter/inducer combinations depicted, and the plasmids used can be found in Noll *et al.* 2019; Noll *et al.* 2021; Chawla *et al.* 2015; Aparicio *et al.* 2019; Liang *et al.* 2021 as well as in the supplementary table 1 of Schuster *et al.* 2021.

7.3 RNA thermometers as molecular process control elements

The use of RNAT in combination with temperature changes for bioprocess control offers several advantages, but also poses some challenges that are discussed below. Temperature is a parameter that has a major influence on the functionality and structure of biomolecules and kinetics of biochemical reactions. Therefore, knowledge of the temperature behavior of the organism used (yields, specific product formation rates, growth etc.) is required in order to estimate the response to changing ambient temperatures and to use it advantageously. Data on temperature behavior were therefore collected for *P. putida* KT2440 pSynpro8oT_*rhlAB* as described in Part II of this thesis. One advantage of these simple RNA switches is that they are functionally interchangeable cross-species [Nocker *et al.* 2001b], as was also shown in this thesis with the use of a fourU RNAT from *Salmonella enterica* and a ROSE RNAT from *P. aeruginosa* in *P. putida* [Noll *et al.* 2019; Noll *et al.* 2021]. The genetic manipulation when working with RNATs poses a challenge. For example, secondary structure formation may complicate the genetic manipulation of constructs as experienced when the custom syntheses of certain sequences were aborted due to the stable structures. This is why partial syntheses had to be carried for the constructs [Noll *et al.* 2019; Noll *et al.* 2021]. Another hurdle is the choice of a suitable RNAT - microorganism combination. It must be possible to use the chosen hybrid at temperatures at which the RNAT responds and at the same time translation can still proceed efficiently after a temperature shift. Furthermore, the activity of the target enzyme expressed under control of the RNAT must be considered. The following example highlights that statement: A cold shock RNAT allows higher translation at low temperatures, but this results in a reduced biochemical reaction rate or enzymatic activity compared to higher temperatures [Giuliodori *et al.* 2010]. *P. putida* with a growth optimum at about 30–32°C in combination with the mentioned ROSE or fourU RNAT ($\leq$ 30°C causes a reduced translation compared to 37–38°C) and the produced rhamnosyltransferase 1 (RhlA & RhlB, from a human pathogen) with functionality at temperatures around 37°C are an ideal combination [Noll *et al.* 2019; Noll *et al.* 2021; Grosso-Becerra *et al.* 2014]. However, there is a good chance to find a suitable RNAT for the desired application, as the database of the descriptive literature for RNATs is dense [Klinkert *et al.* 2009; Wei *et al.* 2016; Shapiro *et al.* 2012; Kortmann *et al.* 2012; Narberhaus *et al.* 2006, 2.1]. Furthermore, based on a simple structure it is possible to design (*in silico*), produce, test and optimize RNATs *de novo* in only 2–3 weeks according to a step-by-step protocol, if no appropriate RNAT with the desired temperature response characteristics can be found in literature. This design and application as control element is facilitated by the fact that RNATs are the so far only known single-component regulators for gene expression functioning independently of protein factors and most importantly do not require inducer molecules to carry out their control tasks [Neupert *et al.* 2008; Neupert *et al.* 2009]. The decisive signal for the regulatory control action is simply a change of the physical parameter temperature. As already mentioned, this has the advantage that the use of expensive chemical inducers (e.g., IPTG, around 8000 € / kg, [Carl Roth GmbH 2021, Karlsruhe, Germany]) can be omitted, making scaling of the process cheaper.

Another argument for the improved scalability of using RNATs as induction system is that it can be used with simple standard bioreactor peripherals. No additional probes or pumps are required, simply a temperature probe and suitable temperature control. It should be noted, however, that temperature shifts alter many biological and physical parameters such as growth rate & enzyme activity, solubility of oxygen in the medium & viscosity, which can be plotted as a function of temperature, for example [Xing *et al.* 2014; Arcus *et al.* 2016; Noll *et al.* 2020b]. However, there is a chance that a system under the temperature-dependent translational control of an RNAT can be used for autoinduction with self-stabilization. If the metabolic heat generated during cell growth is not dissipated, the temperature of the system will rise and autoinduction will occur. Hypothetically, it is also conceivable that during the induced product formation phase, less heat is released. Growth and metabolism of substrates no longer proceed optimally at the ambient higher temperatures, resulting in self-stabilization of the process. This of course requires a suitable host system with corresponding growth temperatures. So far, such a process was never described, and its potential not been harnessed for large-scale bioproduction. Another advantage of RNAT over chemical inducers is that induction of product formation is delay-free. The mRNA transcript is already present, and translation can take place directly after a temperature change. Furthermore, the induction is also reversible in theory. Only the time required until the corresponding controlled protein/enzyme is degraded must be considered. Furthermore, it has been hypothesized that RNATs are capable of modulating mRNA stability and possibly provide an increased resistance to nucleolytic degradation [Giuliodori *et al.* 2010]. Since the opening and closing of an RNAT structure is a probabilistic event, a certain percentage of the RNAT structures present remain in a closed secondary conformation. These secondary structures are arguably more stable and less prone to ribonucleolytic degradation than unfolded mRNAs which extends their half-life [Simons 2001; Fang *et al.* 1997; Giuliodori *et al.* 2010]. For the fourU RNAT structures used in this thesis it was for example calculated that at 38°C *in vitro* around 50% of the wildtype fourU RNAT structures are unfolded whereas almost 80% of the destabilized G14A-C25U mutant are unfolded [Rinnenthal *et al.* 2011]. On the one hand the mutant structure may therefore be more likely to be degraded by endoribonucleases at elevated temperatures than the wildtype structure. On the other hand, single stranded RNA may be stabilized by bound ribosomes. A modulation of temperature dependent ribosome accessibility at the respective binding sites was also assigned to the RNA regulatory elements [Yamanaka *et al.* 1999].

8. Finding the ideal temperature & the role of artificial intelligence

Often, the literature refers to the "optimum temperature" for a bioprocess. However, it should be defined more precisely what exactly this temperature is optimal for. For example, one temperature may be ideal for the growth rate, but may deviate from the ideal temperature for the highest amount of biomass per substrate produced [Seel *et al.* 2016]. Also, the ideal temperature for specific product formation rate may differ from the growth optimum as shown in this thesis. At lower temperatures, for example, protein production rate but also error rate for misfolding are lower compared to elevated temperatures. Some processes for recombinant protein production take advantage of this [Schmidt *et al.* 1999; Sørensen *et al.* 2005; Restaino *et al.* 2013]. Thus, less substrate is wasted for misfolding and non-functional proteins, which could also lead to a better biomass-to-substrate yield at lower growth temperatures. It is also conceivable that one or two temperature setpoints during a bioprocess may not be sufficient. A temperature profile may be needed to find a balance between yields, growth, titer and specific product formation rates. Overall, however, there are many internal interrelationships of temperature-dependent processes that can not easily be mapped and therefore may require modeling approaches. Therefore, it was obvious to summarize the available modeling approaches in biotechnology and to select for the approach that is best suited for the above-mentioned problem [Noll *et al.* 2020a; Noll *et al.* 2020b]. After extensive reviewing of the literature, the mechanistic approaches were ruled out, because a mechanism behind temperature changes is not easily conceivable considering that many if not all biochemical reactions in a cell change. A suitable approach seemed to be an artificial neural network. The advantage is that the mechanism connecting input and output variables does not need to be known *a priori*. It is therefore a black box. Furthermore, the input-output relationship can be completed by collecting training data sets and feeding them into the selected network architecture. The data is then propagated to the output layer via the so-called "hidden layer". Scalar weights for each node connection change the signal strength as a result and the network is “trained” [Thibault *et al.* 1990; Holmes 2014]. In order to collect a training data set, different temperature profiles along with constant temperatures for a bioreactor process with *P. putida* KT2440 pSynpro8oT_*rhlAB* were run during this thesis. The cultivation course of biomass,

glucose and RL were recorded. Later the ANN was fed with the training data using time, biomass, residual glucose and temperature as inputs to compute the output: amount RL produced. The temperature profile with the highest RL recorded during a cultivation is shown below.

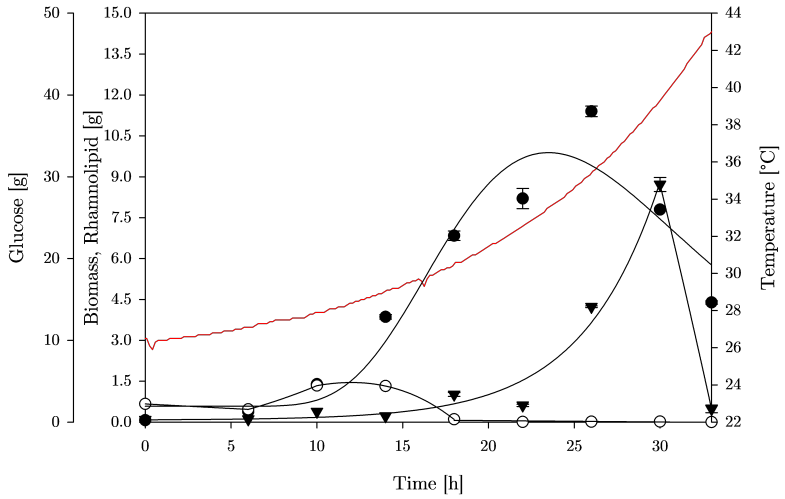

Figure 8.1: Cultivation course of *P. putida* KT2440 pSynpro8oT_*rhlAB* (ROSE RNA thermometer) with an exponential temperature profile displayed as red line [°C]. Cultivation was carried out in a bioreactor in ModR medium with constant feed of 1.5 g glucose per hour starting at 6 h to 33 h. The course for experimentally determined (dots) and fitted values (lines) for biomass (blackdots), rhamnolipid (black triangle) and glucose (open circles) in [g] are shown [Möbus 2020].

P. putida KT2440 pSynpro8oT_*rhlAB* (ROSE RNAT) was cultivated in a bioreactor in ModR medium with a constant glucose feed of 1.5 g_{Glc}/h starting at 6 h to 33 h. The exponential temperature profile shown (Fig. 8.1) yielded at the highest RL value of approx. 9 g (around 13 g/L) less biomass (around 12 g/L) than product. These values were reached after only 30 h consuming just 45 g of glucose. Hence, at this timepoint 36 weight-% of the consumed glucose could be assigned to mono-RL ($Y_{P/S}$ = 0.19 g_{RL}/g_{Glc}) and biomass ($Y_{X/S}$ = 0.17 g_{BM}/g_{Glc}). According to the approximation of the theoretically possible maximum yield (Y_{max}) which is based on ATP-energy balancing [Henkel *et al.* 2012], 0.48 g of mono-RL (Rha-C_{10}-C_{10}) can theoretically be produced per gramm of glucose (catabolism via Entner-Doudoroff-pathway) considering the assumptions stated in section 6 and described elsewhere [Henkel *et al.* 2012]. Hence 40% of Y_{max} was achieved by using an exponential temperature profile. The so far best performing heterologous RL production process, yielded 23.2 g (14.9 g/L) mono-RL from >250 g of consumed glucose ($\sim$ $Y_{P/S}$ = 0.10 $g_{RL}/g_{Glc} \approx$ 21% of Y_{max}) in >70 h using the same strain and medium but a constant temperature of 30°C. Thereby also generating roughly 50% more biomass than RL [Beuker *et al.* 2016a]. In the above shown process following sampling after 30 h, strong foaming with 50% reactor volume loss occurred. It should also be mentioned that the process was simply carried out once. Further repetitions of the process are necessary for confirmation. Nonetheless, this process reveals the potential for the integration of temperature as a control variable in a bioprocess.

9. Conclusion

A part of the Sustainable Development Goals of the United Nations is the use of renewable resources for industrial products like surfactants. This thesis represents a mosaic stone for the latter goal. A bioprocess with a novel process control strategy exploiting RNATs and temperature to produce a biosurfactant is presented. The approach of combining RNATs with temperature variations to produce industrially relevant surfactants like RLs, as presented in this thesis, has so far not been reported previously. The highest titer reported for heterologous RL production so far is 14.9 g/L. However, biomass generation, as a large carbon sink, was a significant drawback in this process with roughly 50% more biomass than product produced. This issue is addressed in this thesis leveraging temperature as control variable and the molecular temperature sensors, ROSE or fourU RNAT. The ROSE RNAT evaluated in the first original research article in the heterologous system *Pseudomonas putida* KT2440 pSynpro8oT_*rhlAB* originates from *P. aeruginosa*. It was found that in the ROSE RNAT-controlled system, the RL production rate was 60% higher at cultivations of 37°C than at 30°C. However, besides the regulatory effect of the RNAT, as revealed by control experiments, multiple unspecific metabolic effects may be equally responsible for the increase in production rate. The experimental data collected in the second original research article confirms the functionality of the fourU RNAT in the heterologous RL production system. The data suggested improved regulatory capabilities of the fourU RNAT compared to the ROSE element and a major effect of temperature on RL production rates and yields. The average RL production rate increased by a factor of 11 between 25°C and 38°C. Control experiments confirmed that a major part of this increase originates from the regulatory effect of the fourU RNAT rather than from an unspecific metabolic effect. With this system $Y_{P/X}$ values well above 1 (about 1.4 g_{RL}/g_{BM}) could be achieved mitigating the initially described drawback of high biomass formation compared to product synthesis. The system was also tested in a proof-of-concept bioreactor process involving a temperature switch. With this simple batch experiment and a temperature switch from 25°C to 38°C not only a partial decoupling of biomass formation from product synthesis was achieved but also an around 25% higher average specific RL production rate (q_{avg}) reached compared to the so far best performing heterologous RL production process reported in literature (q_{avg}: 24 mg/(g h) vs. 32 mg/(g h)). This supports the potential to leverage temperature as control variable in combination with an RNAT e.g., to substitute (often expensive) chemical inducers.

In summary an RNAT-controlled and temperature dependent product formation was established using the example of RL synthesis in *P. putida* KT2440 pSynpro8oT_*rhlAB*. It was found that the type of RNAT used, and the host system are crucial for achieving an optimal separation of growth (30-32°C, *P. putida* KT2440) and product formation (37-38°C, RL). With a bioreactor process, partial decoupling of biomass growth and product formation was achieved. The potential for a more efficient process design was demonstrated, with increased yields and product formation rates. RNATs are functionally interchangeable between species and can be used with simple standard bioreactor peripherals. No additional probes or pumps are required, simply a temperature probe and suitable temperature control. These characteristics predestine the use of an RNAT as molecular control switch in a bioprocess.

To achieve higher titers while reducing side product formation a suitable feeding strategy and more complex temperature profiles may be required. Temperature variations in turn cause several metabolic changes, many of which are complex and interdependent. Models that describe biological processes as a function of temperature are thus essential for improved process understanding. The goal of the peer reviewed review article "Modeling and Exploiting Microbial Temperature Response", shown in this thesis, was to present an overview of various temperature models, aid comprehension of model intent and to facilitate selection and application. Since not all metabolic interdependencies and mechanisms during temperature variation are known for the reasonable connection of input-output relationships, a suitable modeling approach seemed to be neural networks. Neural networks as black box models do not require mechanistic *a priori* knowledge but representative historic datasets. The training of such a neural network was initiated during this thesis. An exponential temperature profile yielded at the highest RL value of approx. 9 g (around 13 g/L) less biomass (around 12 g/L) than product. These values were reached after only 30 h consuming just 45 g of glucose. Hence, at this timepoint 36 weight-% of the consumed glucose could be assigned to mono-RL ($Y_{P/S}$ = 0.19 g_{RL}/g_{Glc}) and biomass ($Y_{X/S}$ = 0.17 g_{BM}/g_{Glc}). The literature value for the theoretically possible maximum yield (Y_{max}) for mono-RL (Rha-C_{10}-C_{10}) from glucose (catabolism via Entner-Doudoroff-pathway), based on ATP-energy balancing, is approximately 0.48 g_{RL}/g_{Glc} however i.a. absence of cell growth and no by-product formation was assumed. Hence 40% of Y_{max} was achieved in the mentioned process, using an exponential temperature profile. The so far best performing heterologous RL production process, yielded 23.2 g (14.9 g/L) mono-RL from >250 g of consumed glucose ($\sim$ $Y_{P/S}$ = 0.10 g_{RL}/g_{Glc} $\approx$ 21% of Y_{max}) in >70 h using the same strain and medium but a constant temperature of 30°C. This again supports the potential of exploiting temperature as a control variable by actively incorporating smart temperature variations in the process thereby increasing yields and time efficiency. Only a few (industrial) processes use temperature in process control or -optimization and none exploits RNATs in combination with temperature variations for industrially relevant surfactants like RLs as reported in this thesis.

10. Outlook

The optimization of an offline temperature profile with a suitable feeding strategy should be continued. This could theoretically also be done in-line/online by using an ANN predictively to control the process. Since there is probably only a narrow optimal glucose control corridor for the reduction of by-product formation and an ideal RL formation, a challenge for bioprocess control will arise. To meet this challenge, the by-product formation in *P. putida* KT2440 would first have to be analyzed. The major carbon sinks would have to be identified and, if necessary, genetic or process design measures taken to reduce the carbon flux into these by-products. This may require a glucose (soft) sensor-feed pump control loop. With the use of the RNAT system exists the opportunity for self-regulating and self-inducible processes. This may depend on the scale: as the scale increases, the metabolic heat to be dissipated becomes greater. However, if this heat is not dissipated by cooling, the temperature rises, which could be used for an autoinduction of the process. Furthermore, the RNAT system could also be applied to other reaction pathways and products such as TCA, amino acids, proteins, etc. For example, a dual RNAT system would be conceivable with an additional cold shock RNAT that, at higher temperatures, can further reduce biomass formation (e.g. by regulating a reaction of the TCA cycle). This could result in an even more efficient incorporation of substrate carbon into the product.

References

Abdel-Mawgoud, A. M., F. Lépine, and E. Déziel (2010). "Rhamnolipids: diversity of structures, microbial origins and roles". In: *Applied microbiology and biotechnology* 86.5, pp. 1323–1336. DOI: 10.1007/s00253-010-2498-2.

Abriata, L. A., D. Albanesi, M. Dal Peraro, and D. De Mendoza (2017). "Signal sensing and transduction by histidine kinases as unveiled through studies on a temperature sensor". In: *Accounts of chemical research* 50.6, pp. 1359–1366. DOI: 10.1021/acs.accounts.6b00593.

Altuvia, S., D. Kornitzer, D. Teff, and A. B. Oppenheim (1989). "Alternative mRNA structures of the *cIII* gene of bacteriophage λ determine the rate of its translation initiation". In: *Journal of molecular biology* 210.2, pp. 265–280. DOI: 10.1016/0022-2836(89)90329-X.

Aparicio, T., V. de Lorenzo, and E. Martinez-Garcia (2019). "Improved Thermotolerance of Genome-Reduced *Pseudomonas putida* EM42 Enables Effective Functioning of the $P_L/cI857$ System". In: *Biotechnology journal* 14.1, p. 1800483. DOI: 10.1002/biot.201800483.

Arcus, V. L., E. J. Prentice, J. K. Hobbs, A. J. Mulholland, M. W. Van der Kamp, C. R. Pudney, E. J. Parker, and L. A. Schipper (2016). "On the temperature dependence of enzyme-catalyzed rates". In: *Biochemistry* 55.12, pp. 1681–1688. DOI: 10.1021/acs.biochem.5b01094.

Arrhenius, S. (1889). "On the reaction rate of the inversion of non-refined sugar upon souring". In: *Zeitschrift für Physikalische Chemie* 4, pp. 226–248. DOI: 10.1515/zpch-1889-0416.

Arsène, F., T. Tomoyasu, and B. Bukau (2000). "The heat shock response of *Escherichia coli*". In: *International journal of food microbiology* 55.1-3, pp. 3–9. DOI: 10.1016/S0168-1605(00)00206-3.

Banat, I. M. (1995). "Biosurfactants production and possible uses in microbial enhanced oil recovery and oil pollution remediation: a review". In: *Bioresource technology* 51.1, pp. 1–12. DOI: 10.1016/0960-8524(94)00101-6.

Banat, I. M., Q. Carboué, G. Saucedo-Castaneda, and J. de Jesús Cázares-Marinero (2020). "Biosurfactants: The green generation of speciality chemicals and potential production using Solid-State fermentation (SSF) technology". In: *Bioresource Technology* 320, p. 124222. DOI: 10.1016/j.biortech.2020.124222.

Becker, J., O. Zelder, S. Häfner, H. Schröder, and C. Wittmann (2011). "From zero to hero—design-based systems metabolic engineering of *Corynebacterium glutamicum* for l-lysine production". In: *Metabolic engineering* 13.2, pp. 159–168. DOI: 10.1016/j.ymben.2011.01.003.

Bennett, A. F. and R. E. Lenski (1993). "Evolutionary adaptation to temperature. II. Thermal niches of experimental lines of *Escherichia coli*". In: *Evolution* 47, pp. 1–12. DOI: 10.1111/j.1558-5646.1993.tb01194.x.

Bergström, S., H. Theorell, and H. Davide (1946). "Pyolipic acid, a metabolic product of *Pseudomonas pyocyanea*, active against *Mycobacterium tuberculosis*". In: *Archives of Biochemistry and Biophysics* 10.1, pp. 1–12.

Beuker, J., T. Barth, A. Steier, A. Wittgens, F. Rosenau, M. Henkel, and R. Hausmann (2016a). "High titer heterologous rhamnolipid production". In: *AMB Express* 6.1, pp. 1–7. DOI: 10.1186/s13568-016-0298-5.

Beuker, J., A. Steier, A. Wittgens, F. Rosenau, M. Henkel, and R. Hausmann (2016b). "Integrated foam fractionation for heterologous rhamnolipid production with recombinant *Pseudomonas putida* in a bioreactor". In: *Amb Express* 6.1, pp. 1–10. DOI: 10.1186/s13568-016-0183-2.

Bona, R. and A. Moser (1997). "Modelling L-glutamic acid production with *Corynebacterium glutamicum* under biotin limitation". In: *Acta biotechnologica* 17.4, pp. 327–337. DOI: 10.1007/PL00008961.

Calero, P., S. I. Jensen, and A. T. Nielsen (2016). "Broad-host-range ProUSER vectors enable fast characterization of inducible promoters and optimization of p-coumaric acid production in *Pseudomonas putida* KT2440". In: *ACS synthetic biology* 5.7, pp. 741–753. DOI: 10.1021/acssynbio.6b00081.

Calero, P., D. C. Volke, P. T. Lowe, C. H. Gotfredsen, D. O'Hagan, and P. I. Nikel (2020). "A fluoride-responsive genetic circuit enables *in vivo* biofluorination in engineered *Pseudomonas putida*". In: *Nature communications* 11.1, pp. 1–11. DOI: 10.1038/s41467-020-18813-x.

Carl Roth GmbH (2021). *IPTG, 100 g*. URL: https://www.carlroth.com/de/de/blau-weiss-selektion/iptg/p/cn08.4 (visited on 08/19/2021).

Carratù, L., S. Franceschelli, C. L. Pardini, G. S. Kobayashi, I. Horvath, L. Vigh, and B. Maresca (1996). "Membrane lipid perturbation modifies the set point of the temperature of heat shock response in yeast". In: *Proceedings of the National Academy of Sciences* 93.9, pp. 3870–3875. DOI: 10.1073/pnas.93.9.3870.

Catalan-Moreno, A., M. Cela, P. Menendez-Gil, N. Irurzun, C. J. Caballero, I. Caldelari, and A. Toledo-Arana (2021). "RNA thermoswitches modulate *Staphylococcus aureus* adaptation to ambient temperatures". In: *Nucleic acids research* 49.6, pp. 3409–3426. DOI: 10.1093/nar/gkab117.

Chavarria, M., P. I. Nikel, D. Perez-Pantoja, and V. de Lorenzo (2013). "The Entner–Doudoroff pathway empowers *Pseudomonas putida* KT2440 with a high tolerance to oxidative stress". In: *Environmental microbiology* 15.6, pp. 1772–1785. DOI: 10.1111/1462-2920.12069.

Chawla, M., R. Credendino, A. Poater, R. Oliva, and L. Cavallo (2015). "Structural stability, acidity, and halide selectivity of the fluoride riboswitch recognition site". In: *Journal of the American Chemical Society* 137.1, pp. 299–306. DOI: 10.1021/ja510549b.

Chong, H. and Q. Li (2017). "Microbial production of rhamnolipids: opportunities, challenges and strategies". In: *Microbial cell factories* 16.1, pp. 1–12. DOI: 10.1186/s12934-017-0753-2.

Chowdhury, S., C. Maris, F. H.-T. Allain, and F. Narberhaus (2006). "Molecular basis for temperature sensing by an RNA thermometer". In: *The EMBO journal* 25.11, pp. 2487–2497. DOI: 10.1038/sj.emboj.7601128.

Cochet, N. and P. Widehem (2000). "Ice crystallization by *Pseudomonas syringae*". In: *Applied microbiology and biotechnology* 54.2, pp. 153–161. DOI: 10.1007/s002530000377.

Corkrey, R., T. A. McMeekin, J. P. Bowman, D. A. Ratkowsky, J. Olley, and T. Ross (2014). "Protein thermodynamics can be predicted directly from biological growth rates". In: *PloS one* 9.5, e96100. DOI: 10.1371/journal.pone.0096100.

Crouzet, J., A. Arguelles-Arias, S. Dhondt-Cordelier, S. Cordelier, J. Pršić, G. Hoff, F. Mazeyrat-Gourbeyre, F. Baillieul, C. Clément, M. Ongena, *et al.* (2020). "Biosurfactants in plant protection against diseases: rhamnolipids and lipopeptides case study". In: *Frontiers in Bioengineering and Biotechnology* 8, pp. 1–11. DOI: 10.3389/fbioe.2020.01014.

Desai, J. D. and I. M. Banat (1997). "Microbial production of surfactants and their commercial potential". In: *Microbiology and Molecular biology reviews* 61.1, pp. 47–64. DOI: 10.1128/mmbr.61.1.47-64.1997.

Deziel, E., F. Lepine, S. Milot, and R. Villemur (2003). "*rhlA* is required for the production of a novel biosurfactant promoting swarming motility in *Pseudomonas aeruginosa*: 3-(3-hydroxyalkanoyloxy) alkanoic acids (HAAs), the precursors of rhamnolipids". In: *Microbiology* 149.8, pp. 2005–2013. DOI: 10.1099/mic.0.26154-0.

Dorman, C. J. (2019). "DNA supercoiling and transcription in bacteria: a two-way street". In: *BMC molecular and cell biology* 20.1, pp. 1–9. DOI: 10.1186/s12860-019-0211-6.

Dubeau, D., E. Déziel, D. E. Woods, and F. Lépine (2009). "*Burkholderia thailandensis* harbors two identical *rhl* gene clusters responsible for the biosynthesis of rhamnolipids". In: *BMC microbiology* 9.1, pp. 1–12. DOI: 10.1186/1471-2180-9-263.

Eichner, H., J. Karlsson, L. Spelmink, A. Pathak, L.-T. Sham, B. Henriques-Normark, and E. Loh (2021). "RNA thermosensors facilitate Streptococcus pneumoniae and Haemophilus influenzae immune evasion". In: *PLoS Pathogens* 17.4, e1009513. DOI: 10.1371/journal.ppat.1009513.

Elsholz, A. K., S. Michalik, D. Zühlke, M. Hecker, and U. Gerth (2010). "CtsR, the Gram-positive master regulator of protein quality control, feels the heat". In: *The EMBO Journal* 29.21, pp. 3621–3629. DOI: 10.1038/emboj.2010.228.

Eslami, P., H. Hajfarajollah, and S. Bazsefidpar (2020). "Recent advancements in the production of rhamnolipid biosurfactants by *Pseudomonas aeruginosa*". In: *RSC Advances* 10.56, pp. 34014–34032. DOI: 10.1039/D0RA04953K.

European Commission (2020). *A new Circular Economy Action Plan - For a cleaner and more competitive Europe - Document 52020DC0098*. URL: https://eur-lex.europa.eu/legal-content/EN/TXT/?qid=1583933814386&uri=COM:2020:98:FIN (visited on 08/04/2021).

European Parliament (2015). *Circular economy: definition, importance and benefits*. URL: https://www.europarl.europa.eu/news/en/headlines/economy/20151201STO05603/circular-economy-definition-importance-and-benefits (visited on 08/04/2021).

Evonik Industries AG (2016). *Evonik commercializes biosurfactants*. URL: https://corporate.evonik.com/media/pressattachments/c483/%20n60276/a28986.pdf (visited on 07/25/2021).

— (2022). *Evonik pioneers industrial-scale manufacturing of biosurfactants*. URL: https://personal-care.evonik.com/en/evonik-pioneers-industrial-scale-manufacturing-of-biosurfactants-168535.html (visited on 02/15/2022).

Fang, L., W. Jiang, W. Bae, and M. Inouye (1997). "Promoter-independent cold-shock induction of cspA and its derepression at 37° C by mRNA stabilization". In: *Molecular microbiology* 23.2, pp. 355–364. DOI: 10.1046/j.1365-2958.1997.2351592.x.

Filloux, A., M. Bally, C. Soscia, M. Murgier, and A. Lazdunski (1988). "Phosphate regulation in *Pseudomonas aeruginosa*: cloning of the alkaline phosphatase gene and identification of *phoB*-and *phoR*-like genes". In: *Molecular and General Genetics MGG* 212.3, pp. 510–513. DOI: 10.1007/BF00330857.

Forterre, P., A. Bergerat, and P. Lopex-Garcia (1996). "The unique DNA topology and DNA topoisomerases of hyperthermophilic archaea". In: *FEMS microbiology reviews* 18.2-3, pp. 237–248. DOI: 10.1016/0168-6445(96)00015-0.

Gaur, V. K., V. Tripathi, P. Gupta, N. Dhiman, R. K. Regar, K. Gautam, J. K. Srivastava, S. Patnaik, D. K. Patel, and N. Manickam (2020). "Rhamnolipids from *Planococcus* spp. and their mechanism of action against pathogenic bacteria". In: *Bioresource technology* 307, p. 123206. DOI: 10.1016/j.biortech.2020.123206.

Giani, C., D. Wullbrandt, R. Rothert, and J. Meiwes (1997). "*Pseudomonas aeruginosa* and its use in a process for the biotechnological preparation of L-rhamnose". US Patent US5501966A.

Giuliodori, A. M., F. Di Pietro, S. Marzi, B. Masquida, R. Wagner, P. Romby, C. O. Gualerzi, and C. L. Pon (2010). "The cspA mRNA is a thermosensor that modulates translation of the cold-shock protein CspA". In: *Molecular cell* 37.1, pp. 21–33. DOI: 10.1016/j.molcel.2009.11.033.

Grosso-Becerra, M. V., G. Croda-Garcia, E. Merino, L. Servin-Gonzalez, R. Mojica-Espinosa, and G. Soberon-Chavez (2014). "Regulation of *Pseudomonas aeruginosa* virulence factors by two novel RNA thermometers". In: *Proceedings of the National Academy of Sciences* 111.43, pp. 15562–15567. DOI: 10.1073/pnas.1402536111.

Hallberg, Z. F., Y. Su, R. Z. Kitto, and M. C. Hammond (2017). "Engineering and *in vivo* applications of riboswitches". In: *Annual review of biochemistry* 86, pp. 515–539. DOI: 10.1146/annurev-biochem-060815-014628.

Hausmann, R., M. Henkel, F. Hecker, and B. Hitzmann (2017). "25 - Present Status of Automation for Industrial Bioprocesses". In: *Current Developments in Biotechnology and Bioengineering*. Ed. by C. Larroche, M. Á. Sanromán, G. Du, and A. Pandey. Elsevier, pp. 725–757. ISBN: 978-0-444-63663-8. DOI: https://doi.org/10.1016/B978-0-444-63663-8.00025-2. URL: https://www.sciencedirect.com/science/article/pii/B9780444636638000252.

Hayes, A., G. Hobbs, C. P. Smith, S. G. Oliver, and P. R. Butler (1997). "Environmental signals triggering methylenomycin production by *Streptomyces coelicolor* A3 (2)". In: *Journal of bacteriology* 179.17, pp. 5511–5515. DOI: 10.1128/jb.179.17.5511-5515.1997.

Helmy, Q., E. Kardena, N. Funamizu, and Wisjnuprapto (2011). "Strategies toward commercial scale of biosurfactant production as potential substitute for it's chemically counterparts". In: *International Journal of Biotechnology* 12.1-2, pp. 66–86. DOI: 10.1504/IJBT.2011.042682.

Henkel, M., M. Müllera, J. Küglera, R. Lovagliob, J. Contierob, C. Syldatka, and R. Hausmann (2012). "Rhamnolipids as biosurfactants from renewable resources: Concepts for next-generation rhamnolipid production". In: *Process Biochemistry* 47.8, pp. 1207–1219. DOI: 10.1016/j.procbio.2012.04.018.

Heyd, M., A. Kohnert, T.-H. Tan, M. Nusser, F. Kirschhöfer, G. Brenner-Weiss, M. Franzreb, and S. Berensmeier (2008). "Development and trends of biosurfactant analysis and purification using rhamnolipids as an example". In: *Analytical and bioanalytical chemistry* 391.5, pp. 1579–1590. DOI: 10.1007/s00216-007-1828-4.

Hoe, N. P. and J. D. Goguen (1993). "Temperature sensing in *Yersinia pestis*: translation of the LcrF activator protein is thermally regulated". In: *Journal of bacteriology* 175.24, pp. 7901–7909. DOI: 10.1128/jb.175.24.7901-7909.1993.

Holmes, J. H. (2014). "Chapter 7 - Knowledge Discovery in Biomedical Data: Theory and Methods". In: *Methods in Biomedical Informatics*. Ed. by I. N. Sarkar. Oxford: Academic Press, pp. 179–240. ISBN: 978-0-12-401678-1. DOI: https://doi.org/10.1016/B978-0-12-401678-1.00007-5. URL: https://www.sciencedirect.com/science/article/pii/B9780124016781000075.

Horváth, I., G. Multhoff, A. Sonnleitner, and L. Vígh (2008). "Membrane-associated stress proteins: more than simply chaperones". In: *Biochimica et Biophysica Acta (BBA)-Biomembranes* 1778.7-8, pp. 1653–1664. DOI: 10.1016/j.bbamem.2008.02.012.

El-Housseiny, G. S., K. M. Aboshanab, M. M. Aboulwafa, and N. A. Hassouna (2019). "Rhamnolipid production by a gamma ray-induced *Pseudomonas aeruginosa* mutant under solid state fermentation". In: *AMB Express* 9.1, pp. 1–11. DOI: 10.1186/s13568-018-0732-y.

Jarvis, F. and M. Johnson (1949). "A glyco-lipide produced by *Pseudomonas aeruginosa*". In: *Journal of the American Chemical Society* 71.12, pp. 4124–4126. DOI: 10.1021/JA01180A073.

Jenzsch, M., S. Gnoth, M. Kleinschmidt, R. Simutis, and A. Lübbert (2006). "Improving the batch-to-batch reproducibility in microbial cultures during recombinant protein production by guiding the process along a predefined total biomass profile". In: *Bioprocess and biosystems engineering* 29.5, pp. 315–321. DOI: 10.1007/s00449-006-0080-1.

Jin, L., W. Black, and T. Sawyer (2021). "Application of environment-friendly rhamnolipids against transmission of enveloped viruses like SARS-CoV2". In: *Viruses* 13.2, p. 322. DOI: 10.3390/v13020322.

Jin, S., Y. Song, W. Deng, M. P. Gordon, and E. Nester (1993). "The regulatory VirA protein of *Agrobacterium tumefaciens* does not function at elevated temperatures". In: *Journal of Bacteriology* 175.21, pp. 6830–6835. DOI: 10.1128/jb.175.21.6830-6835.1993.

Johansson, J., P. Mandin, A. Renzoni, C. Chiaruttini, M. Springer, and P. Cossart (2002). "An RNA thermosensor controls expression of virulence genes in *Listeria monocytogenes*". In: *Cell* 110.5, pp. 551–561. DOI: 10.1016/S0092-8674(02)00905-4.

Kachlany, S. C., S. B. Levery, J. S. Kim, B. L. Reuhs, L. W. Lion, and W. C. Ghiorse (2001). "Structure and carbohydrate analysis of the exopolysaccharide capsule of *Pseudomonas putida* G7". In: *Environmental Microbiology* 3.12, pp. 774–784. DOI: 10.1046/j.1462-2920.2001.00248.x.

Kamp, H. D. and D. E. Higgins (2011). "A protein thermometer controls temperature-dependent transcription of flagellar motility genes in *Listeria monocytogenes*". In: *PLoS pathogens* 7.8, e1002153. DOI: 10.1371/journal.ppat.1002153.

Karlsson, J., H. Eichner, C. Andersson, S. Jacobsson, and E. Loh (2020). "Novel hypercapsulation RNA thermosensor variants in *Neisseria meningitidis* and their association with invasive meningococcal disease: a genetic and phenotypic investigation and molecular epidemiological study". In: *The Lancet Microbe* 1.8, e319–e327. DOI: 10.1016/S2666-5247(20)30146-4.

Katayama, S., O. Matsushita, C.-M. Jung, J. Minami, and A. Okabe (1999). "Promoter upstream bent DNA activates the transcription of the *Clostridium perfringens* phospholipase C gene in a low temperature-dependent manner". In: *The EMBO journal* 18.12, pp. 3442–3450. DOI: 10.1093/emboj/18.12.3442.

Kaza, S., L. Yao, B.-T. Perinaz, and V. W. Frank (2018). "What a Waste 2.0: A Global Snapshot of Solid Waste Management to 2050". In: *World Bank eLibrary* 2. DOI: 10.1596/978-1-4648-1329-0.

KDBIO S.A.S. (2021). *Bioreactor Probe Sensor for Glucose and/or Lactate*. URL: https://www.kdbio.com/products/glucose-lactate-bioreactor-probe-biosensor/ (visited on 08/19/2021).

El-Khordagui, L., S. E. Badawey, and L. A. Heikal (2021). "Chapter 3 - Application of biosurfactants in the production of personal care products, and household detergents and industrial and institutional cleaners". In: *Green Sustainable Process for Chemical and Environmental Engineering and Science*. Ed. by Inamuddin, C. O. Adetunji, and A. M. Asiri. Elsevier, pp. 49–96. ISBN: 978-0-12-823380-1. DOI: https://doi.org/10.1016/B978-0-12-823380-1.00005-8. URL: https://www.sciencedirect.com/science/article/pii/B9780128233801000058.

Klement, T. and J. Büchs (2013). "Itaconic acid–a biotechnological process in change". In: *Bioresource technology* 135, pp. 422–431. DOI: 10.1016/j.biortech.2012.11.141.

Klinkert, B., A. Cimdins, L. C. Gaubig, J. Roßmanith, U. Aschke-Sonnenborn, and F. Narberhaus (2012). "Thermogenetic tools to monitor temperature-dependent gene expression in bacteria". In: *Journal of biotechnology* 160.1-2, pp. 55–63. DOI: 10.1016/j.jbiotec.2012.01.007.

Klinkert, B. and F. Narberhaus (2009). "Microbial thermosensors". In: *Cellular and molecular life sciences* 66.16, pp. 2661–2676. DOI: 10.1007/s00018-009-0041-3.

Kopsahelis, A., C. Kourmentza, C. Zafiri, and M. Kornaros (2018). "Gate-to-gate life cycle assessment of biosurfactants and bioplasticizers production via biotechnological exploitation of fats

and waste oils". In: *Journal of Chemical Technology & Biotechnology* 93.10, pp. 2833–2841. DOI: 10.1002/jctb.5633.

Kortmann, J. and F. Narberhaus (2012). "Bacterial RNA thermometers: molecular zippers and switches". In: *Nature reviews microbiology* 10.4, pp. 255–265. DOI: 10.1038/nrmicro2730.

Kotlajich, M. V., D. R. Hron, B. A. Boudreau, Z. Sun, Y. L. Lyubchenko, and R. Landick (2015). "Bridged filaments of histone-like nucleoid structuring protein pause RNA polymerase and aid termination in bacteria". In: *Elife* 4, e04970. DOI: 10.7554/eLife.04970.

Kouse, A. B., F. Righetti, J. Kortmann, F. Narberhaus, and E. R. Murphy (2021). "Correction draft: RNA-Mediated Thermoregulation of Iron-Acquisition Genes in *Shigella dysenteriae* and Pathogenic *Escherichia coli*". In: *PloS one* 16.6, e0252744. DOI: 10.1371/journal.pone.0252744.

Krajewski, S. S., M. Joswig, M. Nagel, and F. Narberhaus (2014). "A tricistronic heat shock operon is important for stress tolerance of *Pseudomonas putida* and conserved in many environmental bacteria". In: *Environmental microbiology* 16.6, pp. 1835–1853. DOI: 10.1111/1462-2920.12432.

Krell, T., J. Lacal, A. Busch, H. Silva-Jiménez, M.-E. Guazzaroni, and J. L. Ramos (2010). "Bacterial sensor kinases: diversity in the recognition of environmental signals". In: *Annual review of microbiology* 64, pp. 539–559. DOI: 10.1146/annurev.micro.112408.134054.

Krieger, N., D. C. Neto, and D. A. Mitchell (2010). "Production of Microbial Biosurfactants by Solid-State Cultivation". In: *Biosurfactants*. Ed. by R. Sen. New York, NY: Springer New York, pp. 203–210. ISBN: 978-1-4419-5979-9. DOI: 10.1007/978-1-4419-5979-9_15. URL: https://doi.org/10.1007/978-1-4419-5979-9_15.

Krojer, T., J. Sawa, E. Schäfer, H. R. Saibil, M. Ehrmann, and T. Clausen (2008). "Structural basis for the regulated protease and chaperone function of DegP". In: *Nature* 453.7197, pp. 885–890. DOI: 10.1038/nature07004.

Kubicek, C. P. and L. Karaffa (2010). "Citric Acid Processes". In: *Encyclopedia of Industrial Biotechnology*. Ed. by M. C. Flickinger. John Wiley & Sons, Ltd, pp. 1–7. ISBN: 9780470054581. DOI: https://doi.org/10.1002/9780470054581.eib229. URL: https://onlinelibrary.wiley.com/doi/abs/10.1002/9780470054581.eib229.

Lal, A., A. Dhar, A. Trostel, F. Kouzine, A. S. Seshasayee, and S. Adhya (2016). "Genome scale patterns of supercoiling in a bacterial chromosome". In: *Nature communications* 7.1, pp. 1–8. DOI: 10.1038/ncomms11055.

Lang, S. and D. Wullbrandt (1999). "Rhamnose lipids - biosynthesis, microbial production and application potential". In: *Applied microbiology and biotechnology* 51.1, pp. 22–32. DOI: 10.1007/s002530051358.

Lanham, P., K. Mcllravey, and M. Perombelon (1991). "Production of cell wall dissolving enzymes by *Erwinia carotovora* subsp. *atroseptica in vitro* at 27°C and 30,5°C". In: *Journal of applied bacteriology* 70.1, pp. 20–24. DOI: 10.1111/j.1365-2672.1991.tb03781.x.

Li, X., G.-G. Ying, J.-L. Zhao, Z.-F. Chen, H.-J. Lai, and H.-C. Su (2013). "4-Nonylphenol, bisphenol-A and triclosan levels in human urine of children and students in China, and the effects of drinking these bottled materials on the levels". In: *Environment international* 52, pp. 81–86. DOI: 10.1016/j.envint.2011.03.026.

Liang, T., J. Sun, S. Ju, S. Su, L. Yang, and J. Wu (2021). "Construction of T7-Like Expression System in *Pseudomonas putida* KT2440 to Enhance the Heterologous Expression Level". In: *Frontiers in chemistry* 9, p. 556. DOI: 10.3389/fchem.2021.664967.

Lim, C. J., S. Y. Lee, L. J. Kenney, and J. Yan (2012). "Nucleoprotein filament formation is the structural basis for bacterial protein H-NS gene silencing". In: *Scientific reports* 2.1, pp. 1–6. DOI: 10.1038/srep00509.

López-García, P. and P. Forterre (2000). "DNA topology and the thermal stress response, a tale from mesophiles and hyperthermophiles". In: *Bioessays* 22.8, pp. 738–746. DOI: 10.1002/1521-1878(200008)22:8<738::AID-BIES7>3.0.CO;2-5.

— (1997). "DNA topology in hyperthermophilic archaea: reference states and their variation with growth phase, growth temperature, and temperature stresses". In: *Molecular microbiology* 23.6, pp. 1267–1279. DOI: 10.1046/j.1365-2958.1997.3051668.x.

Los, D. (2004). "The effect of low-temperature-induced DNA supercoiling on the expression of the desaturase genes in synechocystis". In: *Cellular and molecular biology* 50 5, pp. 605–12. DOI: 10.1170/T550.

Makkar, R. and S. Cameotra (2002). "An update on the use of unconventional substrates for biosurfactant production and their new applications". In: *Applied microbiology and biotechnology* 58.4, pp. 428–434. DOI: 10.1007/s00253-001-0924-1.

Matsunaga, J., P. J. Schlax, and D. A. Haake (2013). "Role for cis-acting RNA sequences in the temperature-dependent expression of the multiadhesive lig proteins in Leptospira interrogans". In: *Journal of bacteriology* 195.22, pp. 5092–5101. DOI: 10.1128/JB.00663-13.

Matsuno, Y., A. Sugai, H. Higashibata, W. Fukuda, K. Ueda, I. Uda, I. Sato, T. Itoh, T. Imanaka, and S. Fujiwara (2009). "Effect of Growth Temperature and Growth Phase on the Lipid Composition of the Archaeal Membrane from *Thermococcus kodakaraensis*". In: *Bioscience, Biotechnology, and Biochemistry* 73.1, pp. 104–108. DOI: 10.1271/bbb.80520.

Meijaard, E., T. M. Brooks, K. M. Carlson, E. M. Slade, J. Garcia-Ulloa, D. L. Gaveau, J. S. H. Lee, T. Santika, D. Juffe-Bignoli, M. J. Struebig, *et al.* (2020). "The environmental impacts of palm oil in context". In: *Nature plants* 6.12, pp. 1418–1426. DOI: 10.1038/s41477-020-00813-w.

Mizushima, T., K. Kataoka, Y. Ogata, R.-i. Inoue, and K. Sekimizu (1997). "Increase in negative supercoiling of plasmid DNA in *Escherichia coli* exposed to cold shock". In: *Molecular microbiology* 23.2, pp. 381–386. DOI: 10.1046/j.1365-2958.1997.2181582.x.

Mnif, I. and D. Ghribi (2016). "Glycolipid biosurfactants: main properties and potential applications in agriculture and food industry". In: *Journal of the Science of Food and Agriculture* 96.13, pp. 4310–4320. DOI: 10.1002/jsfa.7759.

Möbus, M. (Oct. 2020). "Designing a neural network for temperature-dependent rhamnolipid production". MA thesis. University of Hohenheim.

Müller, M. M., B. Hörmann, C. Syldatk, and R. Hausmann (2010). "*Pseudomonas aeruginosa* PAO1 as a model for rhamnolipid production in bioreactor systems". In: *Applied microbiology and biotechnology* 87.1, pp. 167–174. DOI: 10.1007/s00253-010-2513-7.

Mulligan, C. N. and B. F. Gibbs (1990). "Recovery of biosurfactants by ultrafiltration". In: *Journal of Chemical Technology & Biotechnology* 47.1, pp. 23–29. DOI: 10.1002/jctb.280470104.

Mykytczuk, N. C. S., J. T. Trevors, S. M. Twine, G. D. Ferroni, and L. G. Leduc (2010). "Membrane fluidity and fatty acid comparisons in psychrotrophic and mesophilic strains of *Acidithiobacillus ferrooxidans* under cold growth temperatures". In: *Archives of Microbiology* 192.12, pp. 1005–1018. DOI: 10.1007/s00203-010-0629-x.

Narberhaus, F., T. Waldminghaus, and S. Chowdhury (2006). "RNA thermometers". In: *FEMS microbiology reviews* 30.1, pp. 3–16. DOI: 10.1111/j.1574-6976.2005.004.x.

Nene, S. N., K. S. Joshi, *et al.* (2020). "A comparative study of production of hydrophobin like proteins (HYD-LPs) in submerged liquid and solid state fermentation from white rot fungus *Pleurotus ostreatus*". In: *Biocatalysis and Agricultural Biotechnology* 23, p. 101440. DOI: 10.1016/j.bcab.2019.101440.

Neupert, J. and R. Bock (2009). "Designing and using synthetic RNA thermometers for temperature-controlled gene expression in bacteria". In: *Nature protocols* 4.9, pp. 1262–1273. DOI: 10.1038/nprot.2009.112.

Neupert, J., D. Karcher, and R. Bock (2008). "Design of simple synthetic RNA thermometers for temperature-controlled gene expression in *Escherichia coli*". In: *Nucleic acids research* 36.19, e124–e124. DOI: 10.1093/nar/gkn545.

Niederberger, T. D., N. N. Perreault, S. Tille, B. S. Lollar, G. Lacrampe-Couloume, D. Andersen, C. W. Greer, W. Pollard, and L. G. Whyte (2010). "Microbial characterization of a subzero, hypersaline methane seep in the Canadian High Arctic". In: *The ISME journal* 4.10, pp. 1326–1339. DOI: 10.1038/ismej.2010.57.

Nilsson, M., W.-C. Chiang, M. Fazli, M. Gjermansen, M. Givskov, and T. Tolker-Nielsen (2011). "Influence of putative exopolysaccharide genes on *Pseudomonas putida* KT2440 biofilm stability". In: *Environmental microbiology* 13.5, pp. 1357–1369. DOI: 10.1111/j.1462-2920.2011.02447.x.

Nishiyama, S.-i., T. Umemura, T. Nara, M. Homma, and I. Kawagishi (1999). "Conversion of a bacterial warm sensor to a cold sensor by methylation of a single residue in the presence of an attractant". In: *Molecular microbiology* 32.2, pp. 357–365. DOI: 10.1046/j.1365-2958.1999.01355.x.

Nitschke, M. and S. Costa (2007). "Biosurfactants in food industry". In: *Trends in Food Science & Technology* 18.5, pp. 252–259. DOI: 10.1016/j.tifs.2007.01.002.

Nocker, A., T. Hausherr, S. Balsiger, N.-P. Krstulovic, H. Hennecke, and F. Narberhaus (2001a). "A mRNA-based thermosensor controls expression of rhizobial heat shock genes". In: *Nucleic acids research* 29.23, pp. 4800–4807. DOI: 10.1093/nar/29.23.4800.

Nocker, A., N.-P. Krstulovic, X. Perret, and F. Narberhaus (2001b). "ROSE elements occur in disparate *rhizobia* and are functionally interchangeable between species". In: *Archives of microbiology* 176.1, pp. 44–51. DOI: 10.1007/s002030100294.

Noll, P. and M. Henkel (2020a). "History and evolution of modeling in biotechnology: modeling & simulation, application and hardware performance". In: *Computational and Structural Biotechnology Journal* 18, pp. 3309–3323. DOI: 10.1016/j.csbj.2020.10.018.

Noll, P., L. Lilge, R. Hausmann, and M. Henkel (2020b). "Modeling and exploiting microbial temperature response". In: *Processes* 8.1, p. 121. DOI: 10.3390/pr8010121.

Noll, P., C. Treinen, S. Müller, L. Lilge, R. Hausmann, and M. Henkel (2021). "Exploiting RNA thermometer-driven molecular bioprocess control as a concept for heterologous rhamnolipid production". In: *Scientific Reports* 11, pp. 1–12. DOI: 10.1038/s41598-021-94400-4.

Noll, P., C. Treinen, S. Müller, S. Senkalla, L. Lilge, R. Hausmann, and M. Henkel (2019). "Evaluating temperature-induced regulation of a ROSE-like RNA-thermometer for heterologous rhamnolipid production in *Pseudomonas putida* KT2440". In: *AMB Express* 9.1, pp. 1–10. DOI: 10.1186/s13568-019-0883-5.

Ochsner, U. A., J. Reiser, A. Fiechter, and B. Witholt (1995). "Production of *Pseudomonas aeruginosa* rhamnolipid biosurfactants in heterologous hosts". In: *Applied and environmental microbiology* 61.9, pp. 3503–3506. DOI: 10.1128/aem.61.9.3503-3506.1995.

OECD (2019). *Global Material Resources Outlook to 2060*. URL: https://www.oecd.org/environment/global-material-resources-outlook-to-2060-9789264307452-en.htm (visited on 08/04/2021).

Ogata, Y., R.-i. Inoue, T. Mizushima, Y. Kano, T. Miki, and K. Sekimizu (1997). "Heat shock-induced excessive relaxation of DNA in *Escherichia coli* mutants lacking the histone-like protein HU". In: *Biochimica et Biophysica Acta (BBA)-Gene Structure and Expression* 1353.3, pp. 298–306. DOI: 10.1016/S0167-4781(97)00105-X.

Ogata, Y., T. Mizushima, K. Kataoka, K. Kita, T. Miki, and K. Sekimizu (1996). "DnaK heat shock protein of *Escherichia coli* maintains the negative supercoiling of DNA against thermal stress". In: *Journal of Biological Chemistry* 271.46, pp. 29407–29414. DOI: 10.1074/jbc.271.46.29407.

Ono, S., M. D. Goldberg, T. Olsson, D. Esposito, J. C. Hinton, and J. E. Ladbury (2005). "H-NS is a part of a thermally controlled mechanism for bacterial gene regulation". In: *Biochemical Journal* 391.2, pp. 203–213. DOI: 10.1042/BJ20050453.

Ottemann, K. M., W. Xiao, Y.-K. Shin, and D. E. Koshland (1999). "A piston model for transmembrane signaling of the aspartate receptor". In: *Science* 285.5434, pp. 1751–1754. DOI: 10.1126/science.285.5434.1751.

Pajarron, A. M., C. De Koster, W. Heerma, M. Schmidt, and J. Haverkamp (1993). "Structure identification of natural rhamnolipid mixtures by fast atom bombardment tandem mass spectrometry". In: *Glycoconjugate journal* 10.3, pp. 219–226. DOI: 10.1007/BF00702203.

Pasotti, L., S. Zucca, M. Casanova, G. Micoli, M. G. C. De Angelis, P. Magni, *et al.* (2014). "Half-life measurements of chemical inducers for recombinant gene expression". In: *Journal of biological engineering* 8.1, pp. 1–10. DOI: 10.1186/1754-1611-8-5.

Paulucci, N. S., D. B. Medeot, M. S. Dardanelli, and M. G. de Lema (2011). "Growth Temperature and Salinity Impact Fatty Acid Composition and Degree of Unsaturation in Peanut-Nodulating *Rhizobia*". In: *Lipids* 46.5, pp. 435–441. DOI: 10.1007/s11745-011-3545-1.

Prosseda, G., A. Mazzola, M. L. Di Martino, D. Tielker, G. Micheli, and B. Colonna (2010). "A temperature-induced narrow DNA curvature range sustains the maximum activity of a bacterial promoter *in vitro*". In: *Biochemistry* 49.13, pp. 2778–2785. DOI: 10.1021/bi902003g.

Quinn, J. D., E. H. Weening, T. A. Miner, and V. L. Miller (2019). "Temperature control of *psaA* expression by PsaE and PsaF in *Yersinia pestis*". In: *Journal of bacteriology* 201.16, e00217–19. DOI: 10.1128/JB.00217-19.

Rai, N. and A. Ramaswamy (2015). "Temperature dependent dynamics of DegP-trimer: A molecular dynamics study". In: *Computational and structural biotechnology journal* 13, pp. 329–338. DOI: 10.1016/j.csbj.2015.04.004.

Restaino, O. F., U. Bhaskar, P. Paul, L. Li, M. De Rosa, J. S. Dordick, and R. J. Linhardt (2013). "High cell density cultivation of a recombinant *E. coli* strain expressing a key enzyme in bioengineered heparin production". In: *Applied microbiology and biotechnology* 97.9, pp. 3893–3900. DOI: 10.1007/s00253-012-4682-z.

Rinnenthal, J., B. Klinkert, F. Narberhaus, and H. Schwalbe (2011). "Modulation of the stability of the *Salmonella* fourU-type RNA thermometer". In: *Nucleic acids research* 39.18, pp. 8258–8270. DOI: 10.1093/nar/gkr314.

Sáenz-Marta, C. I., M. de Lourdes Ballinas-Casarrubias, B. E. Rivera-Chavira, and G. V. Nevárez-Moorillón (2015). "Biosurfactants as useful tools in bioremediation". In: *Advances in Bioremediation of Wastewater an Polluted Soil*. Ed. by N. Shiomi. IntechOpen: London, UK, pp. 93–109. ISBN: 978-953-51-2165-7. DOI: 10.5772/60751. URL: https://www.intechopen.com/chapters/48566.

Saragliadis, A., S. S. Krajewski, C. Rehm, F. Narberhaus, and J. S. Hartig (2013). "Thermozymes: Synthetic RNA thermometers based on ribozyme activity". In: *RNA biology* 10.6, pp. 1009–1016. DOI: 10.4161/rna.24482.

Sathesh-Prabu, C., R. Tiwari, D. Kim, and S. K. Lee (2021). "Inducible and tunable gene expression systems for *Pseudomonas putida* KT2440". In: *Scientific reports* 11.1, pp. 1–8. DOI: 10.1038/s41598-021-97550-7.

Schafer, S., M. Wessel, A. Thiessenhusen, and S. N (2011). "Cells and method for producing rhamnolipids". EU Patent EP2598646B1.

Schenk, T., I. Schuphan, and B. Schmidt (1995). "High-performance liquid chromatographic determination of the rhamnolipids produced by *Pseudomonas aeruginosa*". In: *Journal of Chromatography A* 693.1, pp. 7–13. DOI: 10.1016/0021-9673(94)01127-z.

Schilling, M., M. Rueterming, V. Dahl, and F. Cabirol (2013). "Process for the isolation of rhamnolipids". EU Patent EP2735605B1.

Schmidt, M., K. Babu, N. Khanna, S. Marten, and U. Rinas (1999). "Temperature-induced production of recombinant human insulin in high-cell density cultures of recombinant *Escherichia coli*". In: *Journal of biotechnology* 68.1, pp. 71–83. DOI: 10.1016/S0168-1656(98)00189-8.

Schröder, O. and R. Wagner (2000). "The bacterial DNA-binding protein H-NS represses ribosomal RNA transcription by trapping RNA polymerase in the initiation complex". In: *Journal of molecular biology* 298.5, pp. 737–748. DOI: 10.1006/jmbi.2000.3708.

Schuster, L. A. and C. R. Reisch (2021). "A plasmid toolbox for controlled gene expression across the Proteobacteria". In: *Nucleic Acids Research* 49.12, pp. 7189–7202. DOI: 10.1093/nar/gkab496.

Seel, W., J. Derichs, and A. Lipski (2016). "Increased biomass production by mesophilic food-associated bacteria through lowering the growth temperature from 30°C to 10°C". In: *Applied and environmental microbiology* 82.13, pp. 3754–3764. DOI: 10.1128/AEM.00211-16.

Sen, S., D. Apurva, R. Satija, D. Siegal, and R. M. Murray (2017). "Design of a Toolbox of RNA Thermometers". In: *ACS synthetic biology* 6.8, pp. 1461–1470. DOI: 10.1021/acssynbio.6b00301.

Sengupta, P. and P. Garrity (2013). "Sensing temperature". In: *Current Biology* 23.8, R304–R307. DOI: 10.1016/j.cub.2013.03.009.

Servant, P., C. Grandvalet, and P. Mazodier (2000). "The RheA repressor is the thermosensor of the HSP18 heat shock response in *Streptomyces albus*". In: *Proceedings of the National Academy of Sciences* 97.7, pp. 3538–3543. DOI: 10.1073/pnas.97.7.3538.

Shapiro, R. S. and L. E. Cowen (2012). "Thermal control of microbial development and virulence: molecular mechanisms of microbial temperature sensing". In: *MBio* 3.5, e00238–12. DOI: 10.1128/mBio.00238-12.

Shin, M., M. Song, J. H. Rhee, Y. Hong, Y.-J. Kim, Y.-J. Seok, K.-S. Ha, S.-H. Jung, and H. E. Choy (2005). "DNA looping-mediated repression by histone-like protein H-NS: specific requirement of Eσ70 as a cofactor for looping". In: *Genes & development* 19.19, pp. 2388–2398. DOI: 10.1101/gad.1316305.

Shioya, S. (1992). "Optimization and control in fed-batch bioreactors". In: *Modern Biochemical Engineering*. Ed. by A. Fiechter. Springer Berlin Heidelberg, pp. 111–142. ISBN: 978-3-540-47005-2. DOI: 10.1007/BFb0000708. URL: https://doi.org/10.1007/BFb0000708.

Simons, R. (2001). "Antisense RNA". In: *Encyclopedia of Genetics*. Ed. by S. Brenner and J. H. Miller. New York: Academic Press, pp. 83–84. ISBN: 978-0-12-227080-2. DOI: https://doi.org/10.1006/rwgn.2001.0061. URL: https://www.sciencedirect.com/science/article/pii/B0122270800000616.

Sinden, R. R. (1994). "Chapter 3 - DNA Supercoiling". In: *DNA Structure and Function*. Ed. by R. R. Sinden. San Diego: Academic Press, pp. 95–133. ISBN: 978-0-08-057173-7. DOI: 10.1016/B978-0-08-057173-7.50008-0. URL: https://www.sciencedirect.com/science/article/pii/B9780080571737500080.

Sinensky, M. (1974). "Homeoviscous adaptation—a homeostatic process that regulates the viscosity of membrane lipids in *Escherichia coli*". In: *Proceedings of the National Academy of Sciences* 71.2, pp. 522–525. DOI: 10.1073/pnas.71.2.522.

Smirnova, A., H. Li, H. Weingart, S. Aufhammer, A. Burse, K. Finis, A. Schenk, and M. S. Ullrich (2001). "Thermoregulated expression of virulence factors in plant-associated bacteria". In: *Archives of microbiology* 176.6, pp. 393–399. DOI: 10.1007/s002030100344.

Sørensen, H. P. and K. K. Mortensen (2005). "Advanced genetic strategies for recombinant protein expression in *Escherichia coli*". In: *Journal of biotechnology* 115.2, pp. 113–128. DOI: 10.1016/S0167-7799(97)01155-4.

Storz, G. (1999). "An RNA thermometer". In: *Genes & development* 13.6, pp. 633–636. DOI: 10.1101/gad.13.6.633.

Stover, C. K., X. Q. Pham, A. L. Erwin, S. D. Mizoguchi, P. Warrener, M. J. Hickey, F. S. L. Brinkman, W. O. Hufnagle, D. J. Kowalik, M. Lagrou, R. L. Garber, L. Goltry, E. Tolentino, S. Westbrock-Wadman, Y. Yuan, L. L. Brody, S. N. Coulter, K. R. Folger, A. Kas, K. Larbig, R. Lim, K. Smith, D. Spencer, G. K. S. Wong, Z. Wu, I. T. Paulsen, J. Reizer, M. H. Saier, R. E. W. Hancock, S. Lory, and M. V. Olson (2000). "Complete genome sequence of *Pseudomonas aeruginosa* PAO1, an opportunistic pathogen". In: *Nature* 406.6799, pp. 959–964. ISSN: 1476-4687. DOI: 10.1038/35023079.

Striedner, G., M. Cserjan-Puschmann, F. Pötschacher, and K. Bayer (2003). "Tuning the Transcription Rate of Recombinant Protein in Strong *Escherichia coli* Expression Systems through Repressor Titration". In: *Biotechnology progress* 19.5, pp. 1427–1432. DOI: 10.1021/bp034050u.

Takai, K., K. Nakamura, T. Toki, U. Tsunogai, M. Miyazaki, J. Miyazaki, H. Hirayama, S. Nakagawa, T. Nunoura, and K. Horikoshi (2008). "Cell proliferation at 122°C and isotopically heavy CH_4 production by a hyperthermophilic methanogen under high-pressure cultivation". In: *Proceedings of the National Academy of Sciences* 105.31, pp. 10949–10954. DOI: 10.1073/pnas.0712334105.

Thavasi, R. and I. M. Banat (2018). "2 - Downstream processing of microbial biosurfactants". In: *Microbial biosurfactants and their environmental and industrial applications*. Ed. by I. M. Banat and R. Thavasi. CRC Press Boca Raton, pp. 16–27. ISBN: 9781315271767. DOI: 10.1201/b21950-2. URL: https://www.taylorfrancis.com/chapters/edit/10.1201/b21950-2/downstream-processing-microbial-biosurfactants-rengathavasi-thavasi-ibrahim-banat.

Thibault, J., V. Van Breusegem, and A. Chéruy (1990). "On-line prediction of fermentation variables using neural networks". In: *Biotechnology and Bioengineering* 36.10, pp. 1041–1048. DOI: 10.1002/bit.260361009.

Thum, O., P. Engel, C. Gehring, S. Schaffer, and M. Wessel (2017). "Methods of producing rhamnolipids". EU Patent EP3148335.

Tiso, T., N. Ihling, S. Kubicki, A. Biselli, A. Schonhoff, I. Bator, S. Thies, T. Karmainski, S. Kruth, A.-L. Willenbrink, *et al.* (2020). "Integration of genetic and process engineering for optimized rhamnolipid production using *Pseudomonas putida*". In: *Frontiers in bioengineering and biotechnology* 8, p. 976. DOI: 10.3389/fbioe.2020.00976.

Twittenhoff, C., A. K. Heroven, S. Mühlen, P. Dersch, and F. Narberhaus (2020). "An RNA thermometer dictates production of a secreted bacterial toxin". In: *PLoS pathogens* 16.1, e1008184. DOI: 10.1371/journal.ppat.1008184.

Uniprot Database – O34757 (1998). *UniProtKB - O34757 - Sensor histidine kinase DesK*. URL: https://www.uniprot.org/uniprot/O34757 (visited on 08/30/2021).

Uniprot Databse – P0A6Y8 (2007). *UniProtKB - P0A6Y8 - Chaperone protein DnaK*. URL: https://www.uniprot.org/uniprot/P0A6Y8 (visited on 08/30/2021).

United Nations (2015a). *Goal 12: Ensure sustainable consumption and production patterns*. URL: https://www.un.org/sustainabledevelopment/sustainable-consumption-production/ (visited on 08/04/2021).

— (2015b). *THE 17 GOALS*. URL: https://sdgs.un.org/goals (visited on 08/04/2021).

— (2017). *The future of food and agriculture - Trends and challenges*. Rome, Italy: United Nations Food and Agriculture Organization, pp. x–xi. ISBN: 9789251095515.

— (2019). *World Population Prospects 2019:Highlights (ST/ESA/SER.A/423)*. New York, USA: United Nations Department of Economic and Social Affairs, Population Division, p. 1. ISBN: 9789211483161.

Van Bogaert, I. N., K. Saerens, C. De Muynck, D. Develter, W. Soetaert, and E. J. Vandamme (2007). "Microbial production and application of sophorolipids". In: *Applied microbiology and biotechnology* 76.1, pp. 23–34. DOI: 10.1007/s00253-007-0988-7.

Vecino, X., J. Cruz, A. Moldes, and L. Rodrigues (2017). "Biosurfactants in cosmetic formulations: trends and challenges". In: *Critical reviews in biotechnology* 37.7, pp. 911–923. DOI: 10.1080/07388551.2016.1269053.

Vigh, L., B. Maresca, and J. L. Harwood (1998). "Does the membrane's physical state control the expression of heat shock and other genes?" In: *Trends in biochemical sciences* 23.10, pp. 369–374. DOI: 10.1016/S0968-0004(98)01279-1.

Waldminghaus, T., A. Fippinger, J. Alfsmann, and F. Narberhaus (2005). "RNA thermometers are common in α-and γ-proteobacteria". In: *Biological Chemistry* 386.12, pp. 1279–1286. DOI: 10.1515/BC.2005.145.

Waldminghaus, T., L. C. Gaubig, and F. Narberhaus (2007a). "Genome-wide bioinformatic prediction and experimental evaluation of potential RNA thermometers". In: *Molecular Genetics and Genomics* 278.5, pp. 555–564. DOI: 10.1007/s00438-007-0272-7.

Waldminghaus, T., N. Heidrich, S. Brantl, and F. Narberhaus (2007b). "FourU: a novel type of RNA thermometer in *Salmonella*". In: *Molecular microbiology* 65.2, pp. 413–424. DOI: 10.1111/j.1365-2958.2007.05794.x.

Wang, J. C. (1987). "Recent studies of DNA topoisomerases". In: *Biochimica et Biophysica Acta (BBA)-Gene Structure and Expression* 909.1, pp. 1–9. DOI: 10.1016/0167-4781(87)90040-6.

Weber, G. G., J. Kortmann, F. Narberhaus, and K. E. Klose (2014). "RNA thermometer controls temperature-dependent virulence factor expression in *Vibrio cholerae*". In: *Proceedings of the National Academy of Sciences* 111.39, pp. 14241–14246. DOI: 10.1073/pnas.1411570111.

Weber, M. H. and M. A. Marahiel (2003). "Bacterial cold shock responses". In: *Science progress* 86.1-2, pp. 9–75. DOI: 10.3184/003685003783238707.

Wei, Y., E. R. Murphy, M. Larramendy, and S. Soloneski (2016). "Temperature-dependent regulation of bacterial gene expression by RNA thermometers". In: *Nucleic Acids – from Basic Aspects to Laboratory Tools Specific. IntechOpen, London.* Ed. by M. L. Larramendy and S. Soloneski, pp. 157–181. ISBN: 978-953-51-2264-7. DOI: 10.5772/61968. URL: https://www.intechopen.com/chapters/49624.

White-Ziegler, C. A. and T. R. Davis (2009). "Genome-wide identification of H-NS-controlled, temperature-regulated genes in *Escherichia coli* K-12". In: *Journal of bacteriology* 191.3, pp. 1106–1110. DOI: 10.1128/JB.00599-08.

Williams, B. J., J. Dehnbostel, and T. S. Blackwell (2010). "*Pseudomonas aeruginosa*: host defence in lung diseases". In: *Respirology* 15.7, pp. 1037–1056. DOI: 10.1111/j.1440-1843.2010.01819.x.

Xing, W., M. Yin, Q. Lv, Y. Hu, C. Liu, and J. Zhang (2014). "1 - Oxygen Solubility, Diffusion Coefficient, and Solution Viscosity". In: *Rotating Electrode Methods and Oxygen Reduction Electrocatalysts*. Ed. by W. Xing, G. Yin, and J. Zhang. Amsterdam: Elsevier, pp. 1–31. ISBN: 978-0-444-63278-4. DOI: https://doi.org/10.1016/B978-0-444-63278-4.00001-X. URL: https://www.sciencedirect.com/science/article/pii/B978044463278400001X.

Yamanaka, K., M. Mitta, and M. Inouye (1999). "Mutation analysis of the 5' untranslated region of the cold shock cspA mRNA of *Escherichia coli*". In: *Journal of Bacteriology* 181.20, pp. 6284–6291. DOI: 10.1128/JB.181.20.6284-6291.1999.

Zhao, K., M. Liu, and R. R. Burgess (2005). "The global transcriptional response of *Escherichia coli* to induced σ32 protein involves σ32 regulon activation followed by inactivation and degradation of σ32 *in vivo*". In: *Journal of Biological Chemistry* 280.18, pp. 17758–17768. DOI: 10.1074/jbc.M500393200.

Zhulin, I. B. (2001). "The superfamily of chemotaxis transducers: From physiology to genomics and back". In: *Advances in Microbial Physiology* 45, pp. 157–198. DOI: https://doi.org/10.1016/S0065-2911(01)45004-1.

Zulianello, L., C. Canard, T. Köhler, D. Caille, J.-S. Lacroix, and P. Meda (2006). "Rhamnolipids Are Virulence Factors That". In: *Infection and Immunity* 74.6, p. 3134. DOI: 10.1128/IAI.01772-05.

List of Figures

List of Tables